AD 410539

N-63-4-3

ASD-TDR-63-456

The High Temperature Hypersonic Gasdynamics Facility Estimated Mach Number 6 Through 14 Performance

Paul Czysz

TECHNICAL DOCUMENTARY REPORT NO. ASD-TDR-63-456

June 1963

Directorate of Engineering Test
Deputy for Test and Support
Aeronautical Systems Division
Air Force Systems Command
Wright-Patterson Air Force Base, Ohio

Project No. 1426, Task No. 142601

NOTICES

36-899T, 400, 7-22-63

FOREWORD

This report was prepared by Paul Czysz of the Hypersonic Gasdynamics Branch, Aerodynamics Division, Directorate of Engineering Test, Deputy for Test and Support, Aeronautical Systems Division, Wright-Patterson Air Force Base, Ohio. It describes the Mach Number 6 through 14 configuration of the High Temperature Facility and its expected performance. The work covers the period through February 1963.

The development of the High Temperature Hypersonic Gasdynamics Facility is being pursued under the continuing Task No. 142601, "Hypersonic Tunnel Studies," Project No. 1426, "Experimental Simulation of Flight Mechanics."

The assistance of Mr. Norman Fisher in developing and executing the necessary digital computer programs for this study is gratefully acknowledged.

ABSTRACT

The High Temperature Gasdynamics Facility was developed as a result of the Aeronautical Systems Division's effort to extend the state-of-the-art in hypersonic aerodynamic simulation. The High Temperature Facility is a hypersonic wind tunnel supplied with high pressure air, heated from a zirconia dioxide pebble heater. The maximum stagnation pressure and temperature is 40 atmospheres and 4700°R, respectively. This facility is one of four of its kind in this hemisphere and the only Air Force facility of its type. This report discusses the modification of the facility to a two-foot diameter test section with a Mach number range of 6 through 14 and its expected performance. This facility is scheduled to be operational in the Fall of 1963.

This Technical Documentary Report has been reviewed and is approved.

Robert L Colligan Jr

ROBERT L. COLLIGAN, JR.
Colonel, USAF
Deputy for Flight Test

Prepared by:

Paul Czysz

PAUL CZYSZ
Acting Chief, Hypersonic Gasdynamics Branch
Aerodynamics Division

Concurred in:

for Carl E. Reichert

WILLIAM J. DuBOIS, Colonel, USAF
Acting Director, Engineering Test
Deputy for Test and Support

Concurred in:

Hugh S. Lippman

HUGH S. LIPPMAN
Technical Director
Deputy for Test and Support

Approved by:

Robert L. Colligan, Jr.

ROBERT L. COLLIGAN, JR.
Colonel, USAF
Deputy for Flight Test

TABLE OF CONTENTS

LIST OF ILLUSTRATIONS

LIST OF TABLES

LIST OF SYMBOLS

a	speed of sound, $\left[\frac{ft}{sec}\right]$
A	area, (in^2)
c_p	specific heat at constant pressure, $\left[\frac{BTU}{lbm\,^\circ R}\right]$
h	enthalpy, $\left[\frac{BTU}{lbm}\right]$
k	ratio of specific heats for air
K_i	correction factor applied to perfect gas relationship for real gas effects. (Appendix)
M	Mach number
p	pressure, (psia)
q	dynamic pressure, $\frac{\rho V^2}{Z}$, psia
r	coordinate of nozzle normal to center line
Re/l	Reynolds number per foot, $\frac{\rho V}{\mu}$, $\left[\frac{1}{ft}\right]$
R	gas constant = 0.370484, for pressure in $lb/in.^2$, temperature in degrees Rankine and density in lbm/ft^3
t	time, (seconds)
T	temperature ($^\circ R$)
V_s	vacuum sphere volume (ft^3)
V	velocity $\left[\frac{ft}{sec}\right]$
$\dot{V}$	volume flow, (ft^3/min)
$\dot{w}$	mass flow (lbm/sec)
X_e	nozzle length (ft)
δ^*	displacement boundary layer, (in.)
δ	velocity boundary layer, (in.)

LIST OF SYMBOLS (Cont'd)

η	$(1 + \frac{M^2}{5})$ (Appendix)
μ	viscosity $\left[\frac{\text{lbm Sec}}{\text{ft}^2}\right]$
ξ	$\left[\frac{7M^2 - 1}{6}\right]$ (Appendix)
ρ	density $\left[\frac{\text{lbm}}{\text{ft}^3}\right]$

SUBSCRIPTS

0	stagnation conditions
2	behind normal shock
3	inlet to vacuum pump
r	conditions based on reference temperature, Equation 22, Appendix
aw	adiabatic wall
w	wall conditions
∞	free stream static, at nozzle exit
x	based on nozzle length from throat to exit
s	saturation limits of air
n	nozzle

SUPERSCRIPTS

*	critical conditions (M = 1)

INTRODUCTION

Simulation of flight conditions at hypersonic speeds for aerodynamic research is the mission of the High Temperature Hypersonic Gasdynamics Facility (HTF). This facility provides ASD with increased capability for studying basic aerodynamic and thermodynamic problems of hypersonic flight with real gas environments. The HTF operates intermittently at stagnation pressures up to 40 atmospheres and stagnation temperatures approaching 4700°F. This report discusses the operation and performance of the Mach 6 through 14 system presently being installed and scheduled to begin operation in the Fall of 1963.

DESCRIPTION - General

The High Temperature Hypersonic Gasdynamics Facility (HTF) is a blowdown wind tunnel which will operate in a nominal Mach number range of 6 through 14 at stagnation temperatures up to 4700°R. Intermittent operation is provided using the principle of stored air and stored heat. A schematic layout of the facility and associated systems is shown in figure 1. A sketch of the physical layout is shown in figure 2. Air stored at 80 atmospheres is heated as it passes vertically through the bed of the pebble heater. Expansion to the desired Mach number is provided by a series of water-cooled nozzles. After passing through a free-jet test section the air is cooled by passing through a heat exchanger then exhausted into the vacuum system. A sealed plenum chamber installed around the free jet section provides the necessary boundary conditions so that essentially a parallel, shock-free flow is obtained in the test section. A detailed description of the facility operation can be obtained in references 1 and 2.

Air Supply

The air supply consists of a Clark Brothers CMB6, 7-stage, high pressure air compressor which charges the tank farm consisting of 96 Mark I torpedo flasks. The torpedo flasks are connected in four banks and provide a total volume of 2200 cubic feet at 1200 psig. The compressor output is 2 pounds of air per second at 3200 psig, which is dried to a dew point of -80°F by chemical dryers. The air is expanded from the 3200 psig pressure to 1200 psig for storage in the tank farm.

Vacuum System

The vacuum systems consist of a 50-foot diameter sphere of approximately a 60,000 cubic-foot volume. This system is pumped by a series of vacuum pumps of the following capacities:

Manuscript released by the author May 1963 for publication as an ASD Technical Documentary Report.

NAME	NUMBER	MODEL
Roots Connersville	1	20 x 50 @ 880 RPM
	1	14 x 35 @ 920 RPM
	1	12 x 28½ @ 967 RPM
Kinney	6	KD 530
Allis-Chalmers	3	27D
	3	11S
	1	10GG
	1	7DB

This system is shown in figure 8. The performance of the vacuum pumps is shown in figure 9 and the expected run time for a facility utilizing the system is presented in figure 10 with nozzle weight flow as parameter.

Model Support System

The model support system can accomodate two struts each capable of being injected into the air stream. The strut and indexing system is mounted on a pitch sector which has a range of ± 45°. A pressure switch is provided which switches up to 60 pressure lines from the two models to a common pressure measuring system; and mounted between the two struts is a thermocouple reference junction box which switches up to 100 thermocouples from each model to a common amplifier system. The center of rotation of the pitch system is adjustable 14 inches parallel to the nozzle horizontal axis. The model support is designed for three modes of operation, these are: Fixed point,- pitching to a preselected angle of attack for a selected period of time. Pitching,- pitching at a preselected rate to an angle of attack limit, and immediately returning to zero. Pitch and pause,- pitching to a preset limit in increments, pausing at each increment for a preset interval. The model support can be automatically cycled, or manually controlled. The angle of attack readout system is a digital system accurate to 0.01 degree. A sketch of this system is presented in figure 3.

Nozzle

The nozzle is axisymmetric with an exit diameter of 24 inches. The complete nozzle system consists of a series of conical throat sections with different throat areas to provide nominal Mach numbers 8, 10, 12, and 14. The coordinates of these throat sections are given in table 1. The exit Mach number at the end of the conical section is from 5 to 7, so that the static temperature is low enough to be approximately a perfect gas. The straightening section is then a section of a contoured nozzle obtained from reference 9 for a Mach number 10 for a ratio of specific heats equal to 1.40. The contour of this section is tabulated in table 2. A sketch of the nozzle assembly is shown in figure 5. This nozzle is so designed that the throat sections can be replaced without removing the straightening section from the facility. For Mach numbers other than 8 the inflection point is upstream of the separation joint of the throat section and straightening section; so that for the Mach number 10, 12, and 14 throat sections the portion from the end of the conical section to the end of the throat section, is a continuation of the straightening section contour. Based on the experience with the Mach number 4 configuration of this facility, the disturbance due to the joint should be less than that produced by the nozzle wall erroded by the hot gases. The nozzle contours from the beginning of the conical expansion section with the displacement and velocity boundary layer for two Reynolds numbers are shown in figure 17 for Mach 8, 10, 12, and 14 nozzles.

The Mach number 6 and 7 nozzles will be individual nozzles interchangeable with this nozzle system. These are expected to be available in the Fall of 1964.

Test Section and Diffuser

The test section is a free jet type enclosed within a large plenum chamber. The free jet was chosen for obvious reasons of simplicity and to allow for model insertion after the flow had been established. The diffuser is designed to provide a moderately good pressure recovery with the model in the test section. The design is based on references 10 and 11, and these basic principles were successfully applied to the diffuser used in the Mach 4 configuration (ref 2).

Heater Operation

Although a complete description of the operation of the pebble heater is given in references 1 and 2, additional information on the effect of operational methods on flow quality in the test section is necessary. Even during the initial operation of the heater in 1960 it became apparent that long idle times between runs significantly added to the amount of dust in the air stream. During the 1961-1962 operation every attempt was made to make at least three runs, with at least one run over 3000°F during a day of operation. The down time between model changes, maintenance, and so forth, was usually no greater than 48 hours. During this down time the heater was on idle condition with the top of the bed at about 2500°F. As long as this schedule was maintained (approximately 5 months) the amount of zirconia dust was negligible, in fact, no worse than dusting associated with some conventional return flow tunnels. When a long delay did occur, a week's duration or more, the pressure drop across the pebble bed during burning increased markedly. The operation after these long idle periods produces increasing amounts of dust in the air stream and serious reductions in the porosity of the pebble core. In order to continue operation the procedures outlined in reference 2 were used but the dusting was not reduced to the original low levels. If the duration of the idle cycle of the operation between program changes is minimized it appears that the dusting level can be maintained low for most of the refractory life, at least, longer than the five-month figure already achieved and therefore, not seriously impair the quality of the test medium. A cross section of the heater is shown in figure 4.

Performance

The performance of the High Temperature Hypersonic Gasdynamics Facility with the Mach 6 through 14 system is shown in figures 11 through 16. Each figure contains a group of graphs presenting all the pertinent variables for a particular nozzle system. These are:

$$M_\infty\ ,\ \delta^*,\ \delta\ ,\ \dot{w}\ ,\ q_\infty,\ P_\infty\ ,\ T_\infty,\ V_\infty,\ \frac{Re}{\ell}\ ,\ P_{o_2}\ ,\ \frac{M_\infty}{\sqrt{Re/\ell}}\ ,$$

and running time. The details of the formulation for these calculations are presented in the Appendix.

Concluding Remarks

The facility described provides the Air Force with the In-House capability required of a vigorous applied research program in aerothermodynamics. This increased capability is an extension of the capability which provided the means to meet the needs of ASD in its demands for quick reaction capability in applied research during the 1960 through 1962 period. The HTF is not a "production" test facility in the sense of providing solutions to detail vehicle development problems. It is directed toward providing experimental verification and correlation of ideas in such detail as required by the research engineer, and to investigate the fundamental problems of correctly measuring the associated physical phenomena. For this reason the configuration of the HTF is not expected to remain static. If it is to be of value in applied research programs the experimental facility must keep pace with the advancing technology.

APPENDIX

Computation of facility performance.

The basic perfect gas, one dimensional flow equations are listed below. The K terms are corrections applied from references 4, 7, and 8 for real gas effects.

ISENTROPIC FLOW RELATIONSHIPS

Let

$$\eta = \left(1 + \frac{M^2}{5}\right)$$

$\frac{P}{P_0} = \eta^{-3.5}$	$K_1 = \text{CORR}\left(\frac{P}{P_0}\right)$	(1)
$\frac{T}{T_0} = \eta^{-1}$	$K_2 = \text{CORR}\left(\frac{T}{T_0}\right)$	(2)
$\frac{\rho}{\rho_0} = \eta^{-2.5}$	$K_3 = \text{CORR}\left(\frac{\rho}{\rho_0}\right)$	(3)
$\frac{q}{P_0} = 0.7 M^2 \eta^{-0.50}$	$K_4 = \text{CORR}\left(\frac{q}{P_0}\right)$	(4)
$\frac{V}{a^*} = 1.095 M \eta^{-0.50}$	$K_5 = \text{CORR}\left(\frac{V}{a^*}\right)$	(5)
$\frac{A}{A^*} = \frac{125}{216} M^{-1} \eta^3$	$K_6 = \text{CORR}\left(\frac{A}{A^*}\right)$	(6)

ISENTROPIC CRITICAL CONDITIONS

$\frac{P^*}{P_0} = 0.5283$	$K_7 = \text{CORR}\left(\frac{P^*}{P_0}\right)$	(7)
$\frac{T^*}{T_0} = 0.8333$	$K_8 = \text{CORR}\left(\frac{T^*}{T_0}\right)$	(8)

GAS PROPERTY CORRECTIONS

$k = 1.402$	$K_9 = \text{CORR}(k)$	(9)
$c_p = 0.2401$	$K_{10} = \text{CORR}(c_p)$	(10)

NORMAL SHOCK RELATIONSHIPS

Let

$$\xi = \frac{7M^2-1}{6}$$

$$\frac{P_2}{P_1} = \xi \qquad K_{11} = \mathrm{CORR}\left(\frac{P_1}{P_2}\right) \tag{11}$$

$$\frac{T_2}{T_1} = \xi\left(\frac{\xi+6}{6\xi+1}\right) \qquad K_{12} = \mathrm{CORR}\left(\frac{T_2}{T_1}\right) \tag{12}$$

$$\frac{\rho_2}{\rho_1} = \left(\frac{6\xi+1}{\xi+6}\right) \qquad K_{13} = \mathrm{CORR}\left(\frac{\rho_2}{\rho_1}\right) \tag{13}$$

$$\frac{P_{o_2}}{P_o} = \xi^{-2}\left(\frac{6\xi+1}{\xi+6}\right) \qquad K_{14} = \mathrm{CORR}\left(\frac{P_{o_2}}{P_o}\right) \tag{14}$$

These corrections for a non-perfect gas become increasingly inaccurate with decreasing stagnation pressure and therefore are only approximate. A computer program has since been developed for data reduction considering the exact gas composition.

Saturation Limits for Air:

From references 14 and 15 the saturation conditions can be expressed as:

$$P_s = f(T_s)$$

selecting T_o and M_∞ then,

$$T_s = \frac{T_o K_2}{\eta} \tag{15}$$

The corresponding P_s can then be found, so that

$$P_o = \frac{P_s \eta^{3.5}}{K_1} \tag{16}$$

The stagnation temperature and pressure at which saturation occurs can then be found as a function of Mach number. These results are presented in figure 7.

Nozzle Performance:

Once the nozzle exit diameter and throat diameter have been selected, then the displacement boundary layer required to operate at a selected T_o and M is:

$$\delta^*_{REQ'D} = r_e - r^* \left(\frac{A}{A^*} K_e\right)^{0.5} \tag{17}$$

The displacement boundary layer thickness is given by reference 13.

$$\delta^* = \frac{0.5556\, M^{1.311}}{\left[(Re/\ell)_\infty X_e\right]^{0.276}} \tag{18}$$

This can be developed into

$$\delta^* = 1.1387 \times 10^{-3} \frac{T_0^{0.414} X_e^{0.727}}{P_0^{0.276}} M^{1.035} \eta^{0.552} \left(\frac{K_2}{K_3 K_5}\right)^{0.276} \tag{19}$$

From references 13 and 16 the corrections for wall enthalpy ratio can be implied as follows:

$$\frac{\delta^*}{X} = 0.49 \left(\frac{\rho_r V_\infty X_e}{\mu_r}\right)^{-0.30} \tag{20}$$

where

$$T_r = 0.22\,(T_0 - T_\infty) + 0.5\,(T_w - T_\infty) \tag{21}$$

This implies

$$\frac{\rho_r V_\infty X}{\mu_r} \;\alpha\; Re_x \left(\frac{T_\infty}{T_r}\right)^2 \tag{22}$$

from this we have

$$\frac{\delta^*}{\delta^*_{AW}} \cong \left[0.33 + 0.75 \frac{T_w}{T_0}\right]^{0.60} \tag{23}$$

since the data from reference 13 was taken at approximately hw/ho ≈ 0.11, we have

$$\frac{\delta^*}{\delta^*_{\left(\frac{hw}{ho} = 0.11\right)}} = \left[0.80 + 1.81 \frac{T_w}{T_0}\right]^{0.60} \tag{24}$$

The pressure required to operate at a selected M and T_0 is then, combining equations 17, 19, and 24.

$$P_0 = \frac{K_2}{K_3 K_5} \left\{ \frac{1.1387 \times 10^{-3} \left(0.80 + 1.81 \frac{T_w}{T_0}\right)^{0.6} T_0^{0.414} X_e^{0.724} M^{1.05} \eta^{0.552}}{\left[r_e - 0.7607 \sqrt{\frac{K_6 \eta^3}{M}}\, r^* \right]} \right\}^{3.623} \tag{25}$$

The isentropic and normal shock relationship can now be evaluated for the P_0, T_0, and M_∞.

The nozzle weight flow is:

$$\dot{w}_n = 0.4180 \frac{P_0}{\sqrt{T_0}} (\delta^*)^2 K_7 \left(\frac{K_9^*}{K_8} \right) \tag{26}$$

where $K_9{}^*$ is K_9 evaluated at T^*

as a check for equation 5 the freestream velocity was computed as:

$$V_\infty = M_\infty A_\infty \tag{27}$$

In all cases equations 27 and 5 checked identically for three significant figures. The velocity boundary layer, from reference 13 is given by

$$\delta = \frac{0.792 \left(0.80 + 1.81 \frac{T_w}{T_0} \right) M^{0.824}}{\left[(Re/\ell)\ X_e \right]^{0.166}}$$

Conditions at Vacuum Sphere

The temperature at the exit of the heat exchanger is designed to be approximately 610°R. Based on diffuser recovery with a model in the test section, it was assumed that 50 percent of P_{O_2} is recovered at the diffuser exit. Based on a conservative estimate of the pressure drop across the heat exchanger, it was estimated that 25 percent of P_{O_2} would be recorded at the vacuum pump inlet.

$$P_{O_3} = 0.25\, P_{O_2} \tag{28}$$

The gas density is

$$\rho_3 = 0.01846\, P_{O_3} \tag{29}$$

The volume flow is

$$\dot{V}_3 = \frac{\dot{w}_n}{\gamma_3}$$

Running Time

The rate of pressurization of the vacuum system is derived from the continuity equation as follows:

$$\frac{\partial \rho}{\partial t} = \frac{\dot{w}_{in} - \dot{w}_{out}}{V} \tag{30}$$

where

$$\dot{w}_{in} = \dot{w}_n$$

$$\dot{w}_{out} = \frac{p_3 \dot{V}}{RT}$$

$$\rho_3 = \frac{p_3}{RT}$$

then

$$\frac{\partial}{\partial t}\left(\frac{p_3}{RT}\right) = \frac{\dot{w}_n - \frac{p_3\dot{V}}{RT}}{V}$$

and

$$\frac{\partial p}{\partial t} = \frac{\dot{w}_n RT - p_3\dot{V}}{V} \tag{31}$$

for the general case:

The volume flow and pressure are both functions of time, so that numerical integration is required. This solution for the pump characteristics in figure 9 is presented in figure 10 with nozzle weight flow as parameter.

If the assumption of constant pumping speed is valid, then equation 31 can be integrated as follows:
From equation 31,

$$\frac{dp}{\frac{\dot{w}_n RT}{V} - p} = \frac{\dot{V}}{V}\,dt \tag{32}$$

this may be integrated directly as

$$\ln\left(\frac{\dot{w}_n RT}{V} - p\right) = \frac{\dot{V}}{V}\,dt$$

when

$$t = 0 \qquad p_3 = p_i$$

$$\ln\left[\frac{\frac{\dot{w}_n RT}{\dot{V}} - p_3}{\frac{\dot{w}_n RT}{\dot{V}} - p_i}\right] = \frac{\dot{V}}{V}\,t$$

then

$$t_{\substack{constant\\pumping}} = \frac{V}{\dot{V}}\left[\ln\left(\frac{\dot{w}_n RT - p_3\dot{V}}{\dot{w}_n RT - p_i\dot{V}}\right)\right] \tag{33}$$

For calculation of the running times included in the performance of the nozzle systems, figures 11 through 16, equation 33 was used with the following assumptions:

$p_3 < 5 \times 10^{-1}$ mm Hg $\qquad \dot{V} = 30{,}000$ cfm

$p_3 \geq 5 \times 10^{-1}$ mm Hg $\qquad \dot{V} = 10{,}000$ cfm

$T_3 = 610°R$

for the case of no pumps, $\dot{V} = 0$, we have then from equation 31

$$\frac{dp}{dt} = \frac{\dot{w}_n RT}{V} \tag{34}$$

which can be integrated as

$$t_{\substack{no \\ pumps}} = \frac{(p_3 - p_i)V}{\dot{w}_n RT} \tag{35}$$

REFERENCES

1. Milling, Robert W., Captain, USAF, The High Temperature Hypersonic Gasdynamics Facility. ASD Technical Note 61-107, AD No. 266-728.

2. Czysz, Paul, The High Temperature Hypersonic Gasdynamics Facility, Mach Number 4 Operation, ASD-TDR-63-236.

3. Ames Research Staff (NASA) Equations, Tables, and Charts for Compressible Flows. NACA Report 1135, 1953.

4. Hansen, C. Fredrick, Approximations for the Thermodynamic and Transport Properties of High Temperature Air. NACA Report TN 4150, April 1958.

5. Moeckel, W. E. and Weston, Kenneth C., Composition and Thermodynamic Properties of Air in Chemical Equilibrium. NACA Report TN 4265, April 1958.

6. National Bureau of Standards Circular 564, Tables of Thermal Properties of Gases, November 1955.

7. Yoshikawa, Kenneth K. and Katzen, Elliott D., Charts for Air Flow Properties in Equilibrium and Frozen Flows in Hypervelocity Nozzles, NASA TN D-693, April 1961.

8. Jorgensen, Leland H., and Baum, Gayle M., Charts for Equilibrium Flow Properties of Air in Hypervelocity Nozzles. NASA TN D-1333, ADVANCE COPY, Aug 1962.

9. Cresci, Robert J., Tabulation of Coordinates for Hypersonic Axisymmetric Nozzles, WADD TN 58-300, Parts 1 and 2. Oct 1958 and July 1960.

10. Scaggs, N. E. and Petrie, S. L., Experimental Blockage Studies for a Hypersonic Wind Tunnel Diffuser, Ohio State University Research Foundation Report TN (ALOSU) 761-2, Dec 1961.

11. Harris, William G. and McCormick, Ralph B., Diffuser Investigation in an Axisymmetric Open Jet, Hypersonic Wind Tunnel. PREPRINT of a paper presented by Boeing Aircraft Company, Seattle, Washington at AGARD-Sta Meeting, 1959.

12. Burke, A. F. and Bird, K. D., The Use of Conical and Contoured Expansion Nozzles in Hypervelocity Facilities, Cornell Aeronautical Laboratory, Report CAL No. 112, July 1962.

13. Burke, Andrew F., Turbulent Boundary Layers on Highly Cooled Surfaces at High Mach Numbers. Proceedings of Symposium on Aerothermoelasticity, ASD TR 61-645.

14. Erickson, Wayne D., and Creekmore, Helen S., A Study of Equilibrium Real Gas Effects in Hypersonic Air Nozzles Including Charts of Thermodynamic Properties for Equilibrium Air. NASA TN D-231, April 1960.

REFERENCES

1. Milling, Robert W., Captain, USAF, The High Temperature Hypersonic Gasdynamics Facility. ASD Technical Note 61-107, AD No. 266-728.

2. Czysz, Paul, The High Temperature Hypersonic Gasdynamics Facility, Mach Number 4 Operation, ASD-TDR-63-236.

3. Ames Research Staff (NASA) Equations, Tables, and Charts for Compressible Flows. NACA Report 1135, 1953.

4. Hansen, C. Fredrick, Approximations for the Thermodynamic and Transport Properties of High Temperature Air. NACA Report TN 4150, April 1958.

5. Moeckel, W. E. and Weston, Kenneth C., Composition and Thermodynamic Properties of Air in Chemical Equilibrium. NACA Report TN 4265, April 1958.

6. National Bureau of Standards Circular 564, Tables of Thermal Properties of Gases, November 1955.

7. Yoshikawa, Kenneth K. and Katzen, Elliott D., Charts for Air Flow Properties in Equilibrium and Frozen Flows in Hypervelocity Nozzles, NASA TN D-693, April 1961.

8. Jorgensen, Leland H., and Baum, Gayle M., Charts for Equilibrium Flow Properties of Air in Hypervelocity Nozzles. NASA TN D-1333, ADVANCE COPY, Aug 1962.

9. Cresci, Robert J., Tabulation of Coordinates for Hypersonic Axisymmetric Nozzles, WADD TN 58-300, Parts 1 and 2. Oct 1958 and July 1960.

10. Scaggs, N. E. and Petrie, S. L., Experimental Blockage Studies for a Hypersonic Wind Tunnel Diffuser, Ohio State University Research Foundation Report TN (ALOSU) 761-2, Dec 1961.

11. Harris, William G. and McCormick, Ralph B., Diffuser Investigation in an Axisymmetric Open Jet, Hypersonic Wind Tunnel. PREPRINT of a paper presented by Boeing Aircraft Company, Seattle, Washington at AGARD-Sta Meeting, 1959.

12. Burke, A. F. and Bird, K. D., The Use of Conical and Contoured Expansion Nozzles in Hypervelocity Facilities, Cornell Aeronautical Laboratory, Report CAL No. 112, July 1962.

13. Burke, Andrew F., Turbulent Boundary Layers on Highly Cooled Surfaces at High Mach Numbers. Proceedings of Symposium on Aerothermoelasticity, ASD TR 61-645.

14. Erickson, Wayne D., and Creekmore, Helen S., A Study of Equilibrium Real Gas Effects in Hypersonic Air Nozzles Including Charts of Thermodynamic Properties for Equilibrium Air. NASA TN D-231, April 1960.

15. Handbook of Supersonic Aerodynamics. NAVORD Report 1488 Vol 5, August 1953.

16. Persh, Jerome, A Theoretical Investigation of Boundary Layer Flow with Heat Transfer at Supersonic and Hypersonic Speeds. NAVORD Report 3854.

TABLE 1

COORDINATES OF CONICAL THROAT SECTIONS

Nozzle Mach = 8		Nozzle Mach = 10	
X	Y	X	Y
0.0000	1.7500	0.0000	1.7500
0.2500	1.5749	0.2500	1.5749
0.5000	1.3999	0.5000	1.3999
0.7500	1.2248	0.7500	1.2248
1.0000	1.0498	1.0000	1.0498
1.2500	0.8747	1.2500	0.8747
1.5000	0.6997	1.5000	0.6997
1.5995	0.6300	1.7500	0.5246
		1.9233	0.4033
2.8595	0.6300		
3.8595	0.8380	2.7299	0.4033
4.8595	1.0460	3.7299	0.6251
5.8595	1.2540	4.7299	0.8469
6.8595	1.4620	5.7299	1.0688
7.8595	1.6701	6.7299	1.2906
8.8595	1.8781	7.7299	1.5124
9.8595	2.0861	8.7299	1.7342
10.8595	2.2941	9.7299	1.9560
11.8595	2.5021	10.7299	2.1779
12.8595	2.7101	11.7299	2.3997
13.8595	2.9181	12.7299	2.6215
14.8595	3.1261	13.7299	2.8433

TABLE 1 (Cont'd)

COORDINATES OF CONICAL THROAT SECTIONS

Nozzle Mach = 8		Nozzle Mach = 10	
X	Y	X	Y
15.8595	3.3341	14.7299	3.0651
16.8595	3.5421	15.5443	3.2458
17.8595	3.7502		
18.8595	3.9582		
18.8690	3.9601		

Nozzle Mach = 12		Nozzle Mach = 14	
X	Y	X	Y
0.0000	1.7500	0.0000	1.7500
0.2500	1.5749	0.2500	1.5749
0.5000	1.3999	0.5000	1.3999
0.7500	1.2248	0.7500	1.2248
1.0000	1.0498	1.0000	1.0498
1.2500	0.8747	1.2500	0.8747
1.5000	0.6997	1.5000	0.6997
1.7500	0.5246	1.7500	0.5246
2.0000	0.3496	2.0000	0.3496
2.1799	0.2236	2.2500	0.1745
		2.3105	0.1322
2.6271	0.2236		
3.6271	0.4592	2.5749	0.1322
4.6271	0.6948	3.5749	0.3767
5.6271	0.9305	4.5749	0.6212

TABLE 1 (Cont'd)

COORDINATES OF CONICAL THROAT SECTIONS

Nozzle Mach = 12		Nozzle Mach = 14	
X	Y	X	Y
6.6271	1.1662	5.5749	0.8657
7.6271	1.4018	6.5749	1.1102
8.6271	1.6374	7.5749	1.3547
9.6271	1.8731	8.5749	1.5991
10.6271	2.1087	9.5749	1.8436
11.6271	2.3444	10.5749	2.0881
12.4559	2.5397	10.5853	2.0907

TABLE 2

COORDINATES OF STRAIGHTENING SECTION

X	Y	X	Y
10.000	1.9467	51.000	9.0332
11.000	2.1916	52.000	9.1521
12.000	2.4318	53.000	9.2693
13.000	2.6672	54.000	9.3848
14.000	2.8981	55.000	9.4987
15.000	3.1245	56.000	9.6109
16.000	3.3465	57.000	9.7216
17.000	3.5642	58.000	9.8308
18.000	3.7778	59.000	9.9386
19.000	3.9873	60.000	10.0448
20.000	4.1928	61.000	10.1497
21.000	4.3944	62.000	10.2532
22.000	4.5922	63.000	10.3553
23.000	4.7863	64.000	10.4561
24.000	4.9768	65.000	10.5556
25.000	5.1638	66.000	10.6538
26.000	5.3473	67.000	10.7507
27.000	5.5274	68.000	10.8464
28.000	5.7043	69.000	10.9409
29.000	5.8779	70.000	11.0342
30.000	6.0485	71.000	11.1264
31.000	6.2160	72.000	11.2173
32.000	6.3805	73.000	11.3071

TABLE 2 (Cont'd)

COORDINATES OF STRAIGHTENING SECTION

X	Y	X	Y
33.000	6.5421	74.000	11.3958
34.000	6.7009	75.000	11.4834
35.000	6.8570	76.000	11.5698
36.000	7.0104	77.000	11.6551
37.000	7.1612	78.000	11.7393
38.000	7.3094	79.000	11.8225
39.000	7.4552	80.000	11.9045
40.000	7.5986	81.000	11.9854
41.000	7.7396	81.185	12.0003
42.000	7.8783		
43.000	8.0148		
44.000	8.1491		
45.000	8.2813		
46.000	8.4115		
47.000	8.5397		
48.000	8.6659		
49.000	8.7902		
50.000	8.9126		

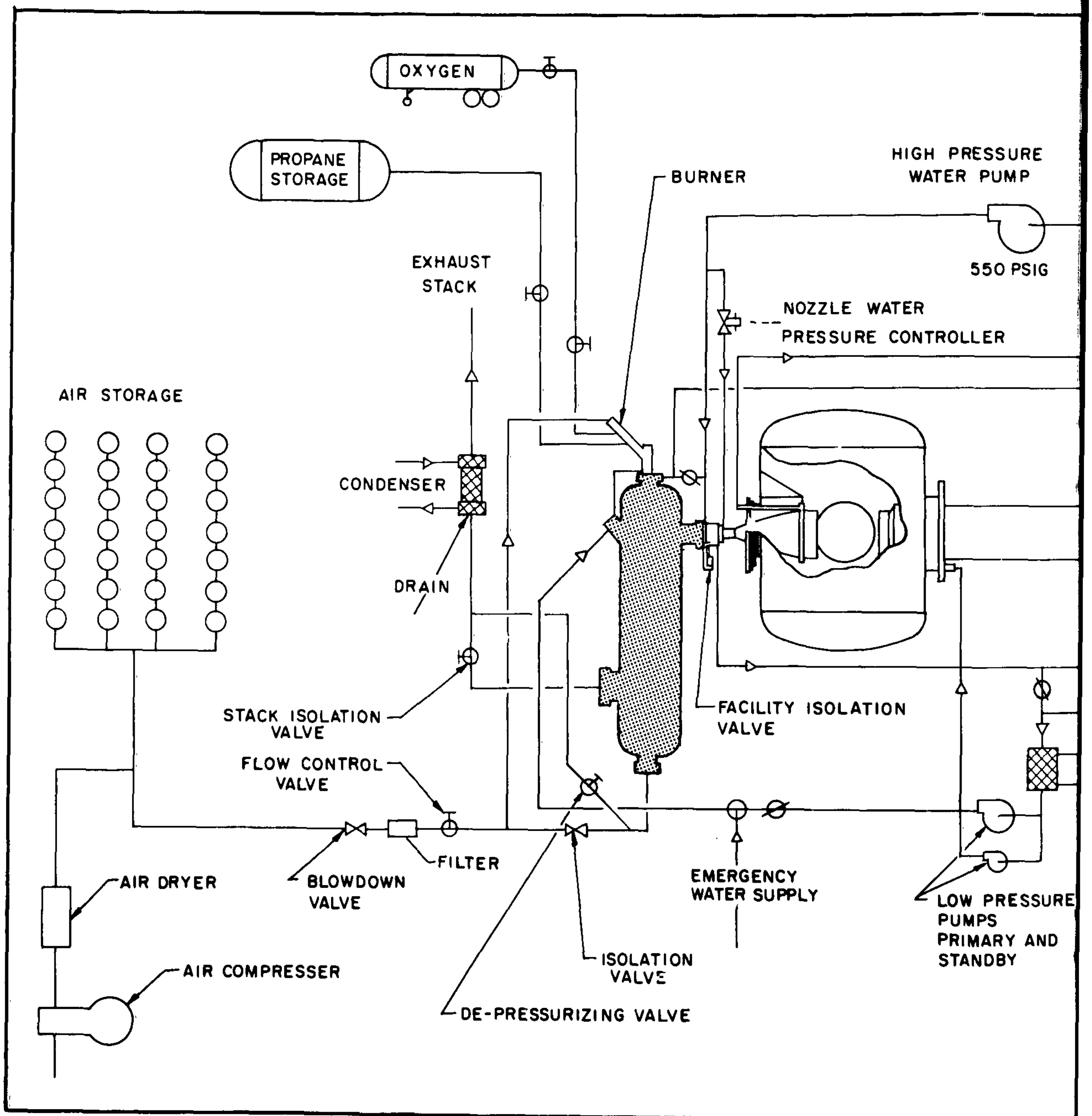

1

Figure 1. Schematic of Facility Systems

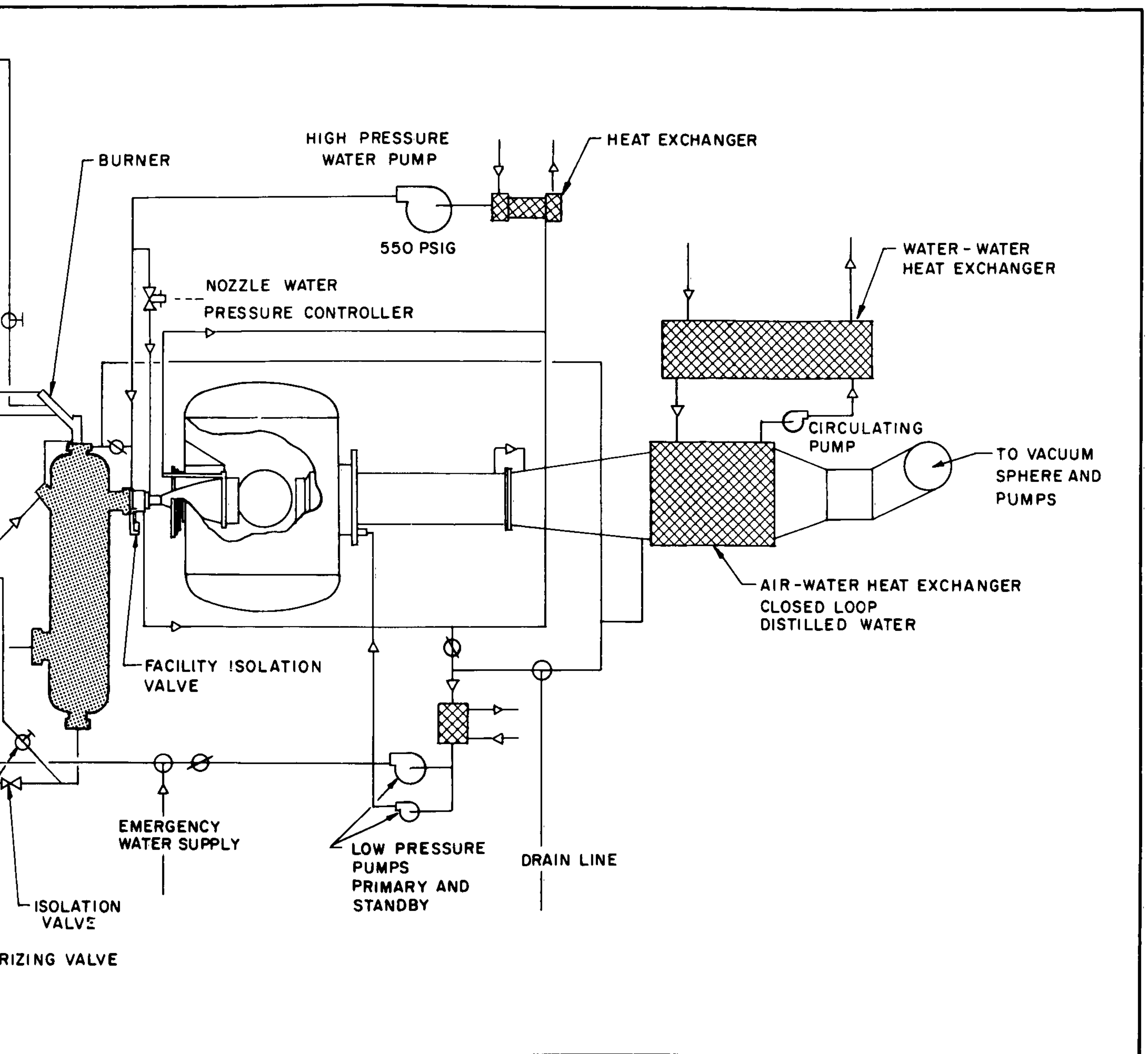

Figure 1. Schematic of Facility Systems

2

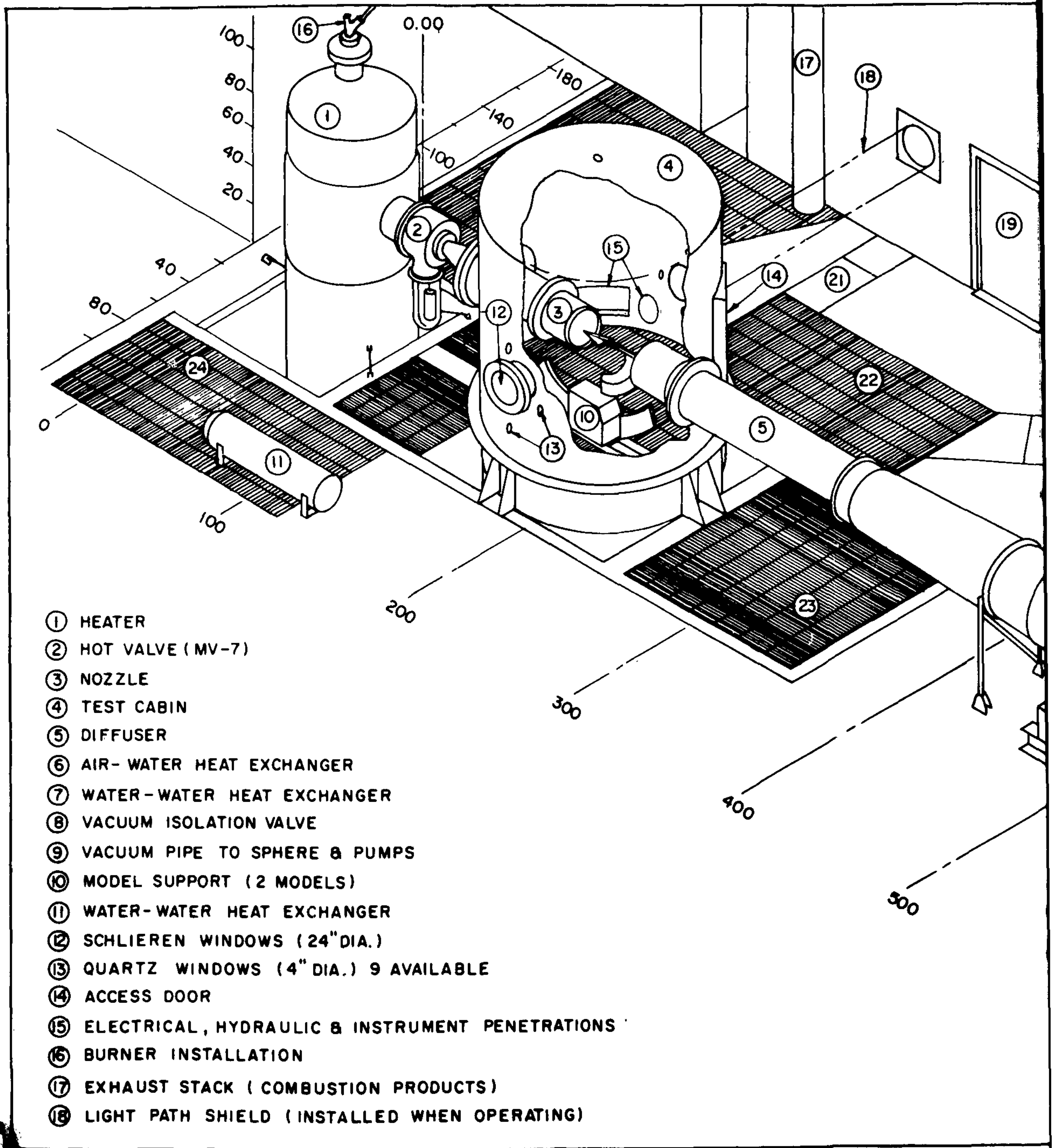

Figure 2. Facility Drawing

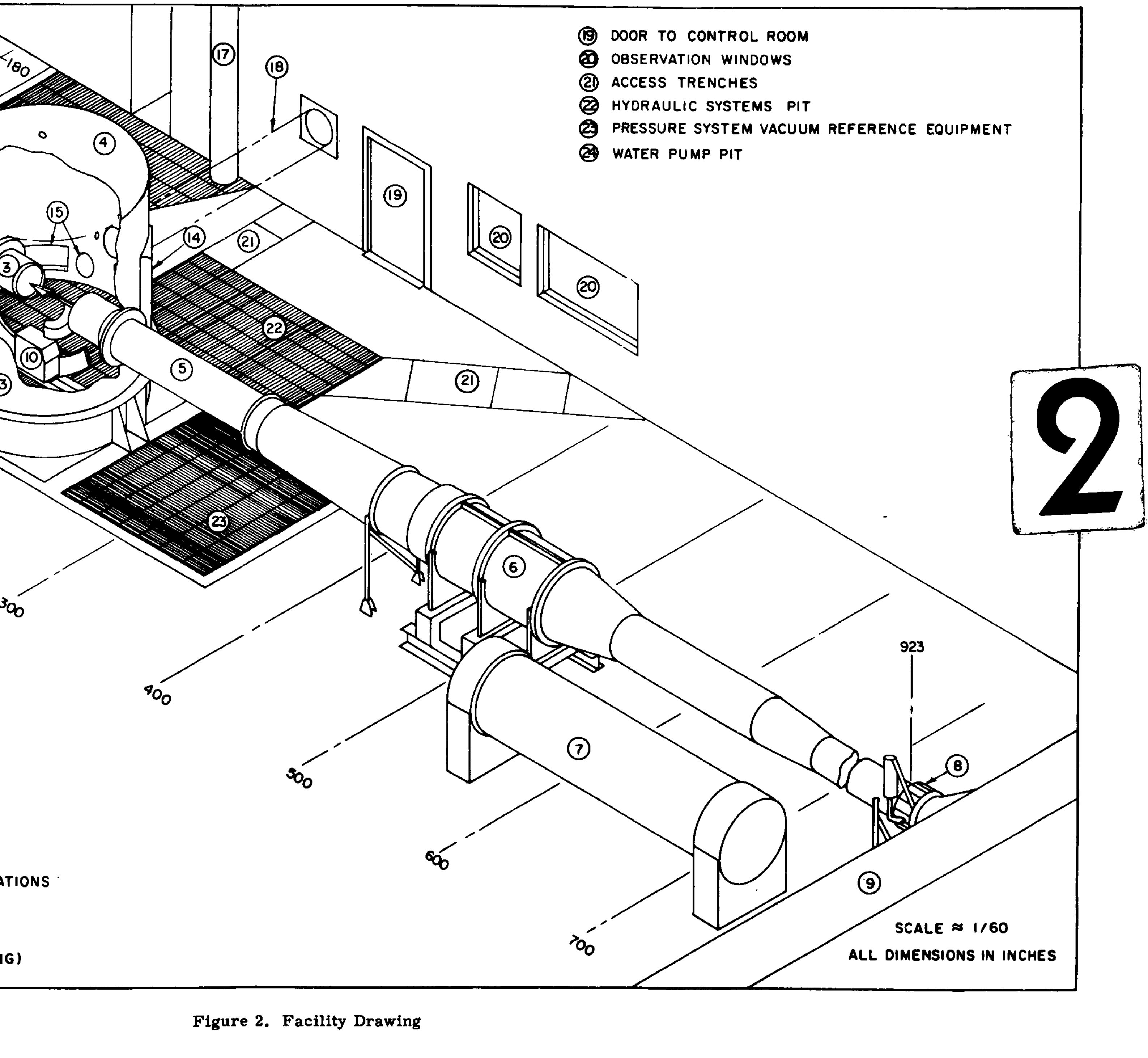

Figure 2. Facility Drawing

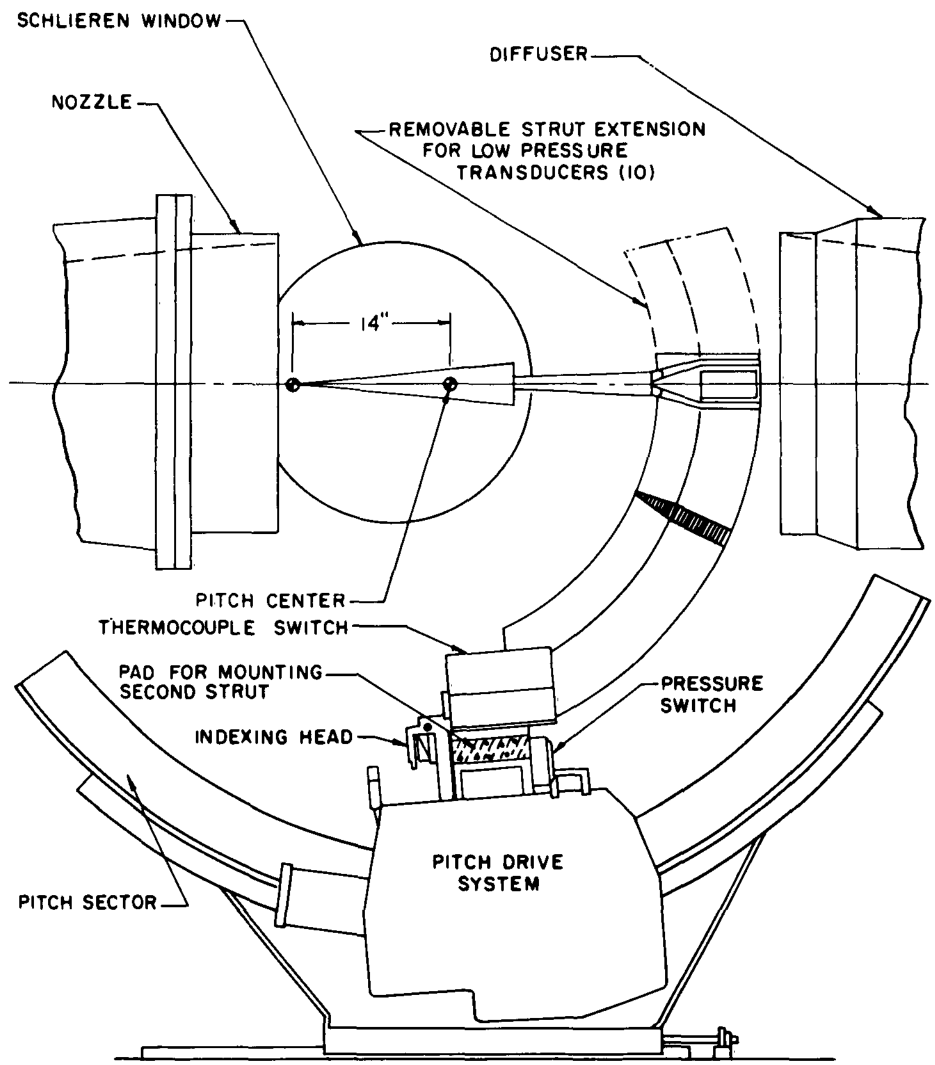

Figure 3. Model Support System

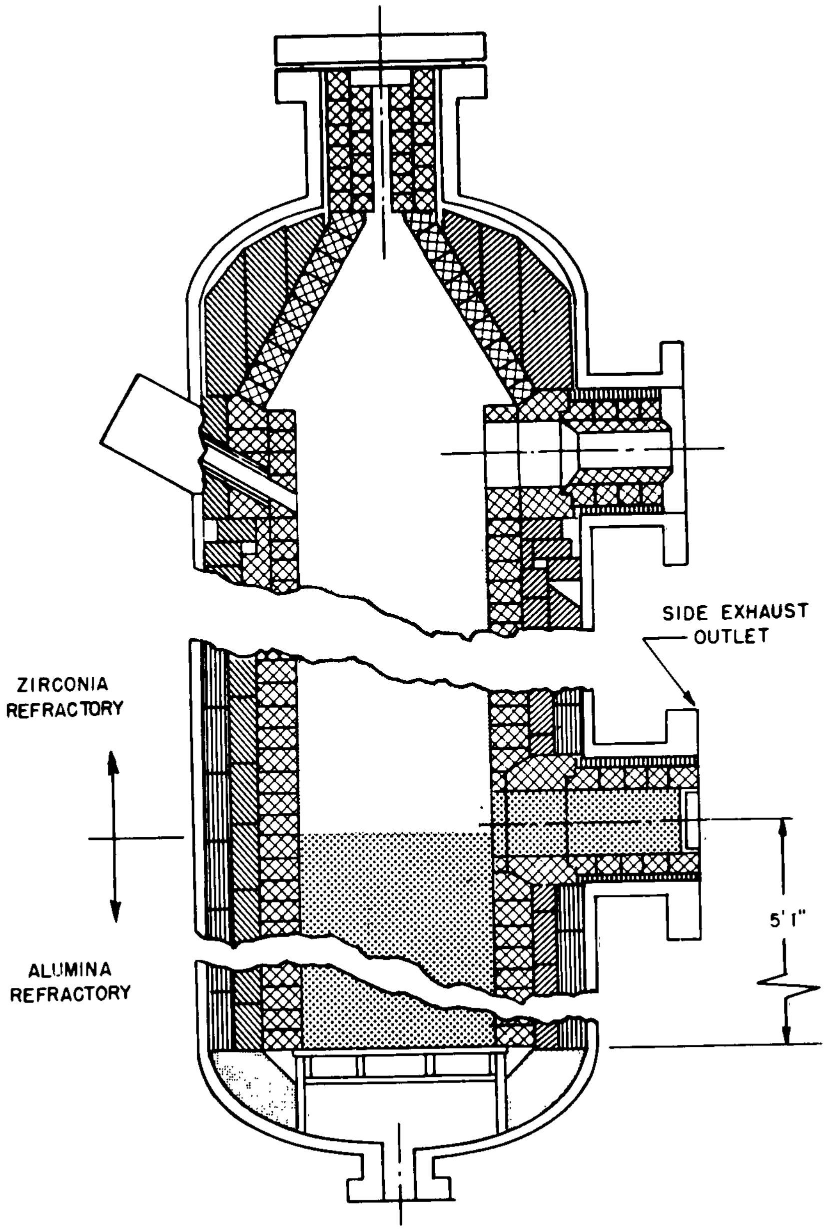

Figure 4. Heater Details

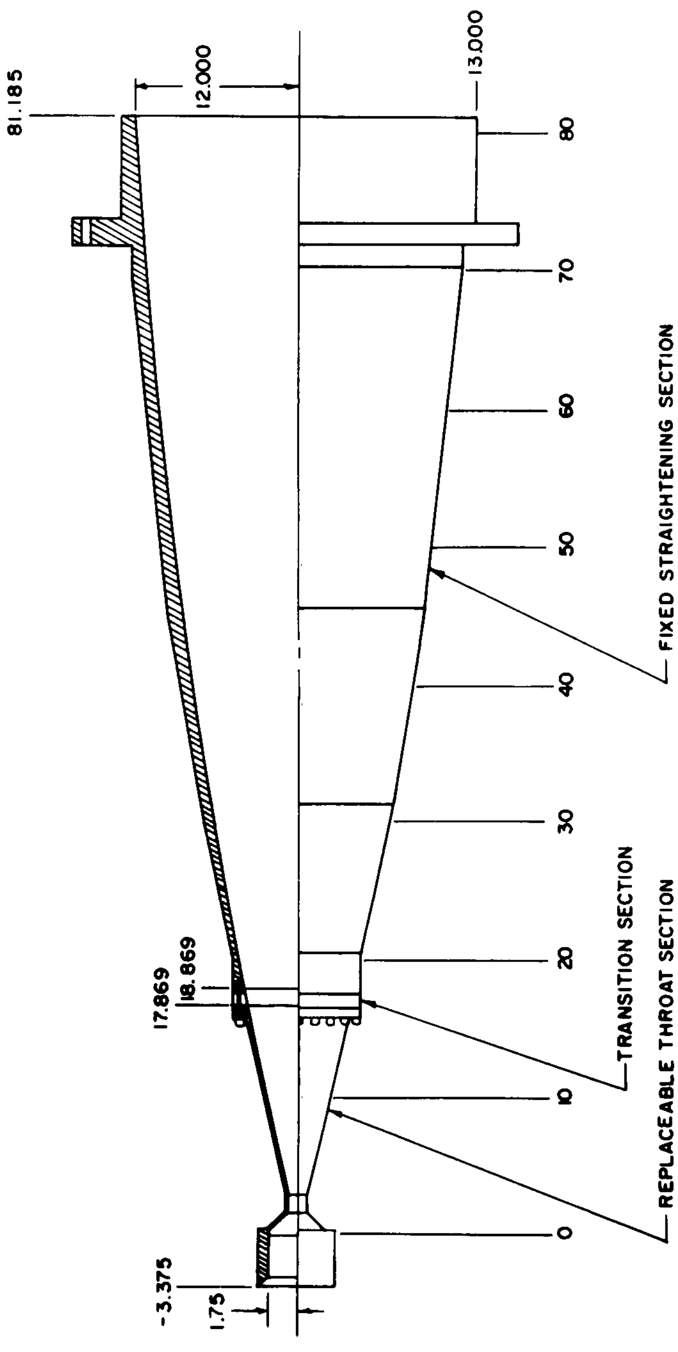

Figure 5. Mach Number 8 - 14 Nozzle Liner

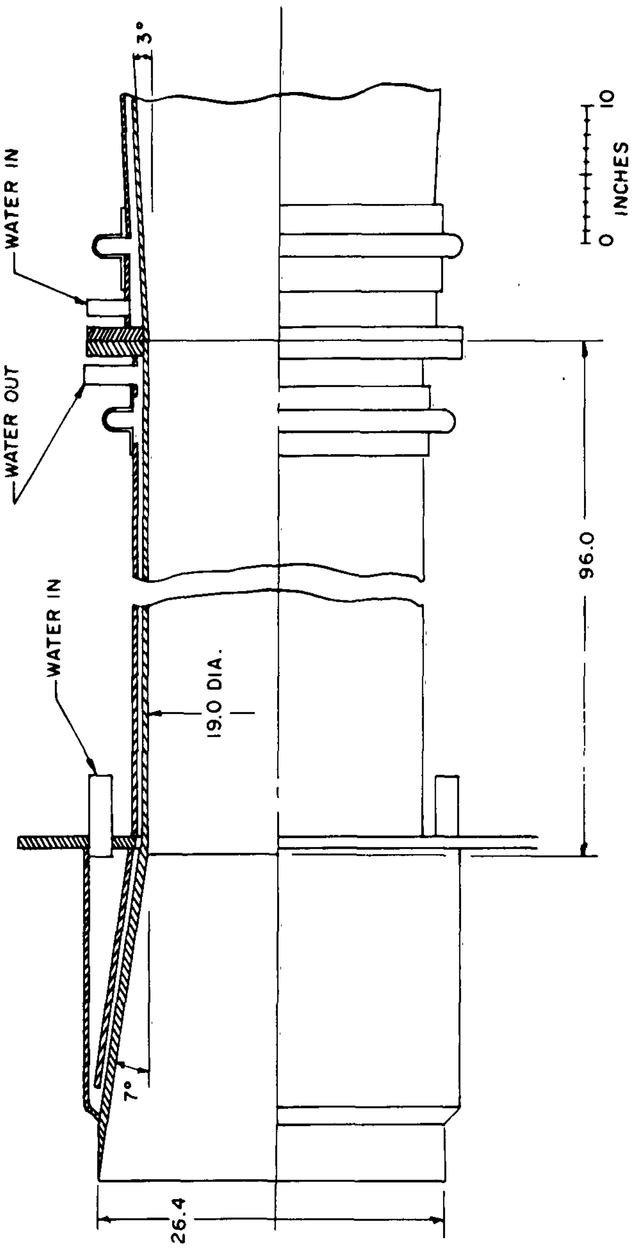

Figure 6. Diffuser Assembly

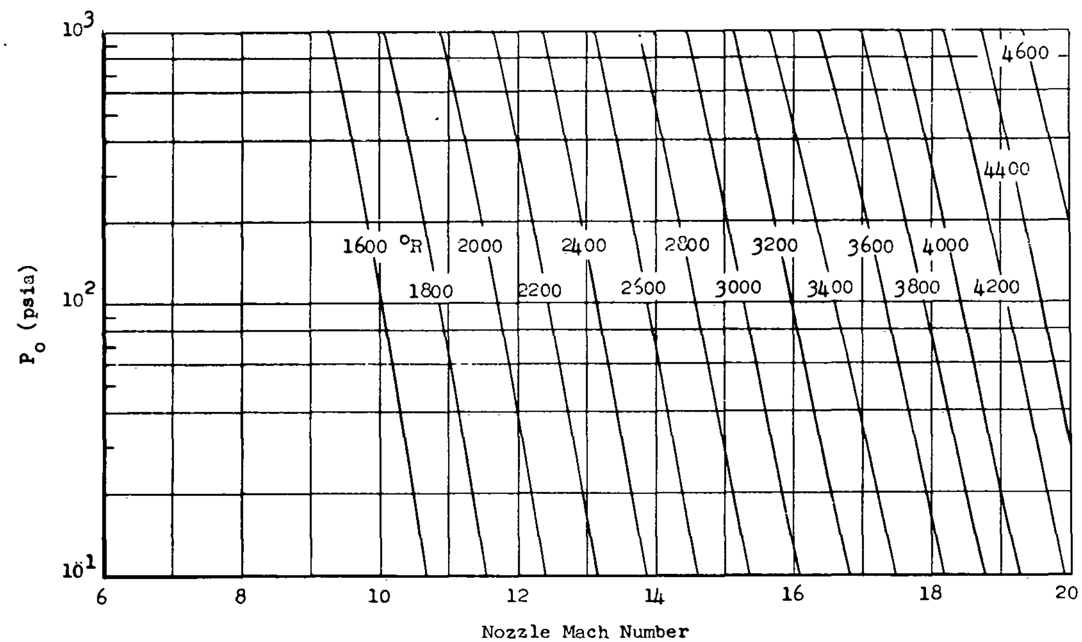

Figure 7. Stagnation Pressure and Temperature at Which Saturated Air Occurs in the Test Section vs. Test Section Mach Number

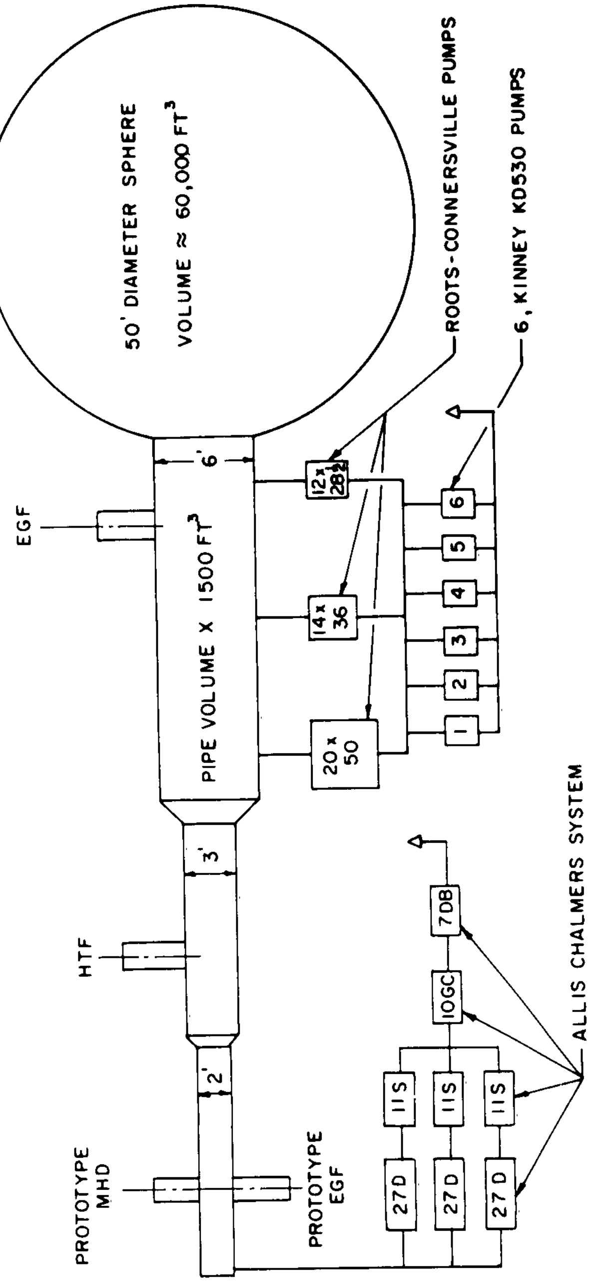

Figure 8. Schematic Diagram of Vacuum System

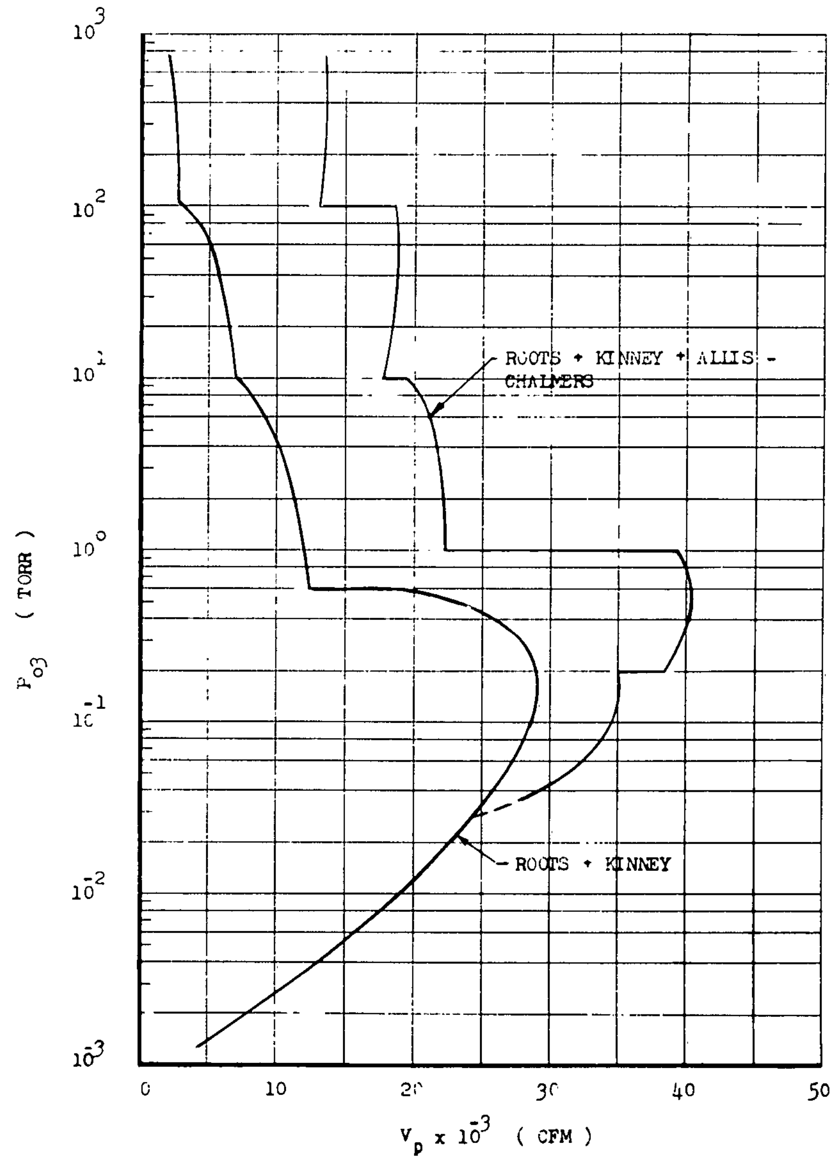

Figure 9. Vacuum Pump System Performance

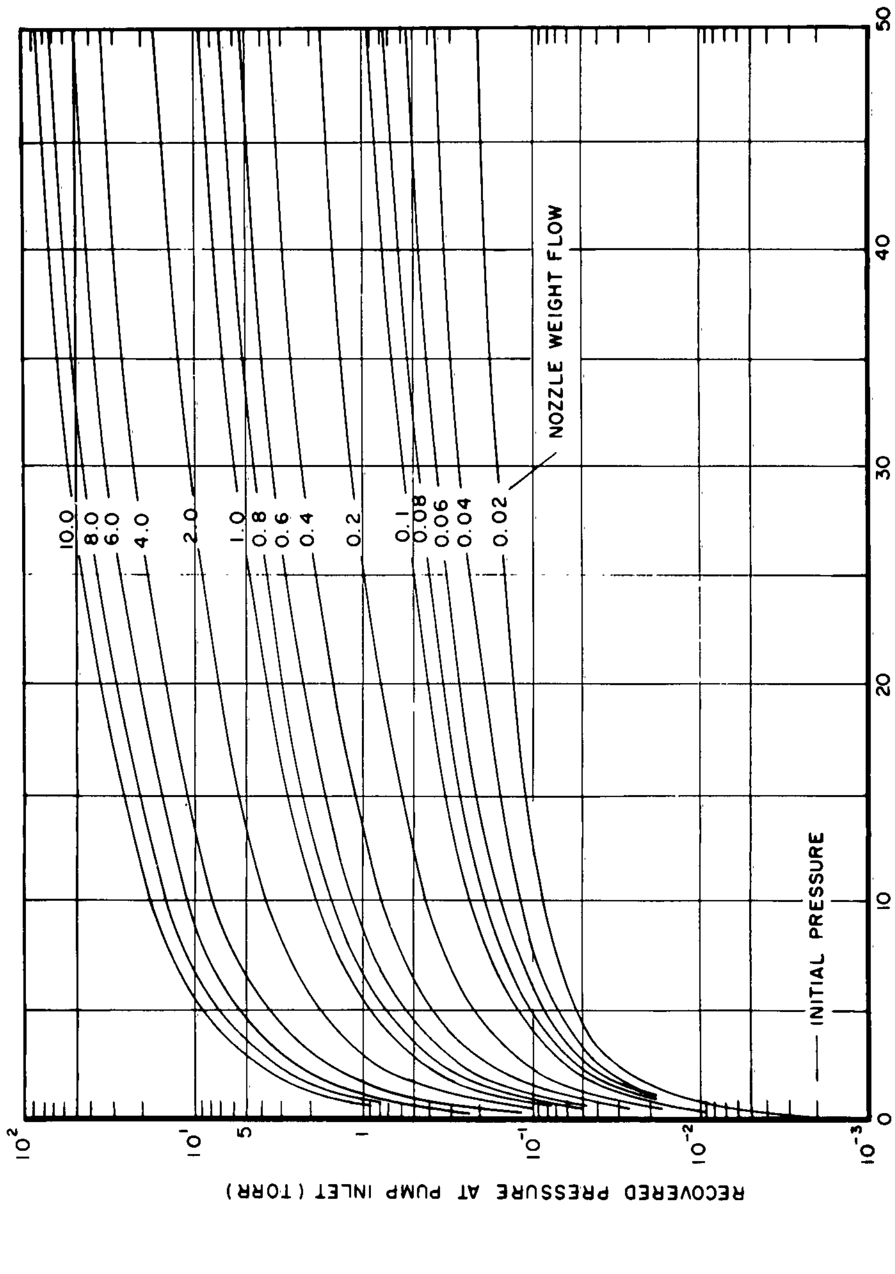

Figure 10. Running Time for Values of Nozzle Weight Flow Using the Root-Connersville and Kinney Pumps

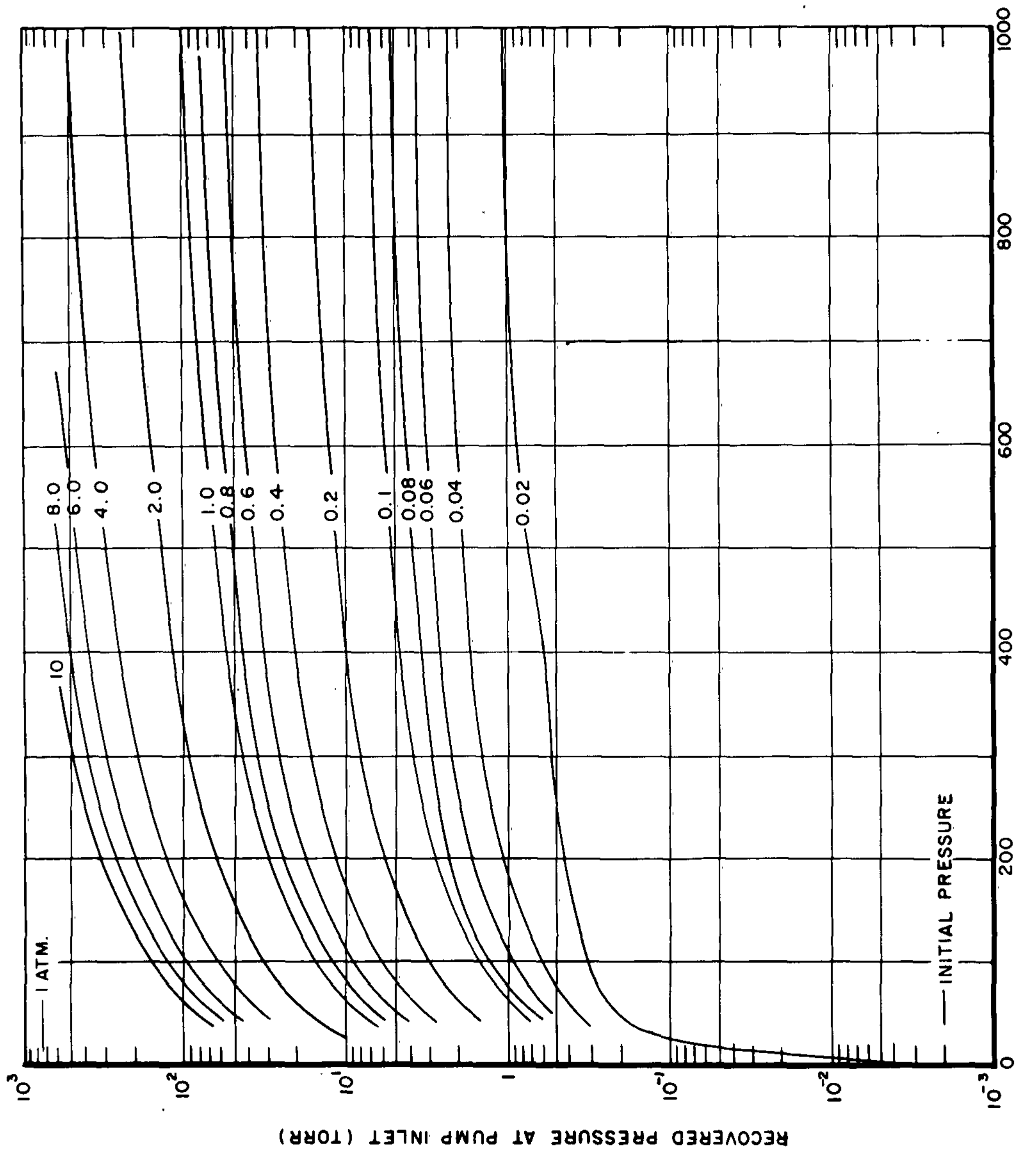

Figure 10 Cont'd

Figure 11 - Performance Curves For Mach 6 Nozzle

Nozzle Length:	81.185 inches
Throat Diameter:	1.260 inches
Exit Diameter:	12.580 inches

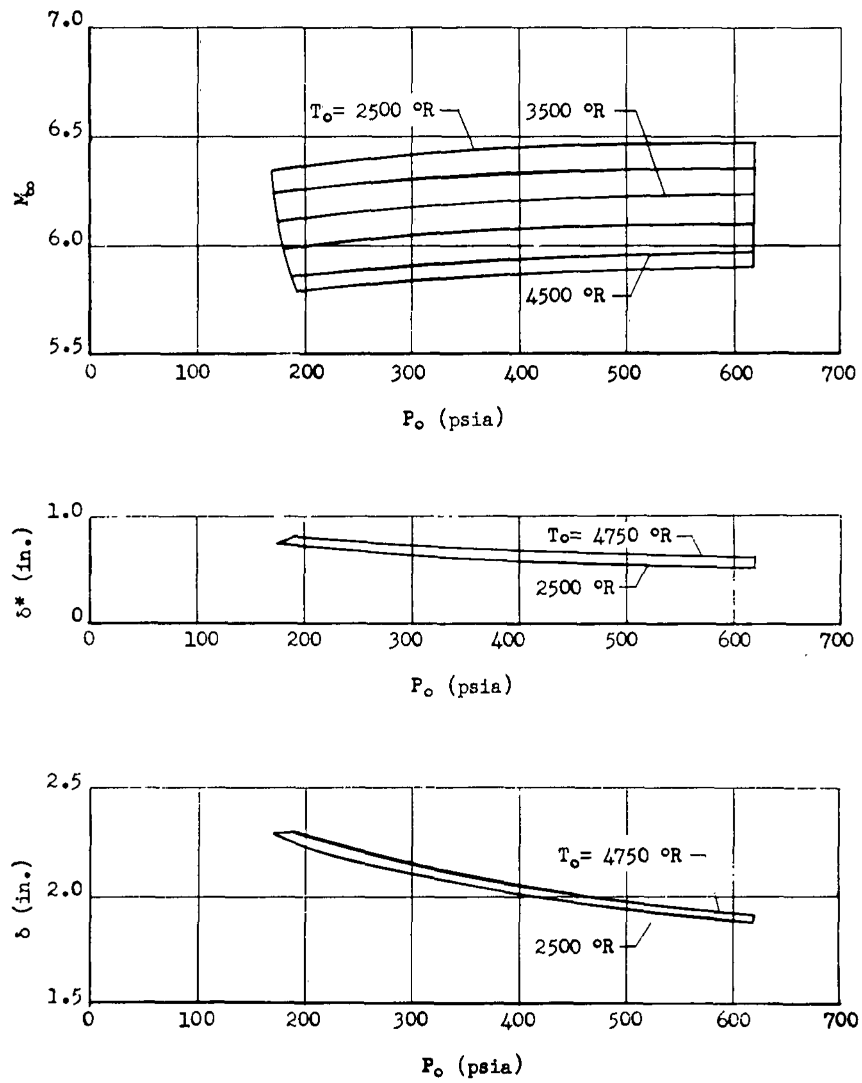

Figure 11 Cont'd

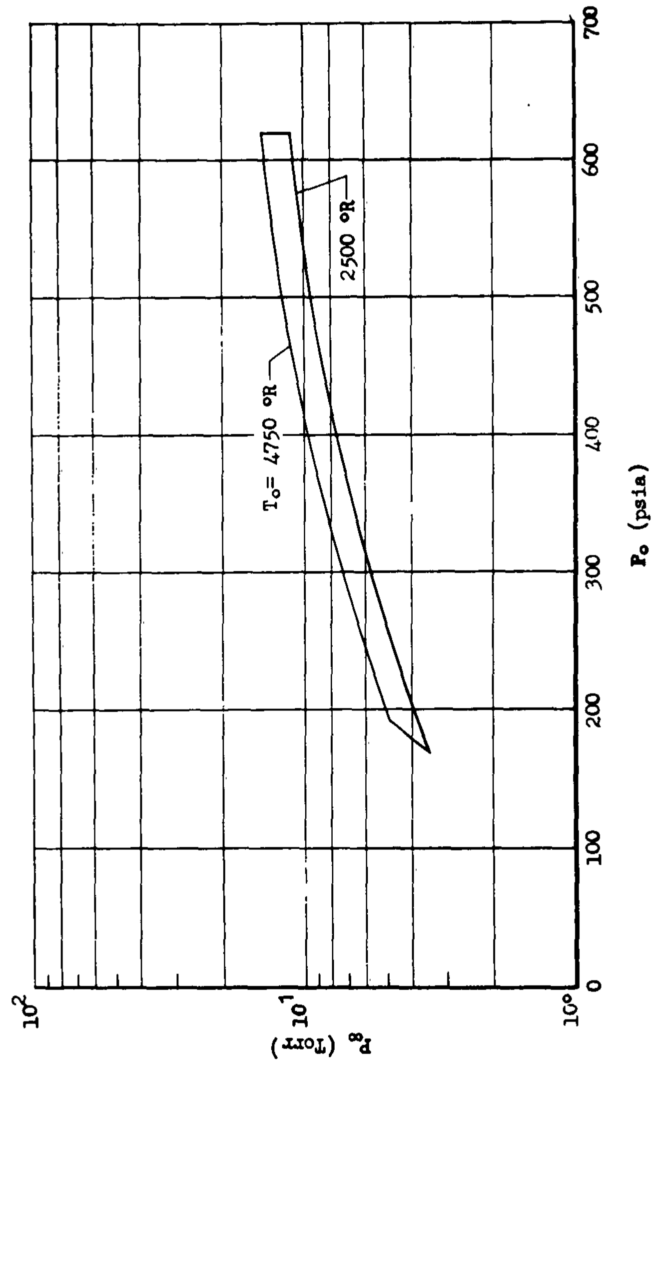

Figure 11 Cont'd

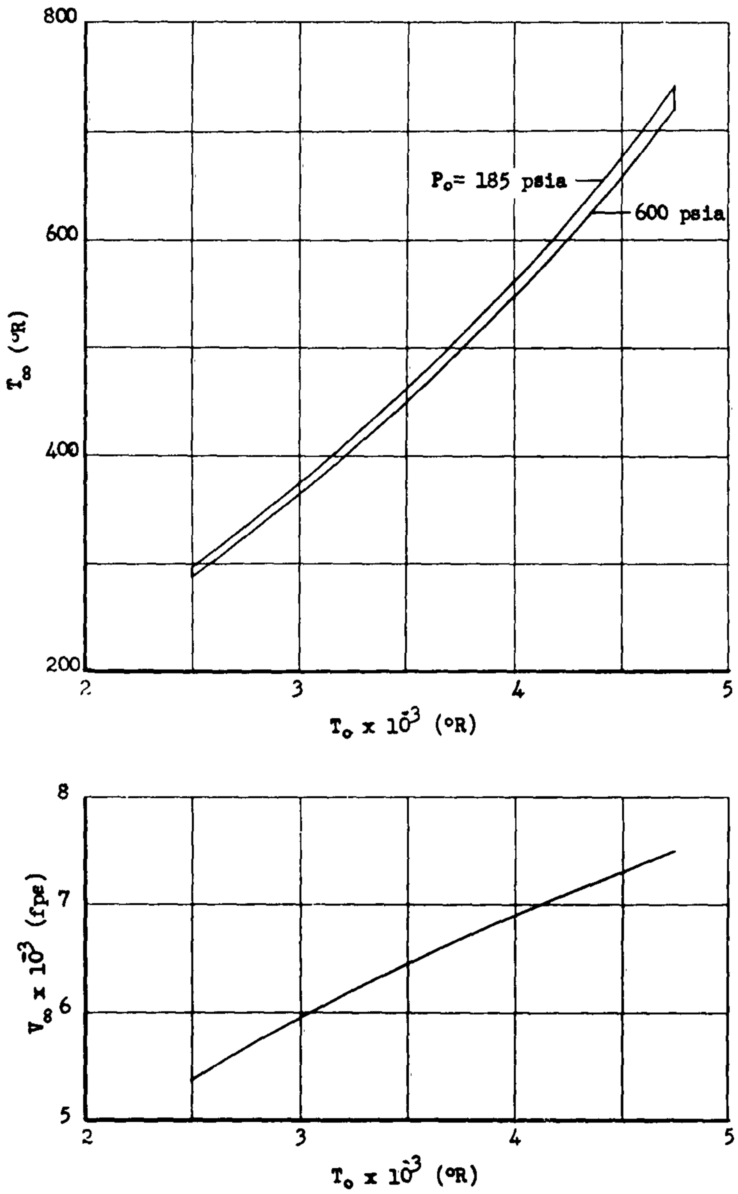

Figure 11 Cont'd

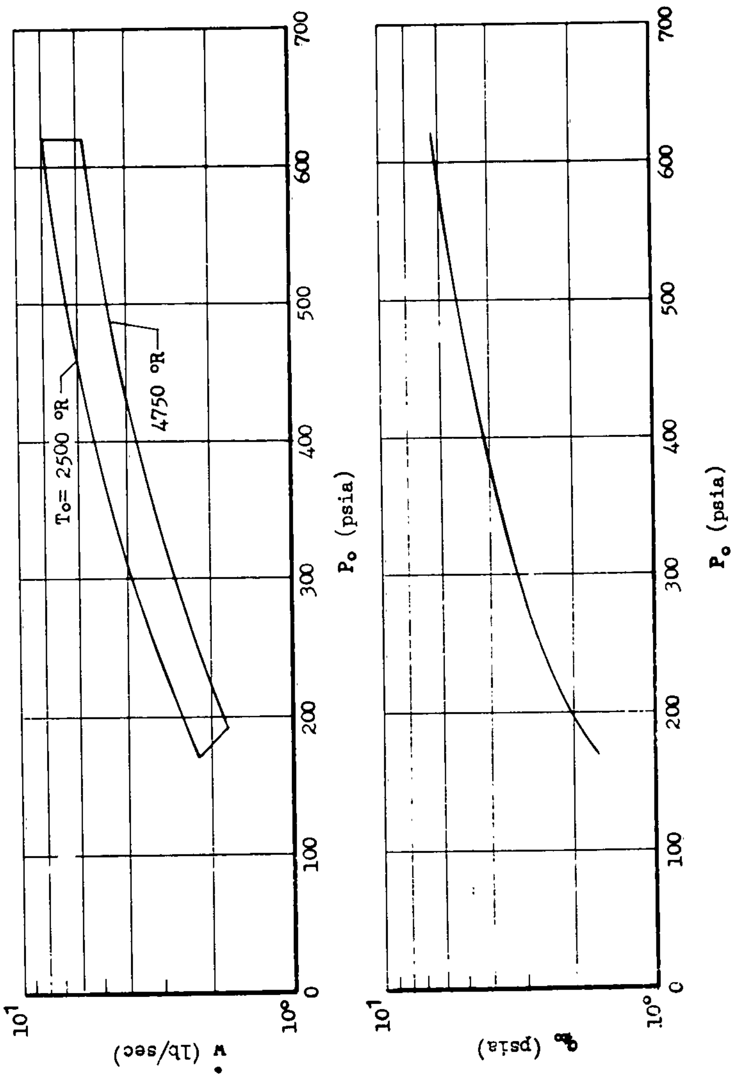

Figure 11 Cont'd

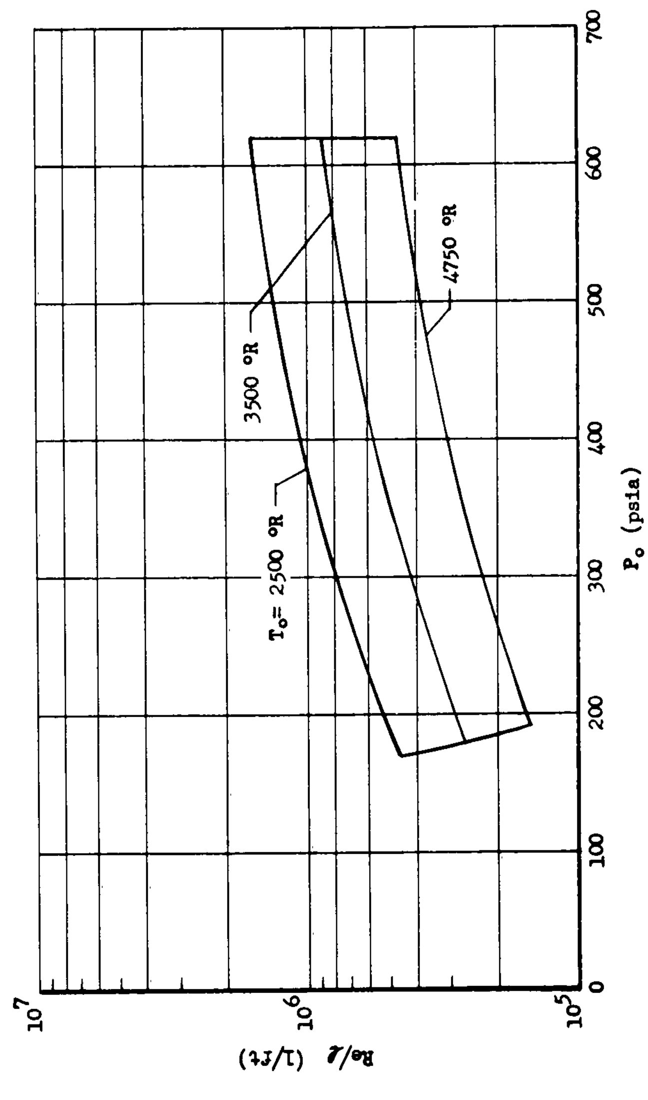

Figure 11 Cont'd

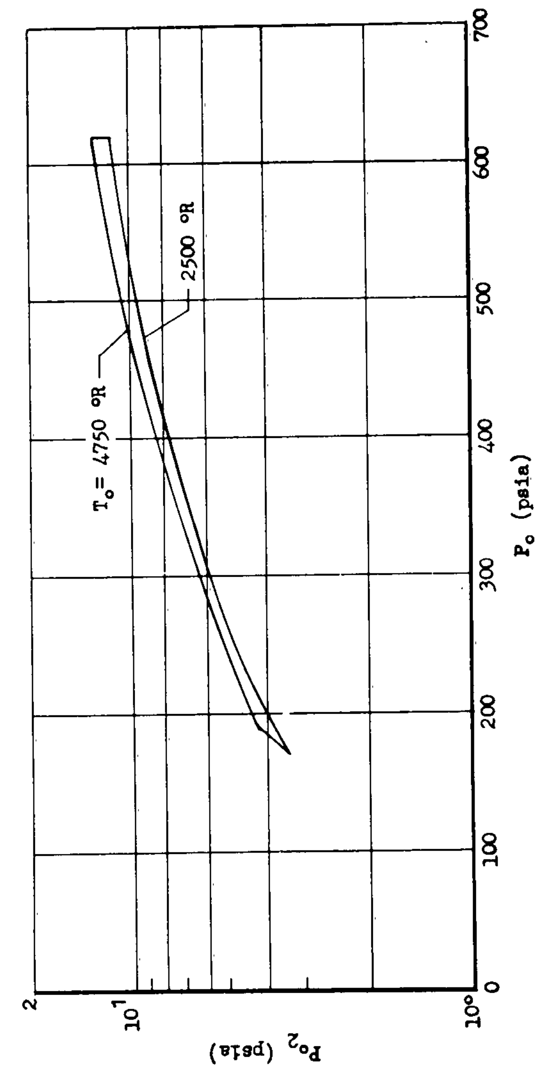

Figure 11 Cont'd

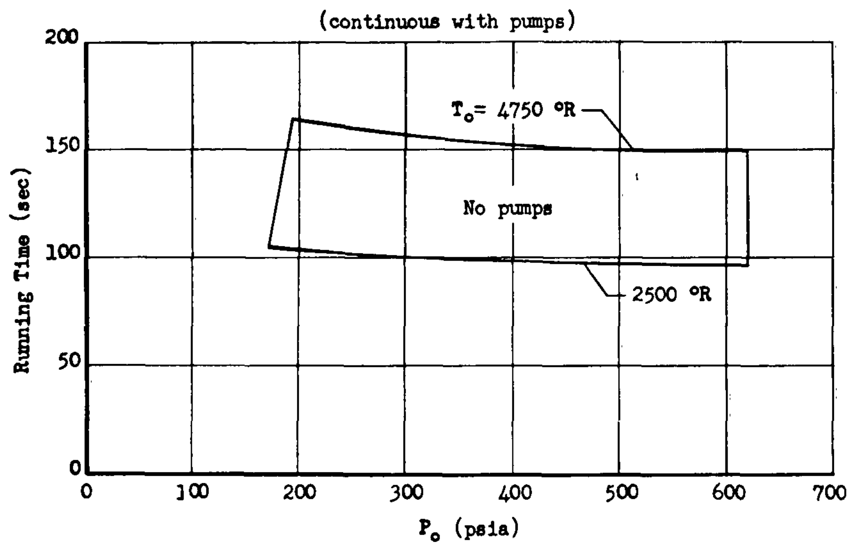

Figure 11 Cont'd

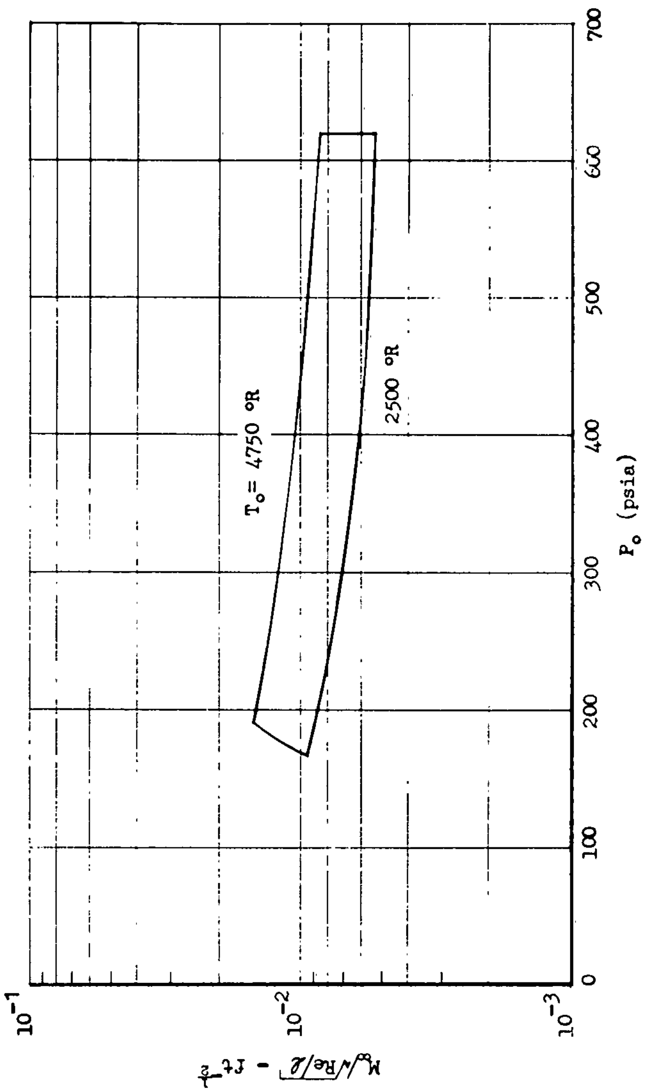

Figure 11 Cont'd

Figure 12 - Performance Curves For Mach 7 Nozzle

Nozzle Length: 81.185 inches
Throat Diameter: 1.260 inches
Exit Diameter: 16.520 inches

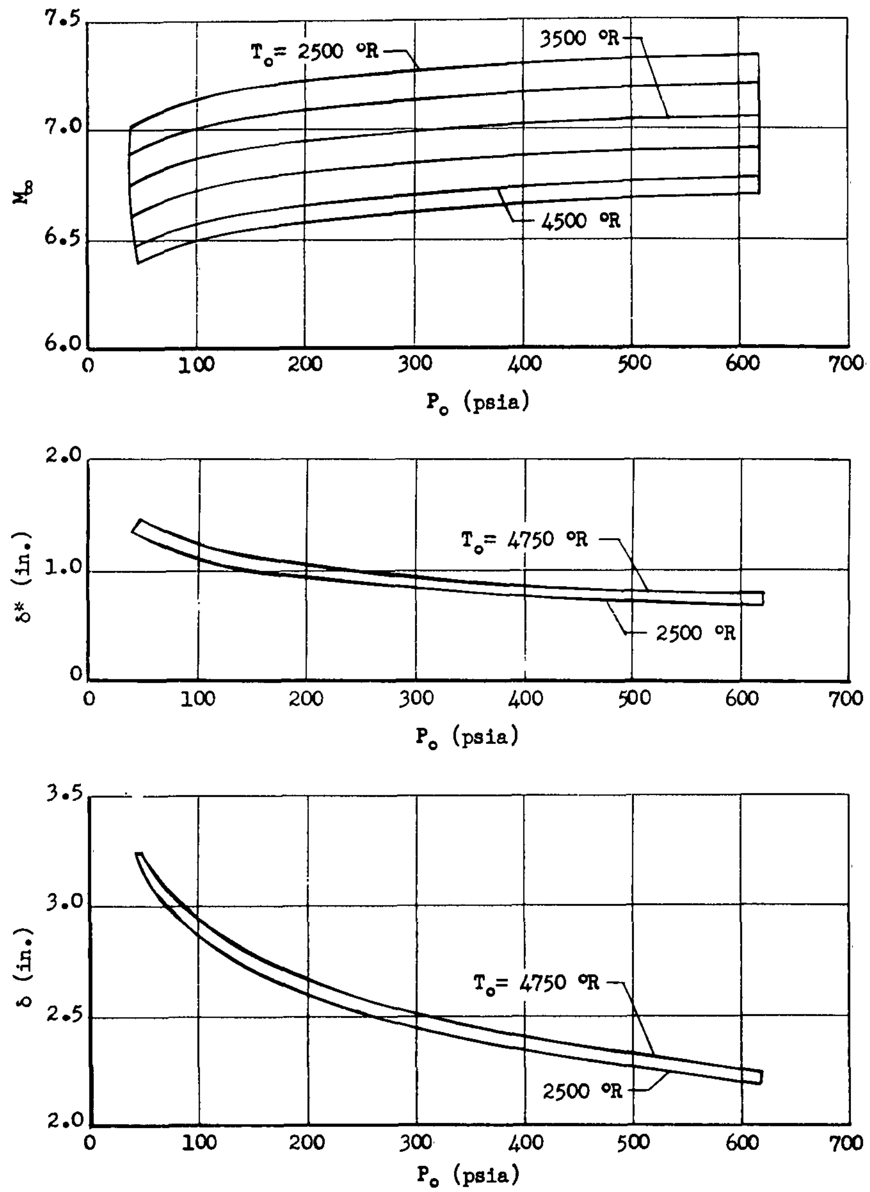

Figure 12 Cont'd

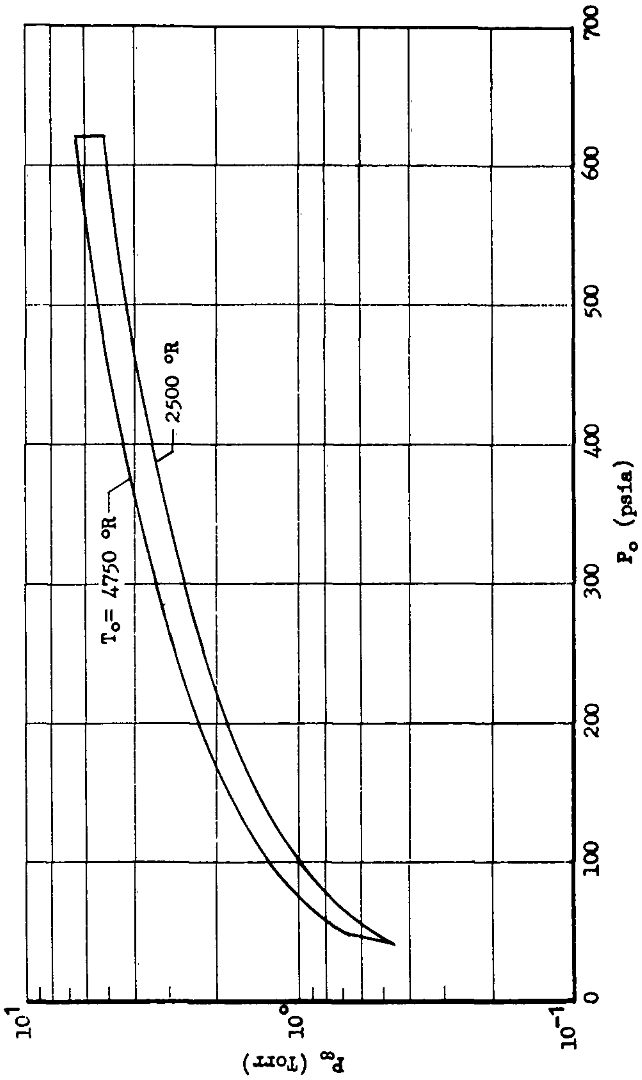

Figure 12 Cont'd

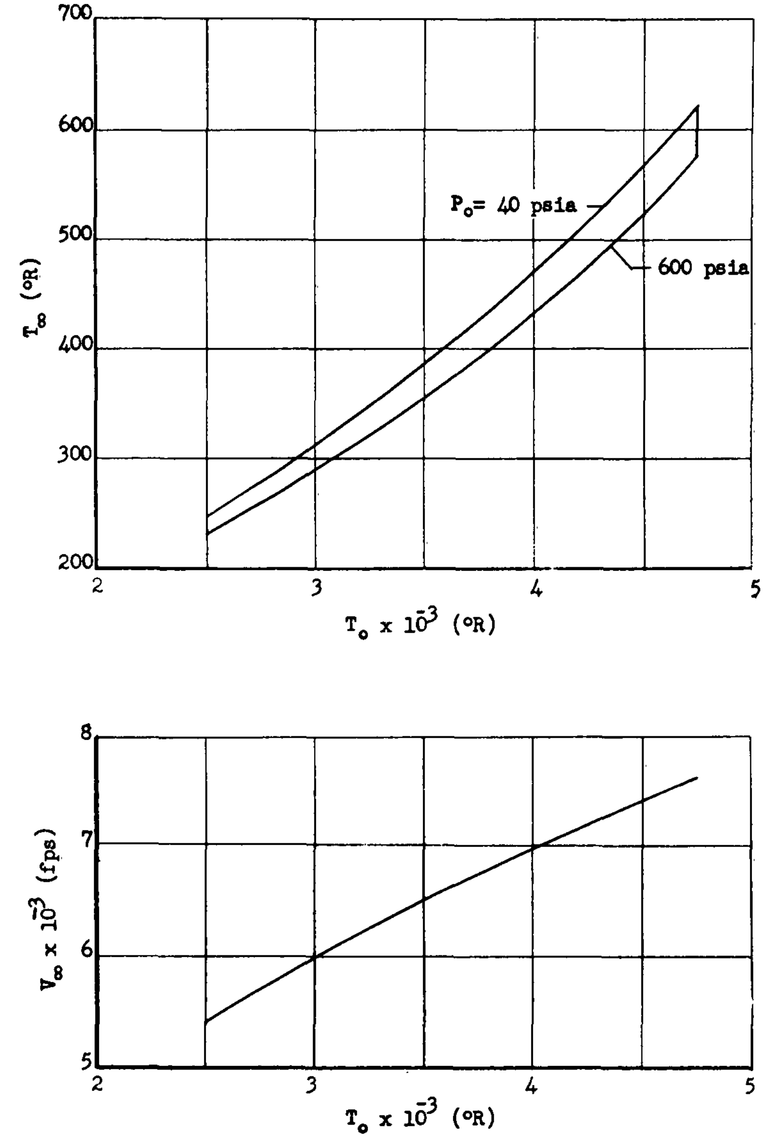

Figure 12 Cont'd

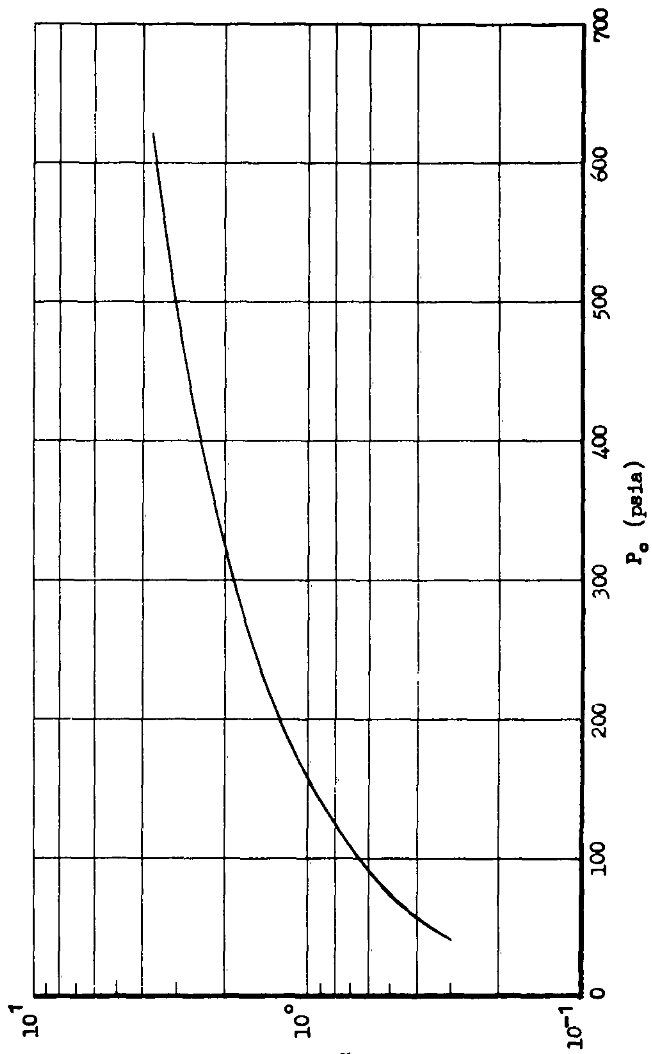

Figure 12 Cont'd

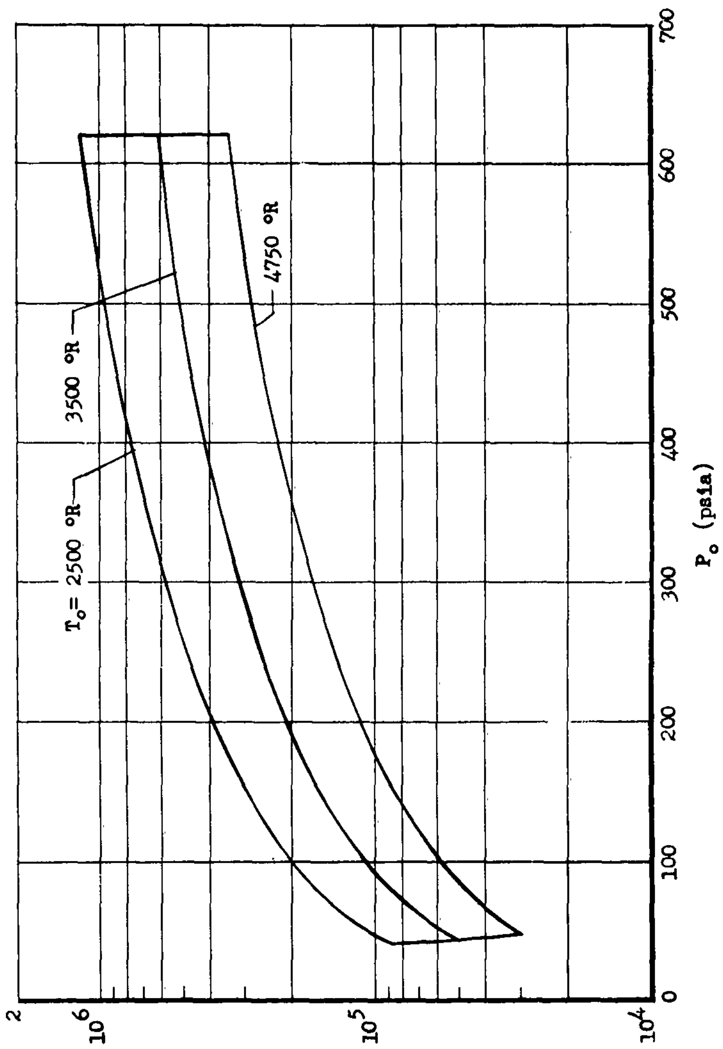

Figure 12 Cont'd

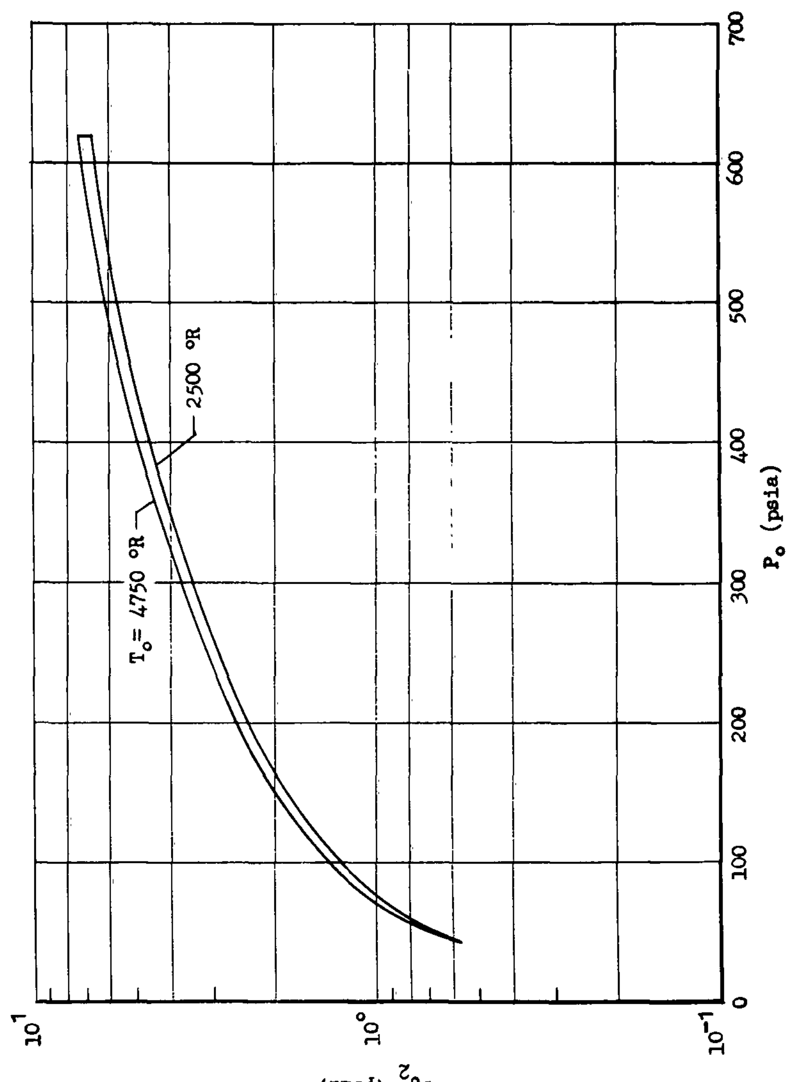

Figure 12 Cont'd

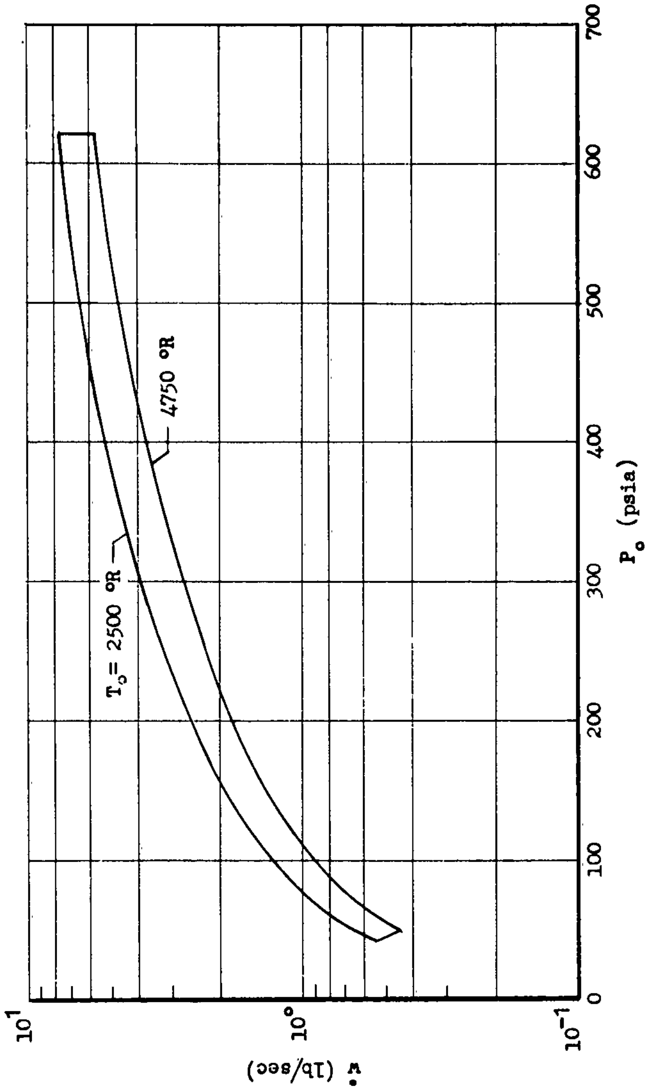

Figure 12 Cont'd

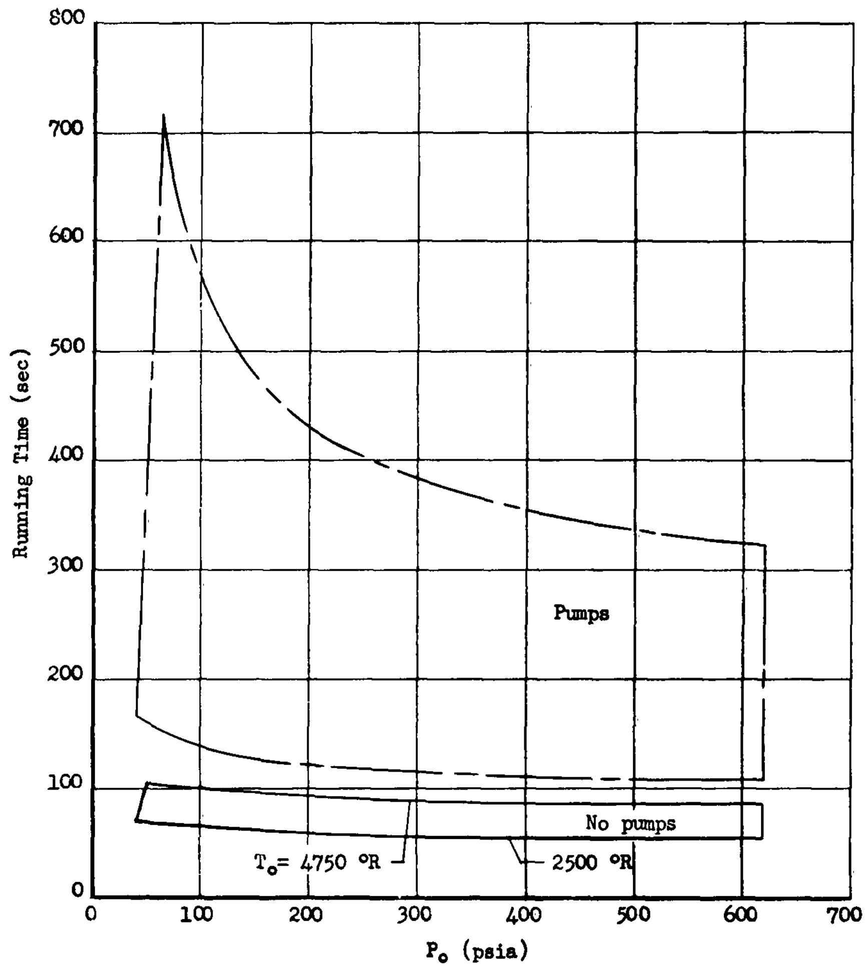

Figure 12 Cont'd

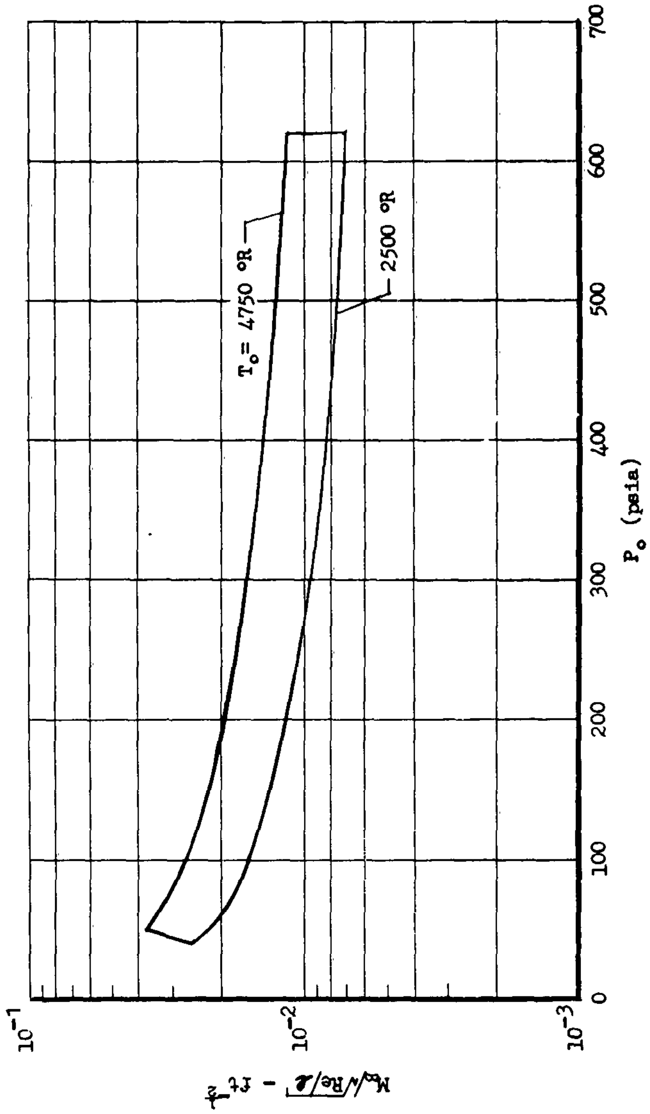

Figure 12 Cont'd

Figure 13 - Performance Curves For Mach 8 Nozzle

Nozzle Length:	81.185 inches
Throat Diameter:	1.260 inches
Exit Diameter:	24.000 inches

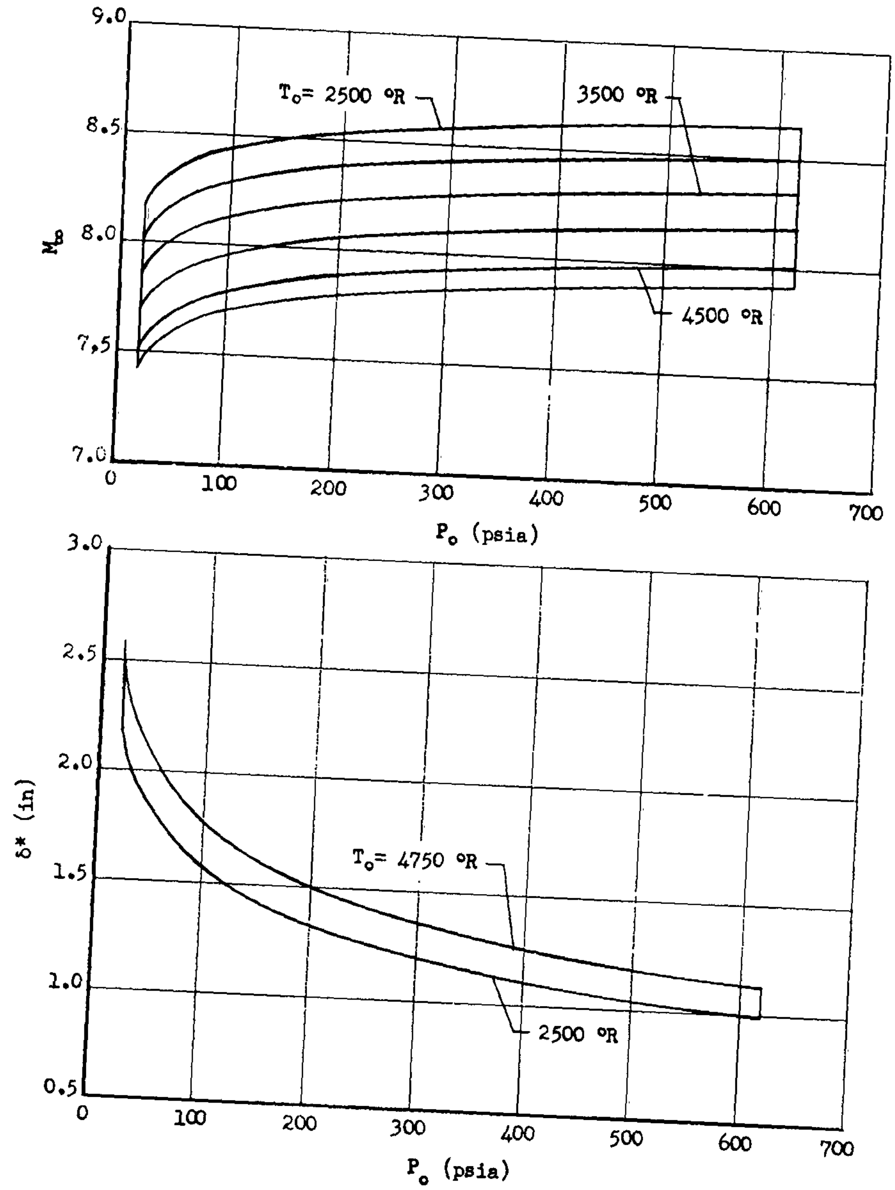

Figure 13 Cont'd

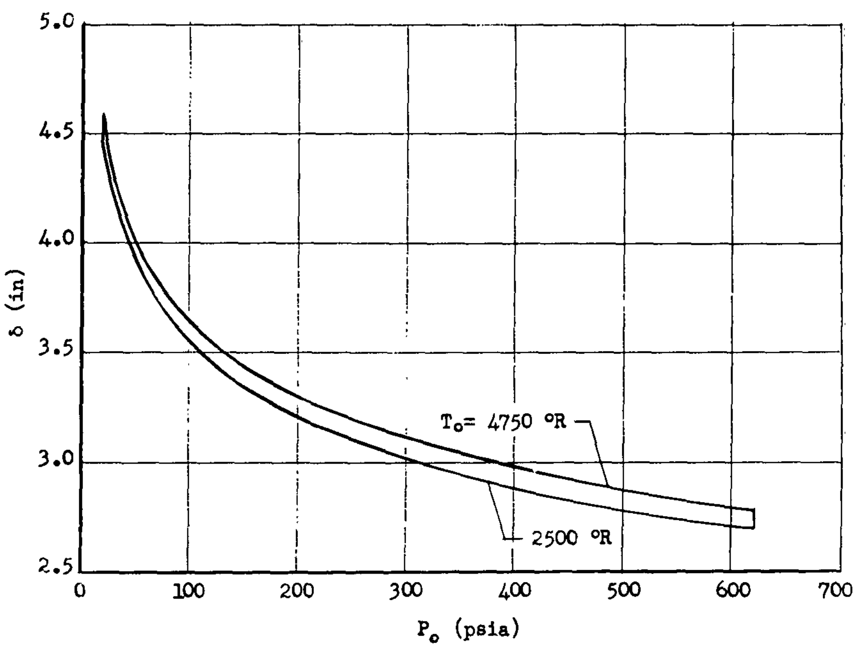

Figure 13 Cont'd

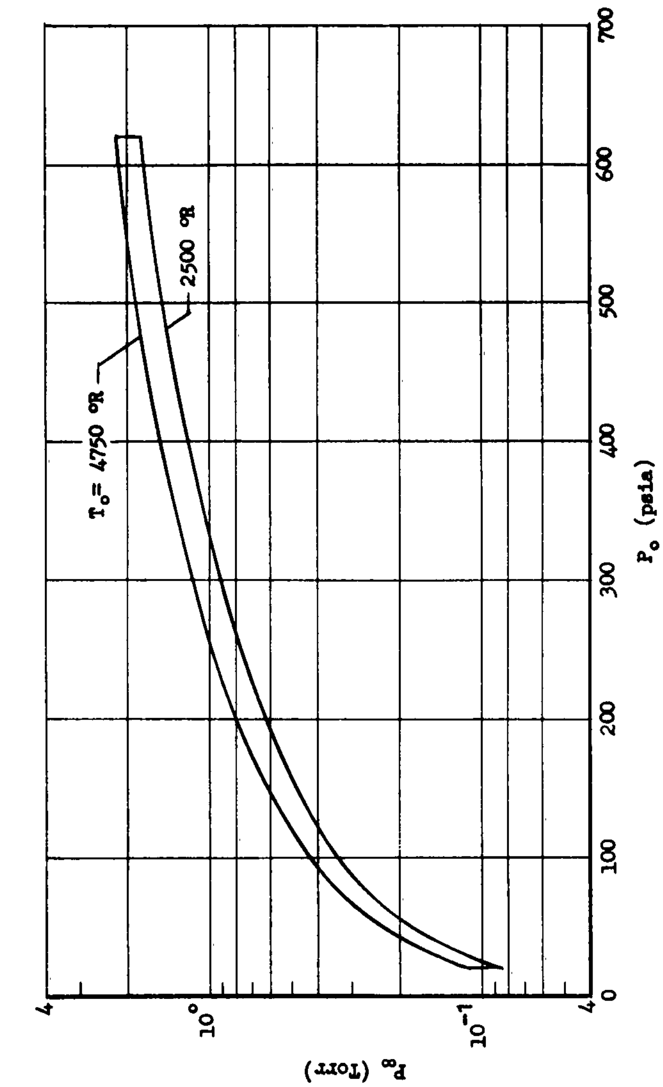

Figure 13 Cont'd

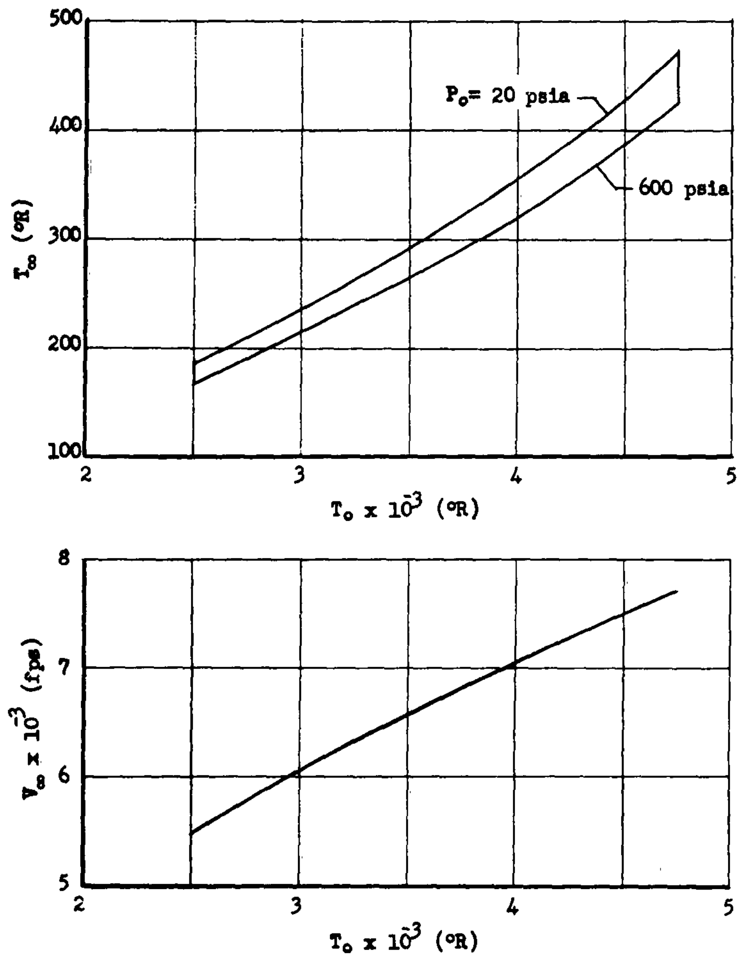

Figure 13 Cont'd

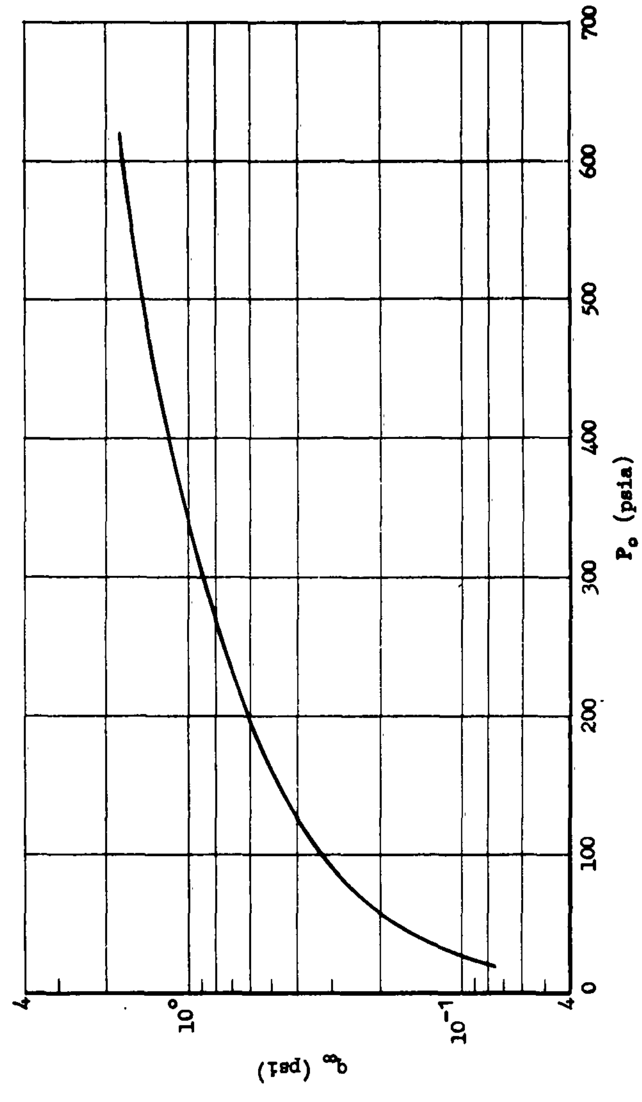

Figure 13 Cont'd

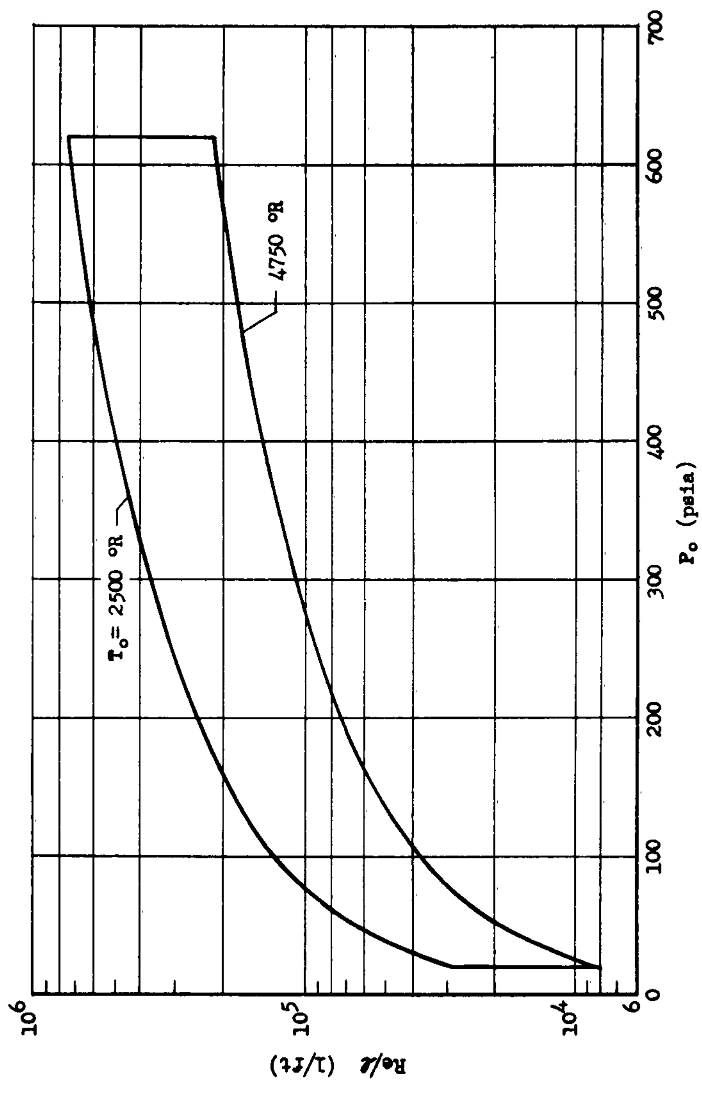

Figure 13 Cont'd

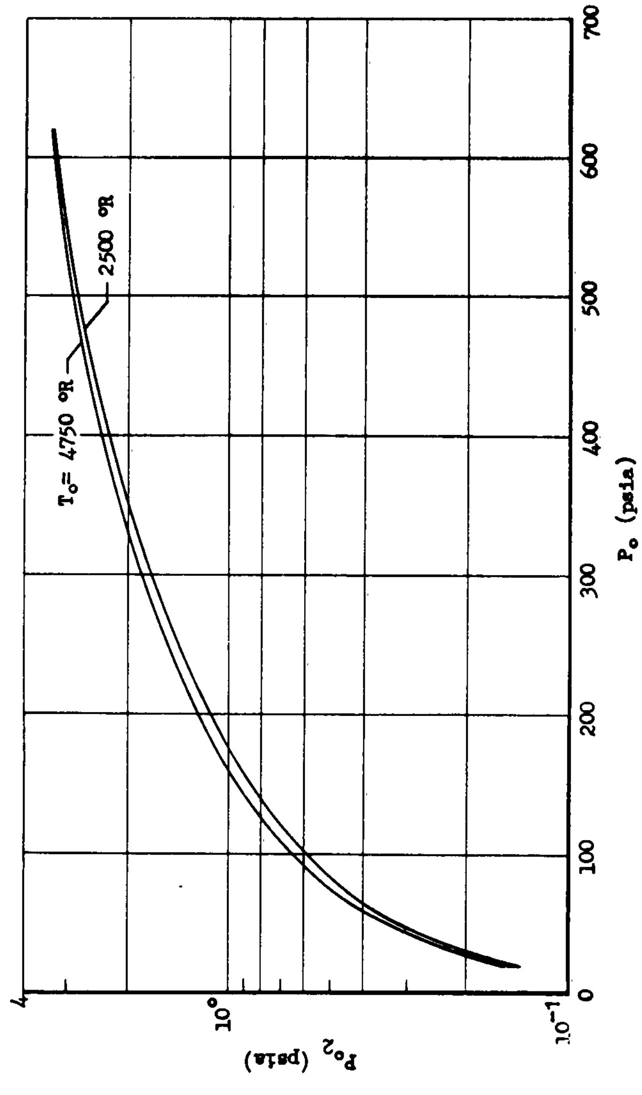

Figure 13 Cont'd

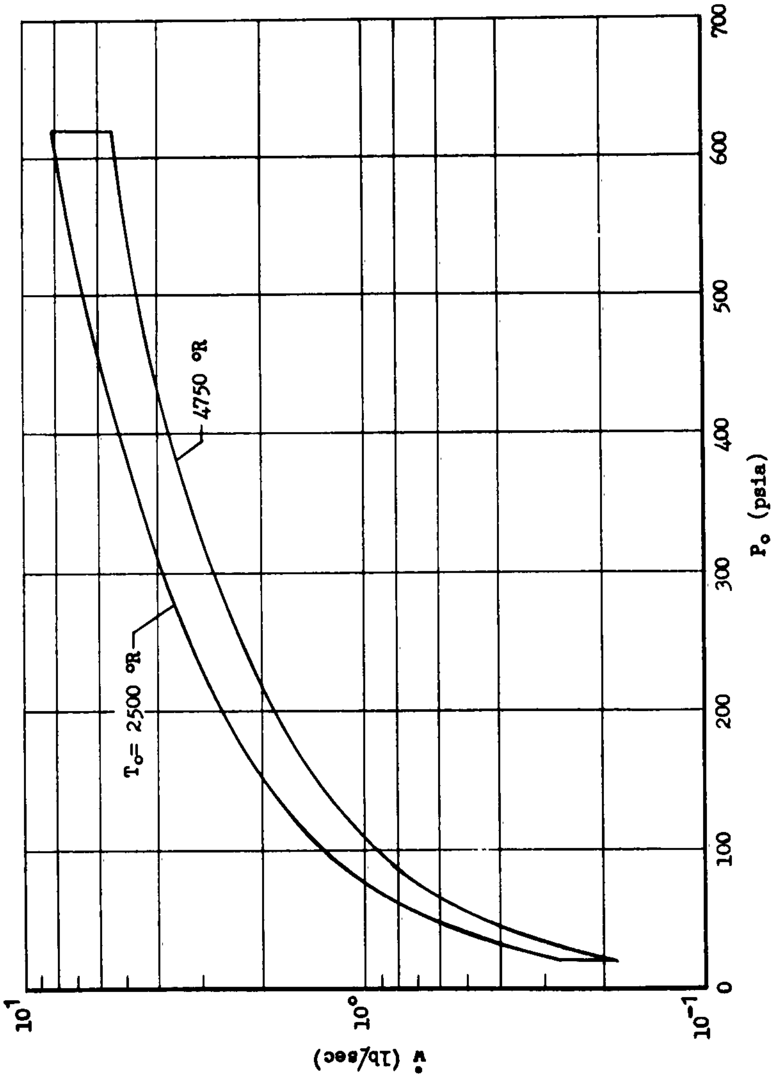

Figure 13 Cont'd

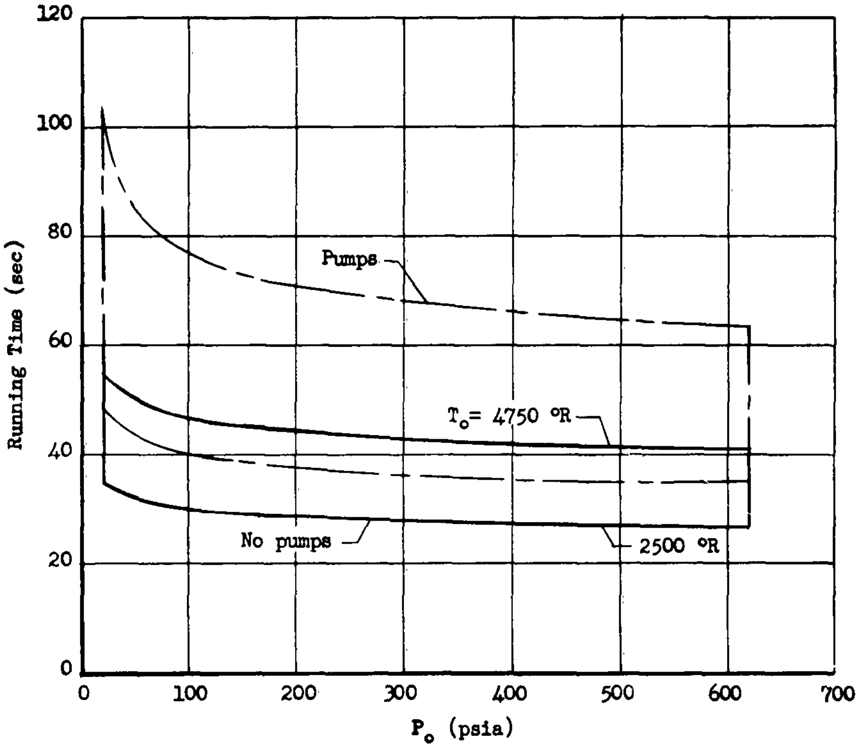

Figure 13 Cont'd

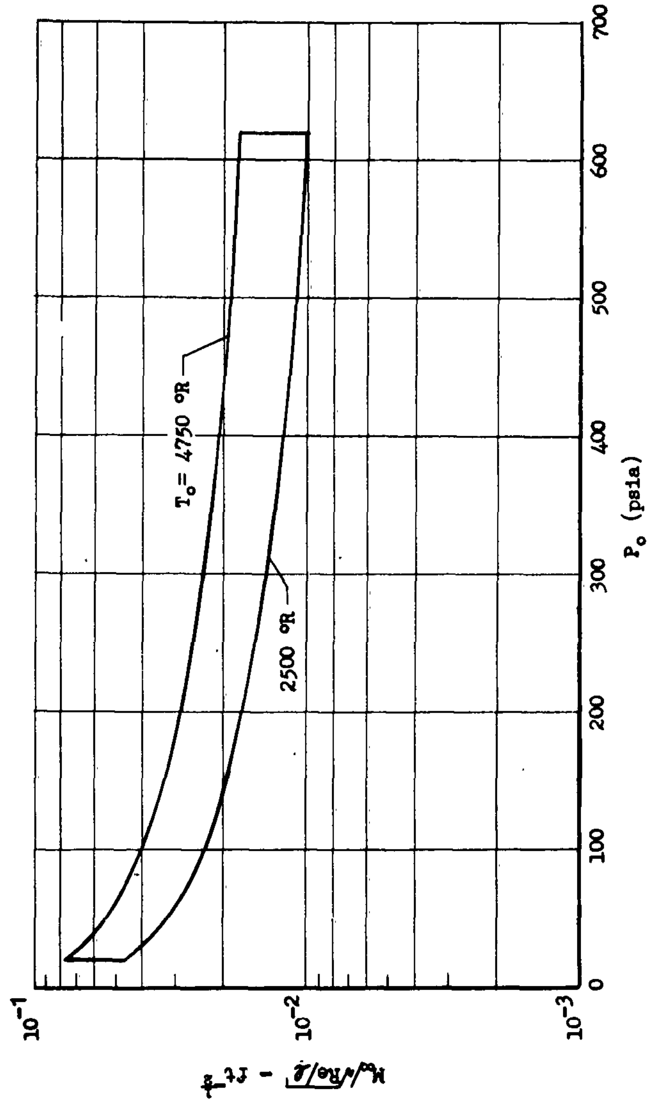

Figure 13 Cont'd

Figure 14 - Performance Curves For Mach 10 Nozzle

Nozzle Length:	81.185 inches
Throat Diameter:	0.807 inches
Exit Diameter:	24.000 inches

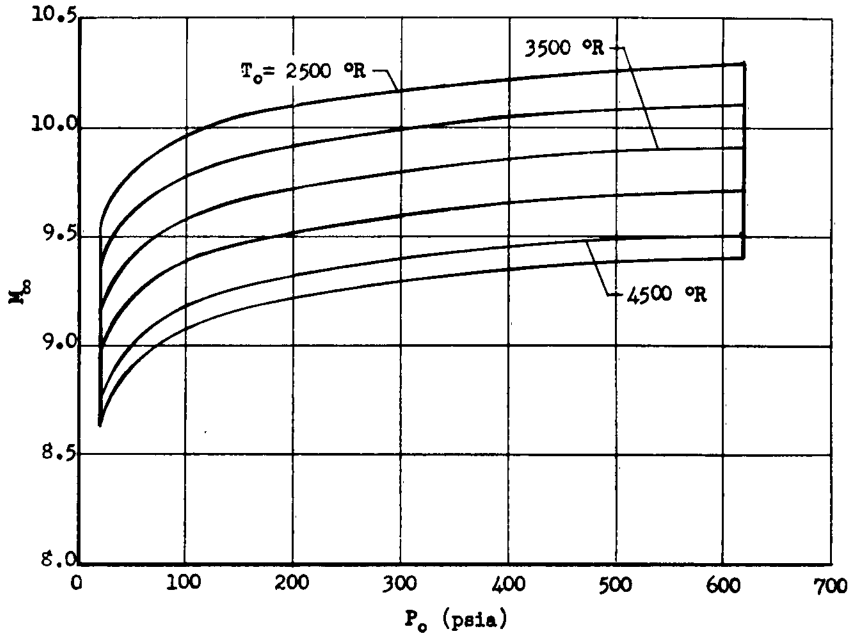

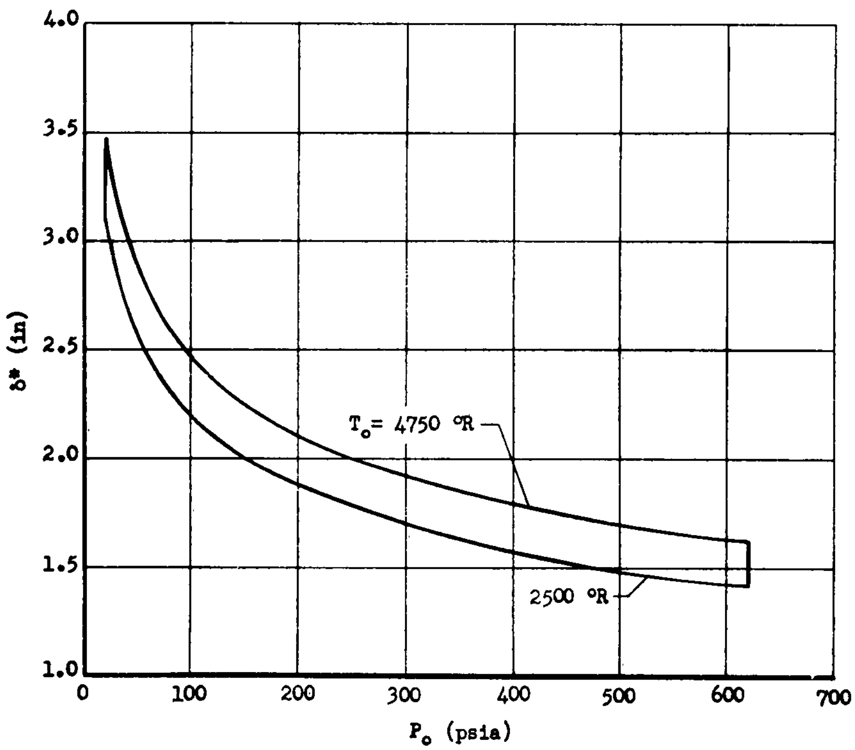

Figure 14 Cont'd

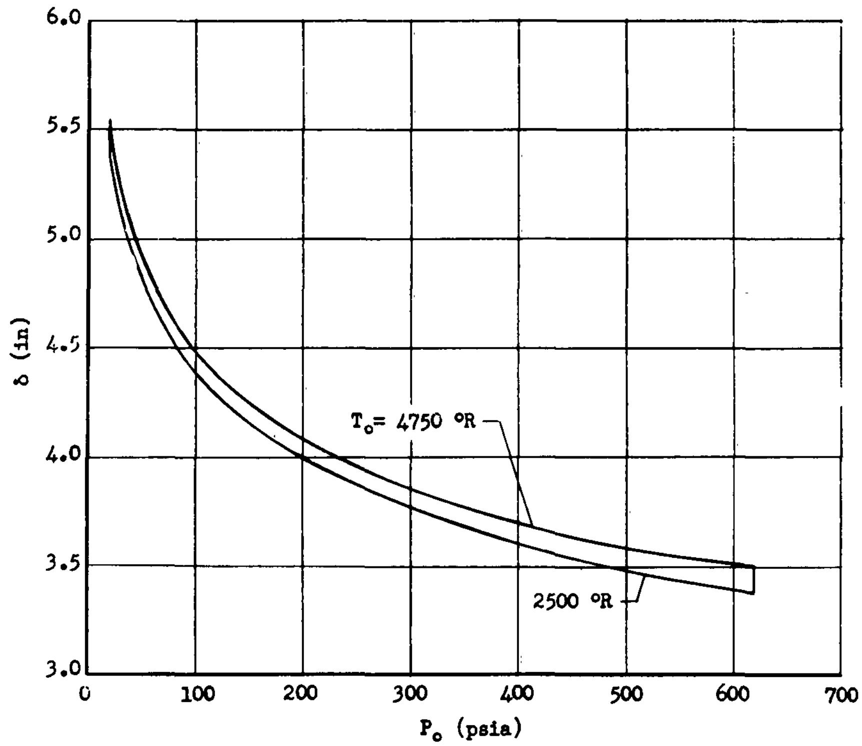

Figure 14 Cont'd

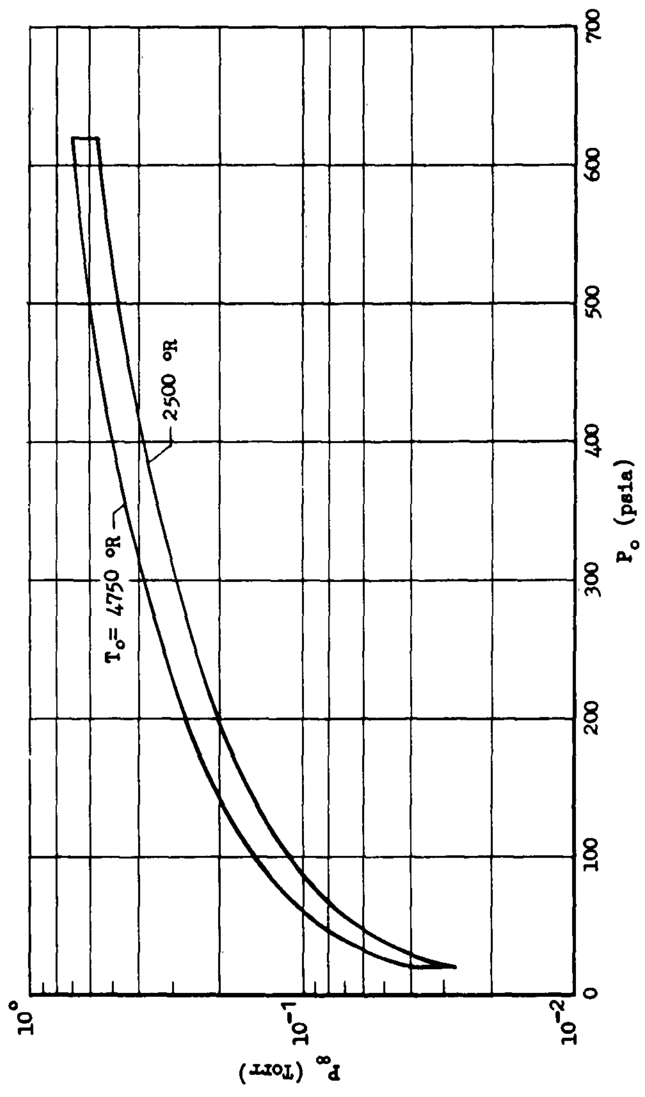

Figure 14 Cont'd

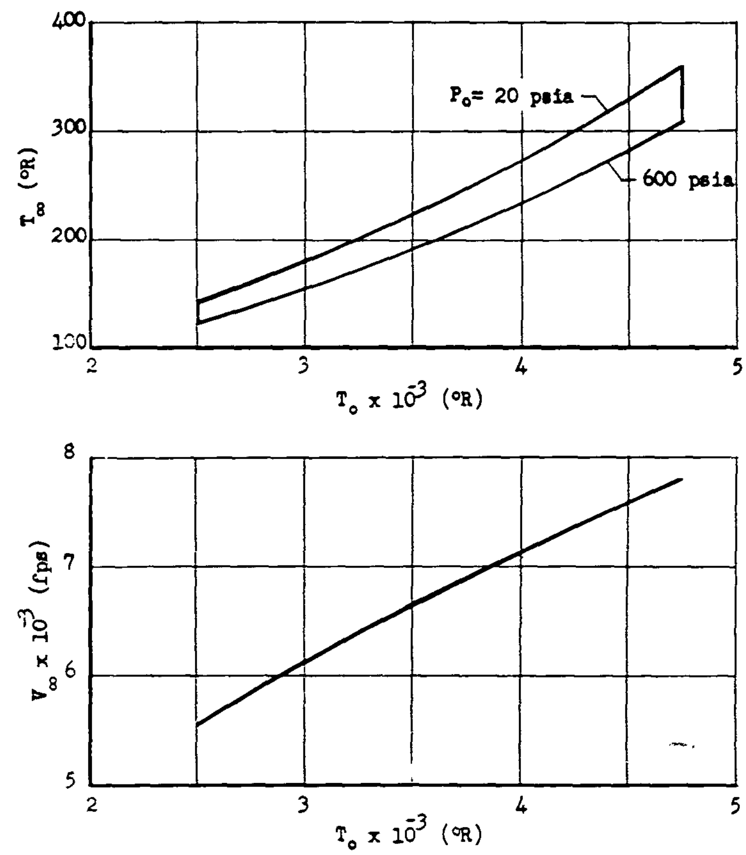

Figure 14 Cont'd

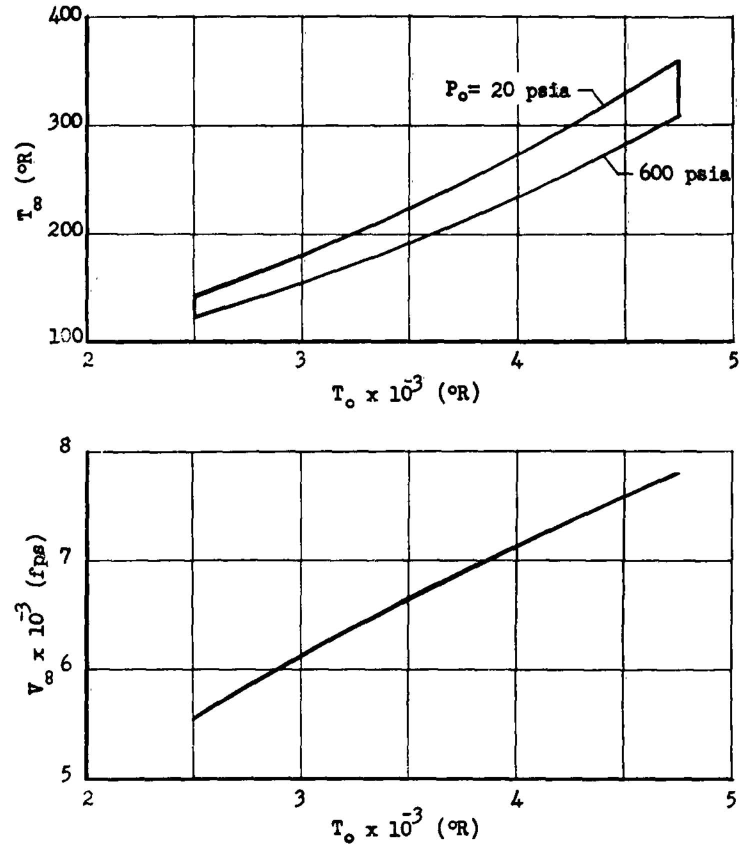

Figure 14 Cont'd

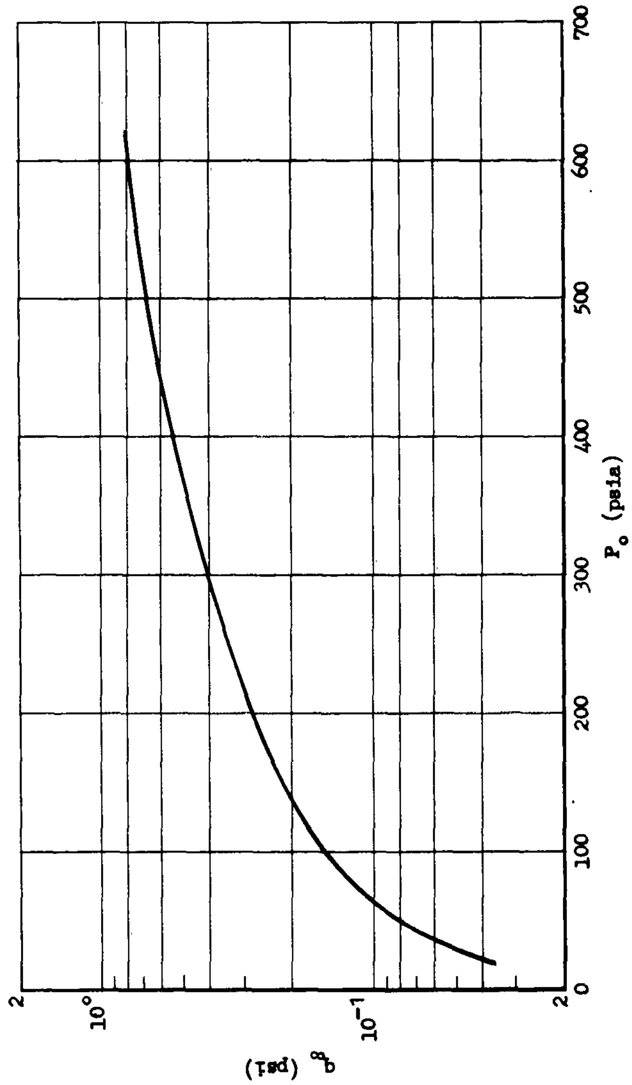

Figure 14 Cont'd

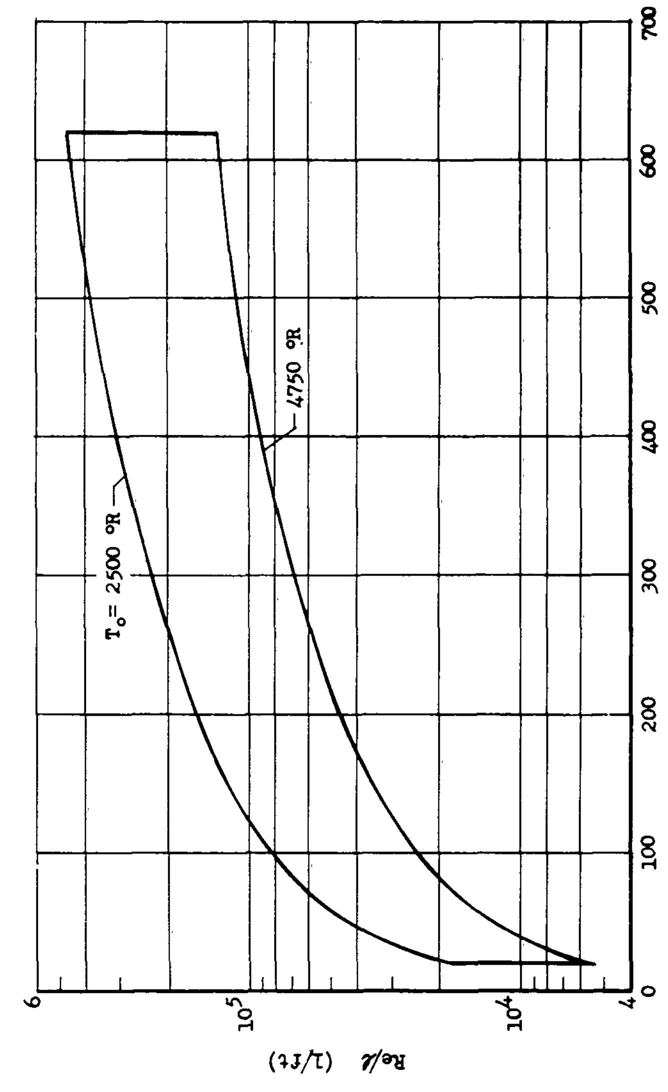

Figure 14 Cont'd

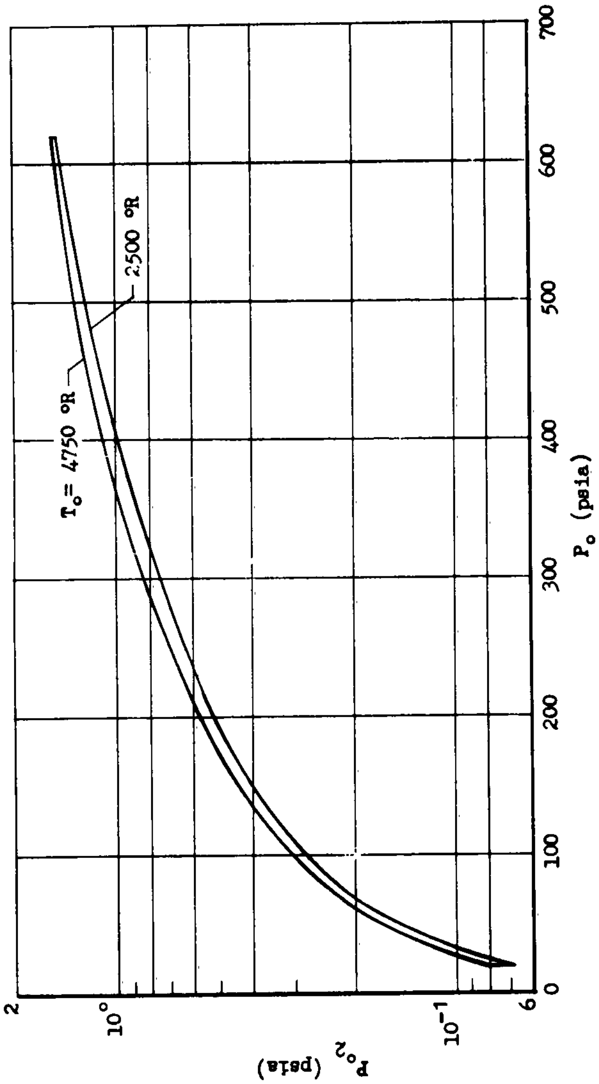

Figure 14 Cont'd

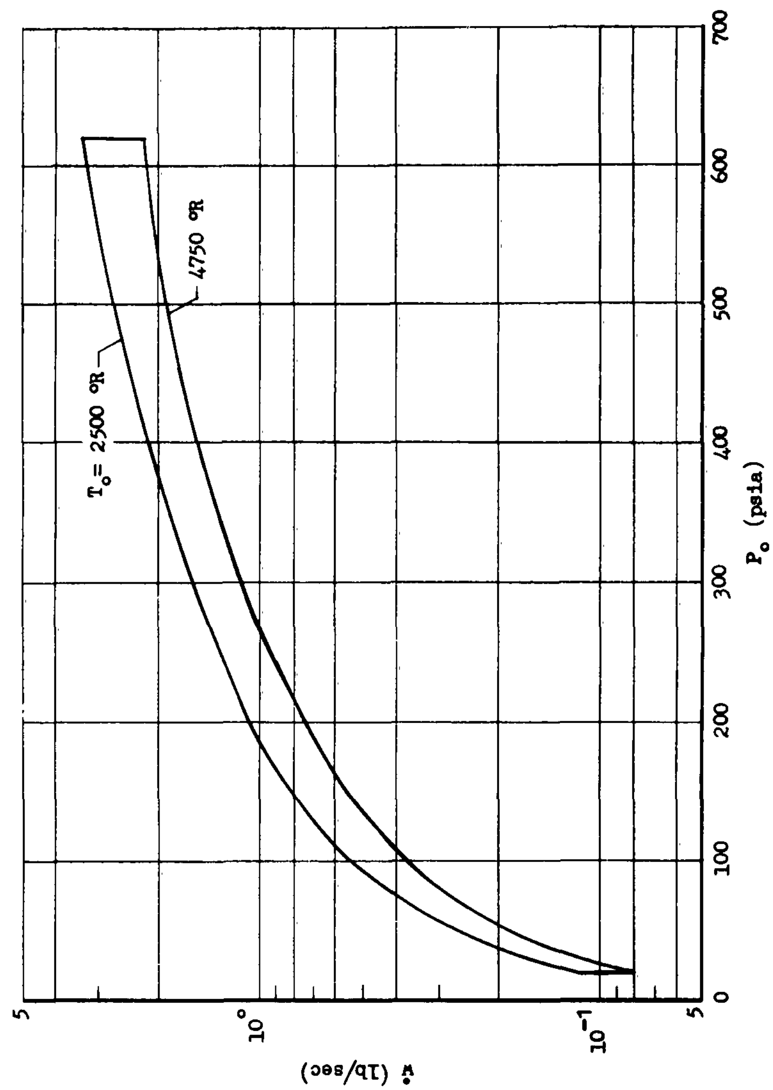

Figure 14 Cont'd

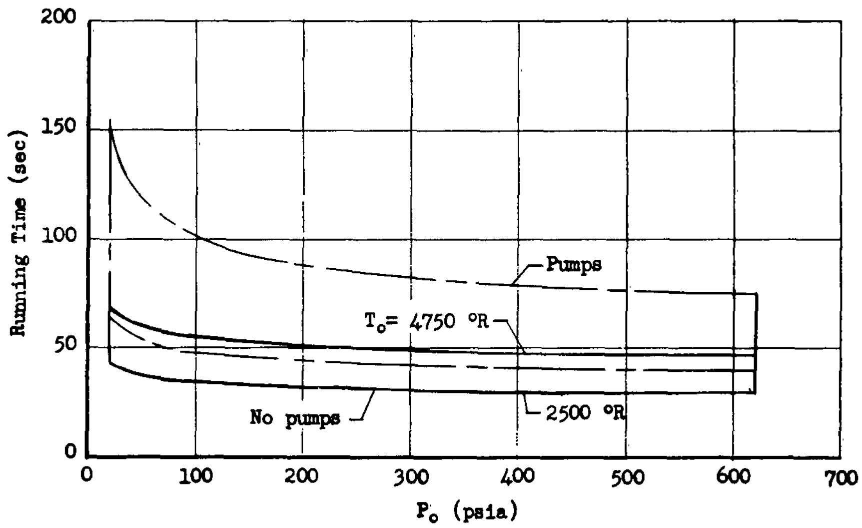

Figure 14 Cont'd

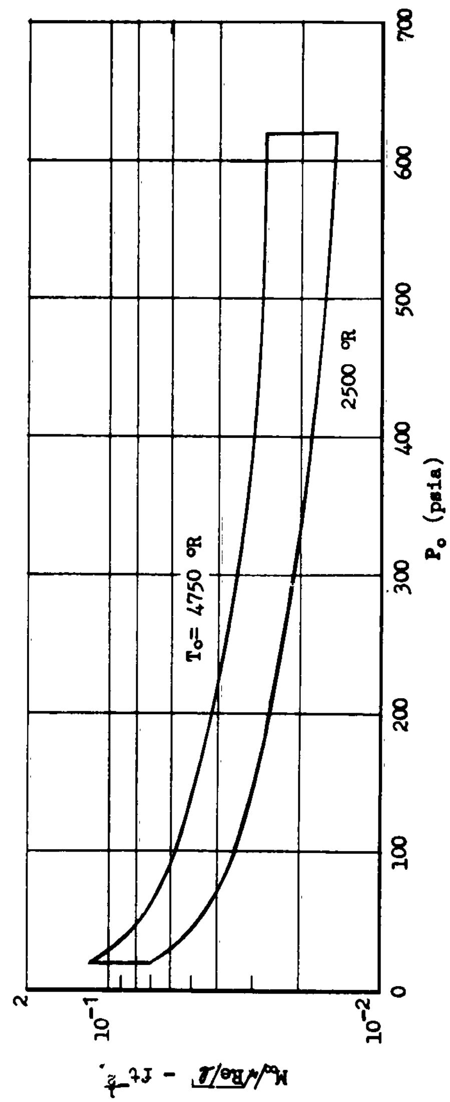

Figure 14 Cont'd

Figure 15 - Performance Curves For Mach 12 Nozzle

Nozzle Length:	81.185 inches
Throat Diameter:	0.447 inches
Exit Diameter:	24.000 inches

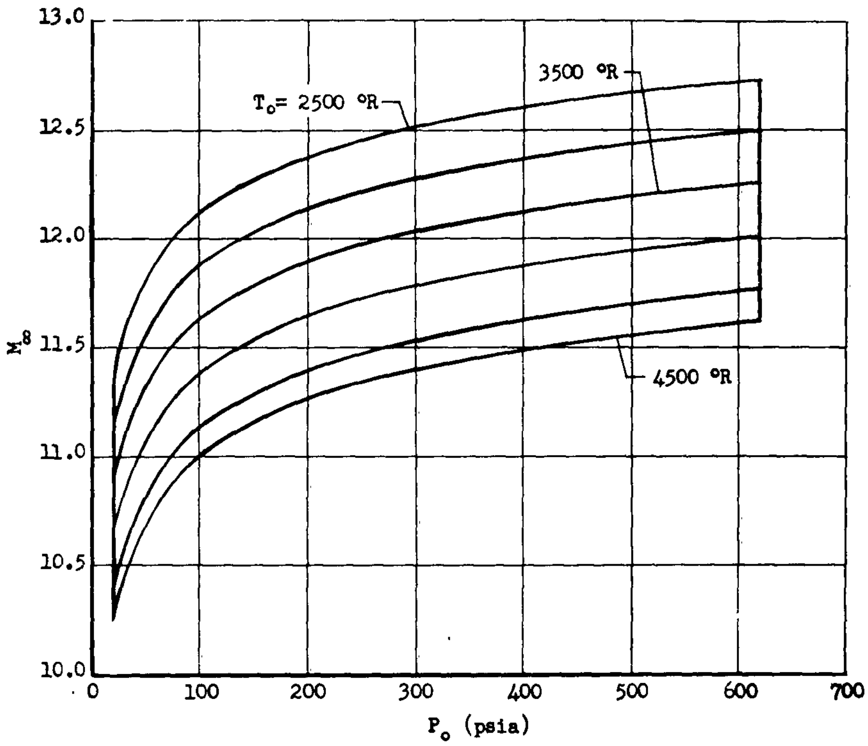

Figure 15 Cont'd

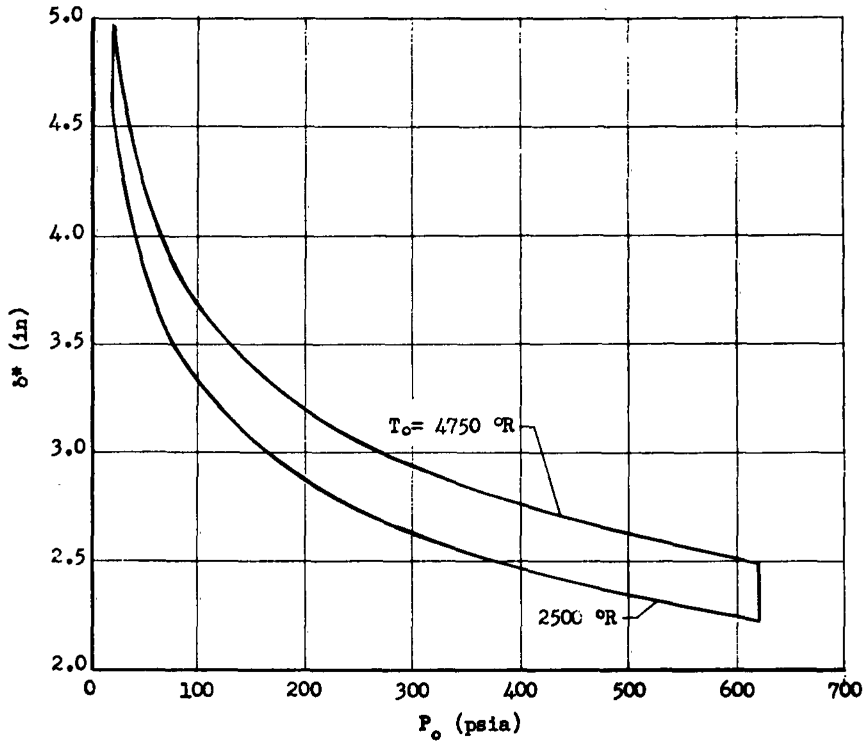

Figure 15 Cont'd

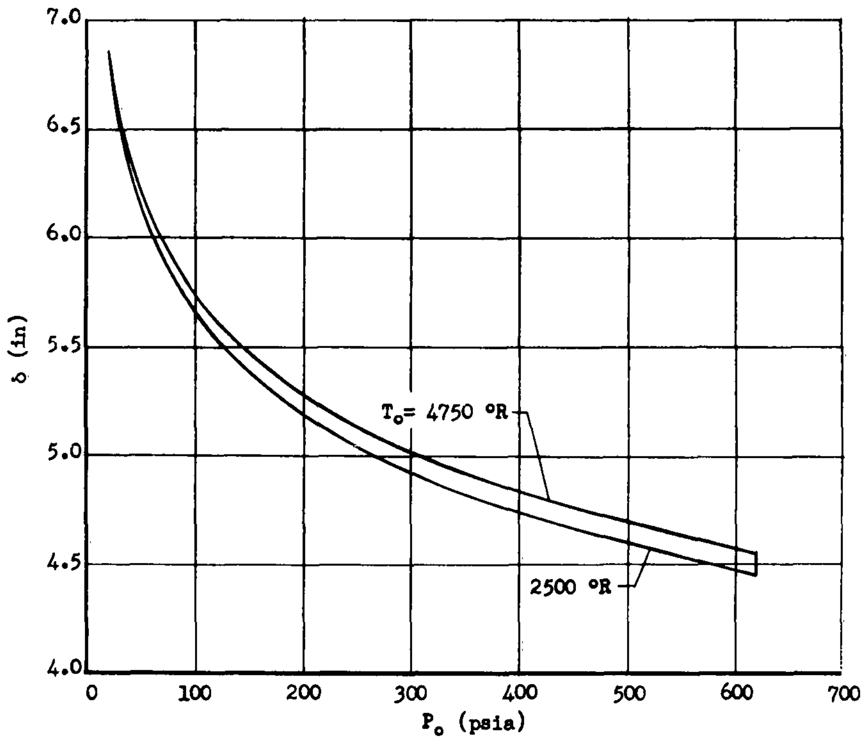

Figure 15 Cont'd

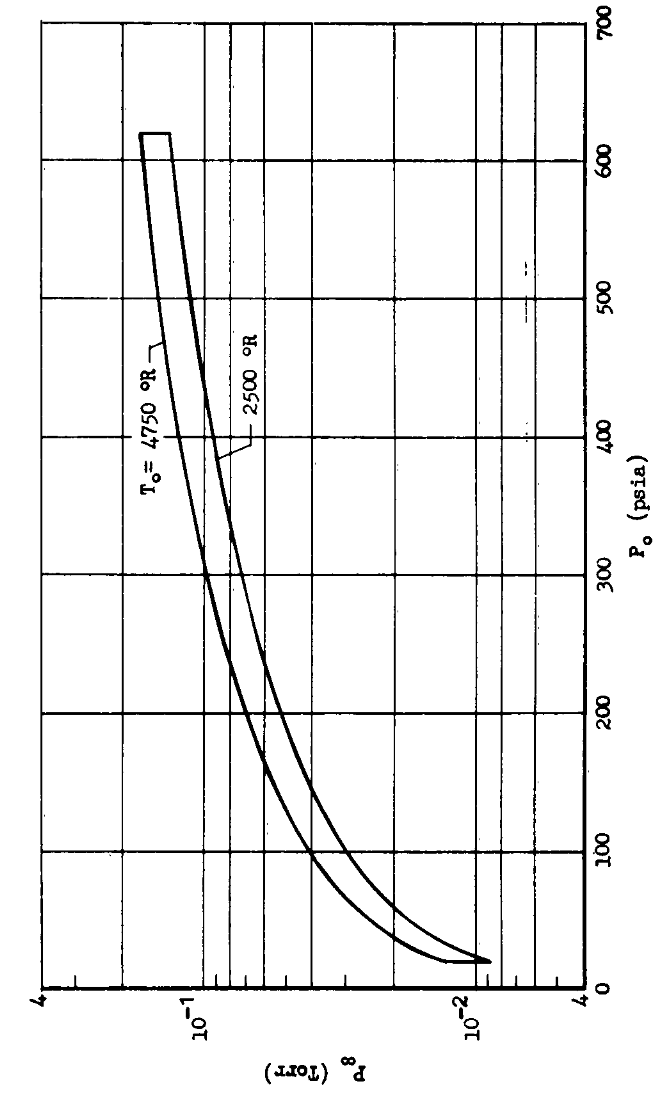

Figure 15 Cont'd

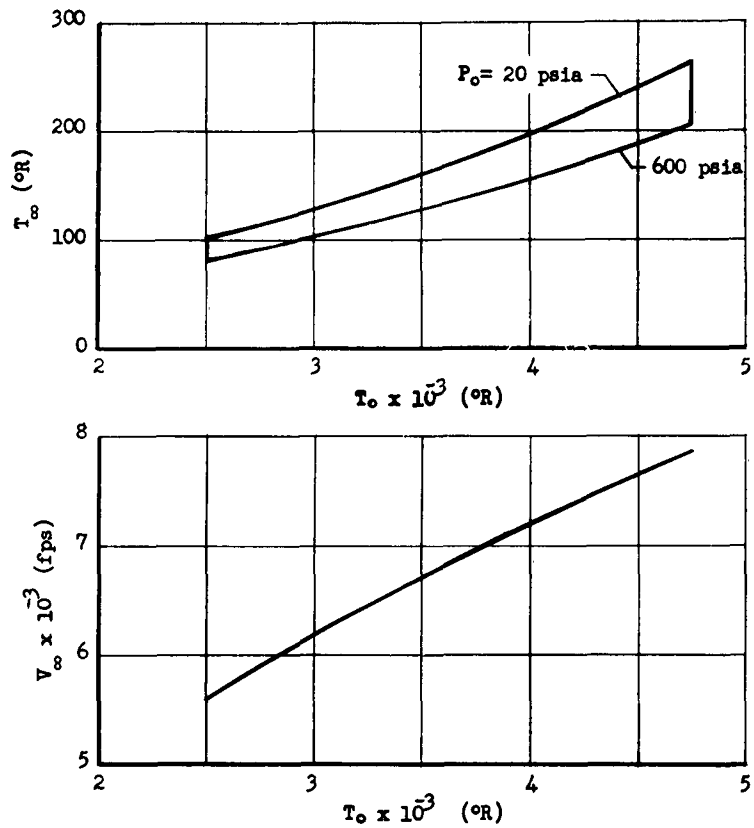

Figure 15 Cont'd

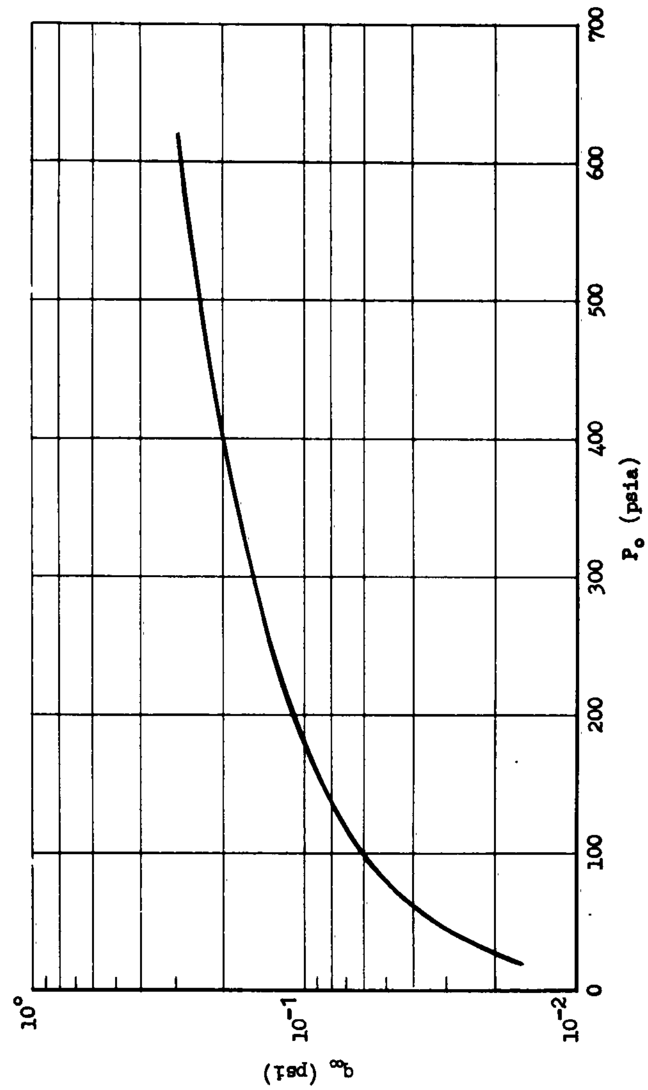

Figure 15 Cont'd

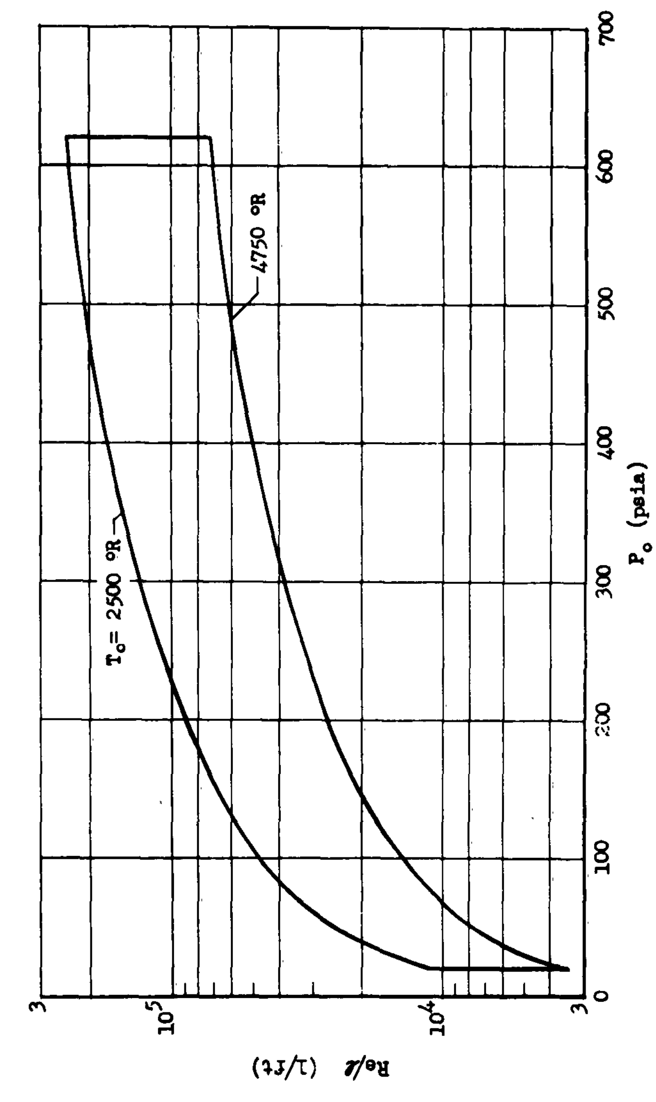

Figure 15 Cont'd

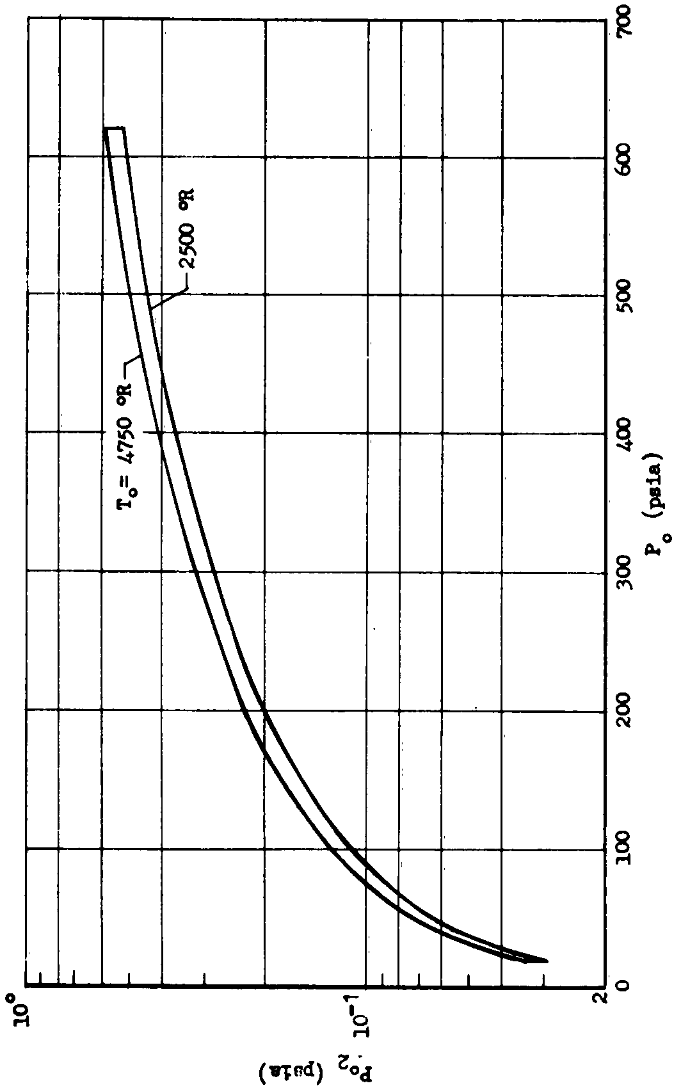

Figure 15 Cont'd

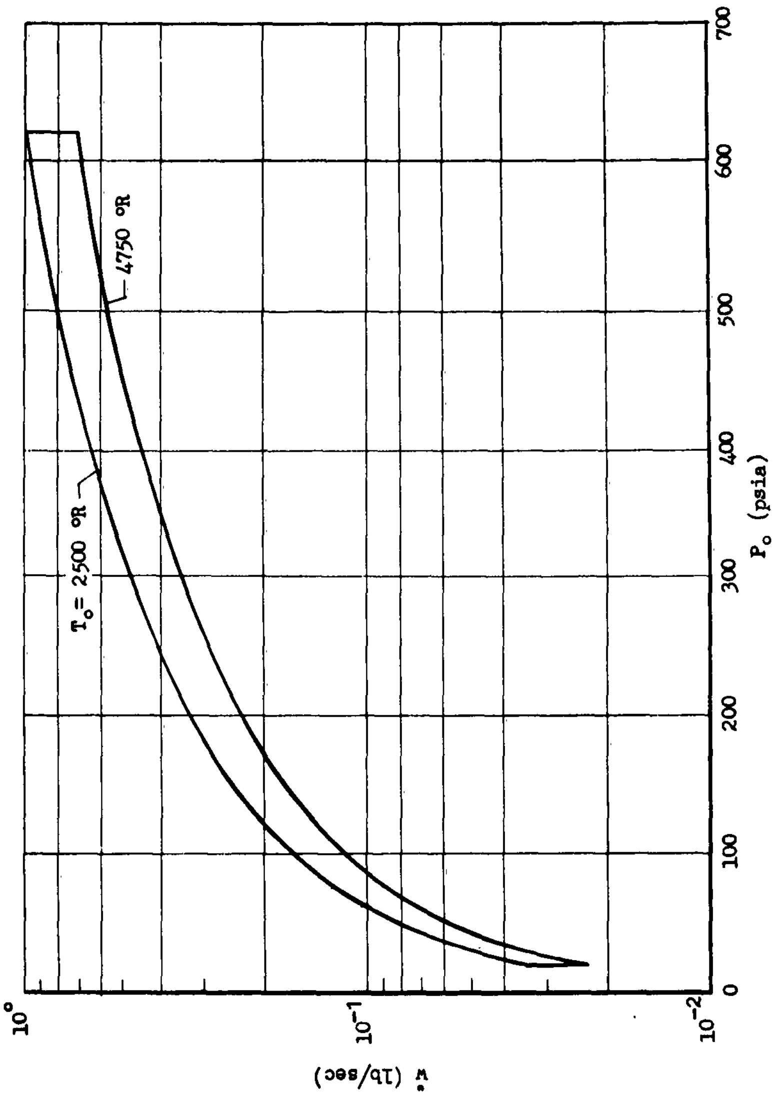

Figure 15 Cont'd

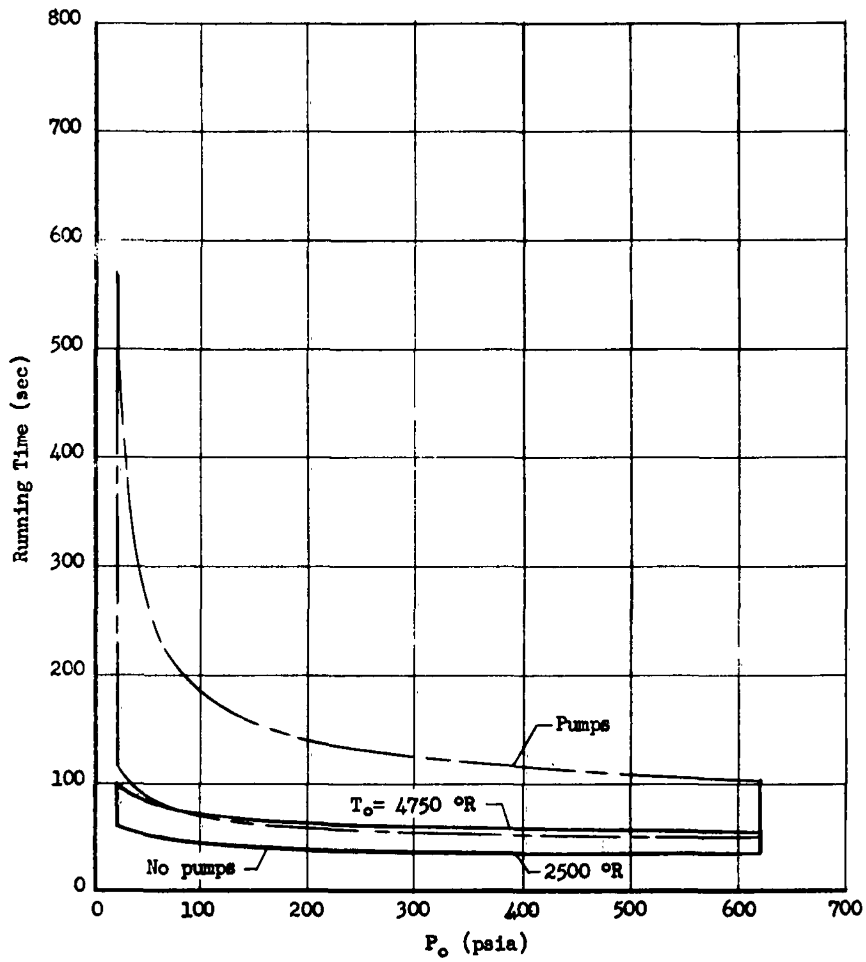

Figure 15 Cont'd

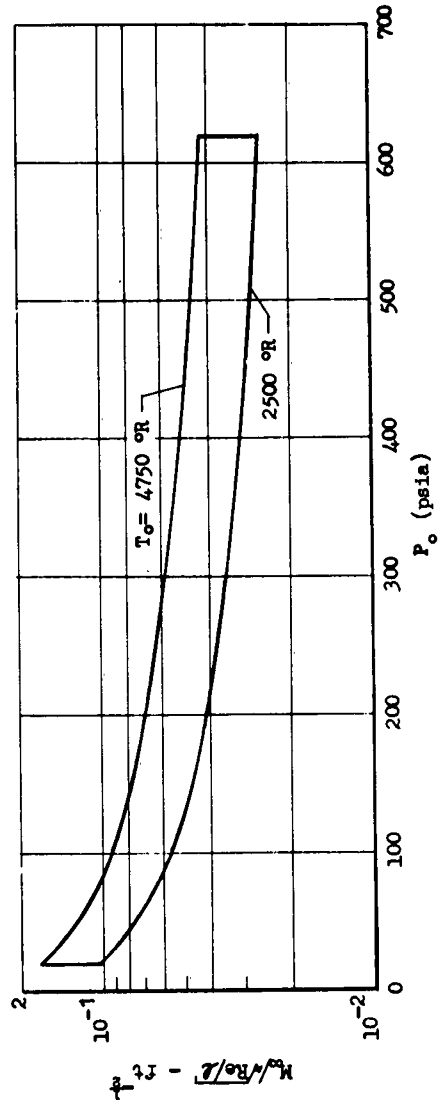

Figure 15 Cont'd

Figure 16 - Performance Curves For Mach 14 Nozzle

Nozzle Length:	81.185 inches
Throat Diameter:	0. 2644 inch
Exit Diameter:	24.000 inches

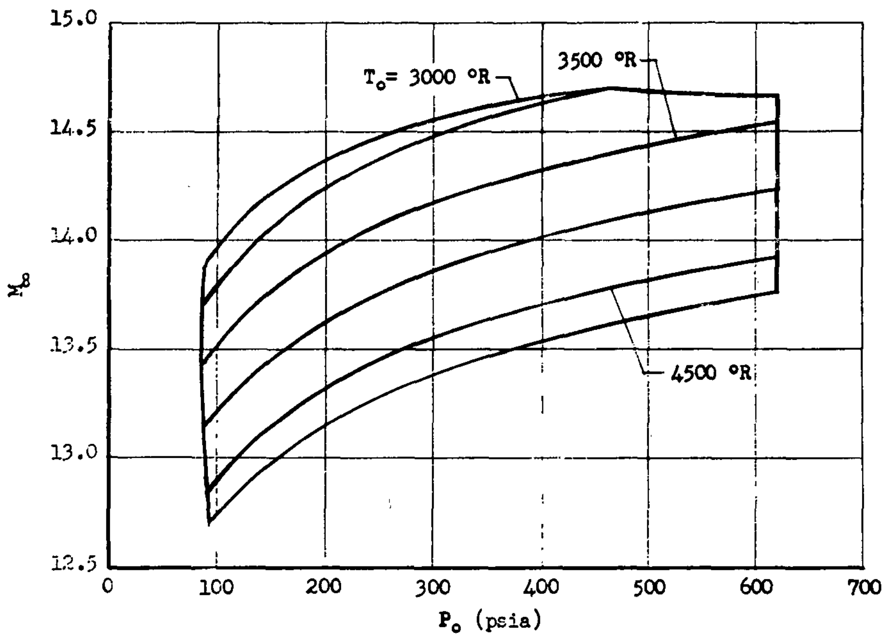

Figure 16 Cont'd

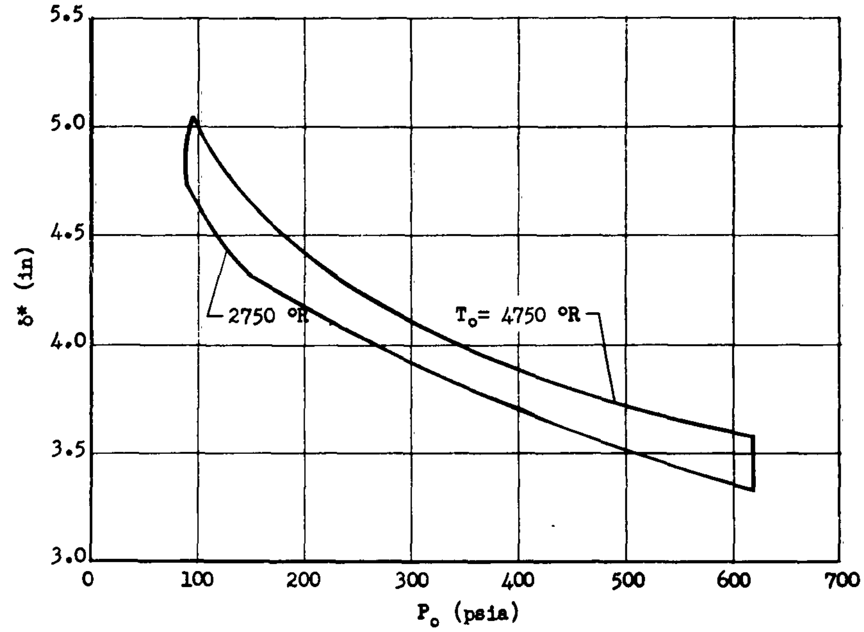

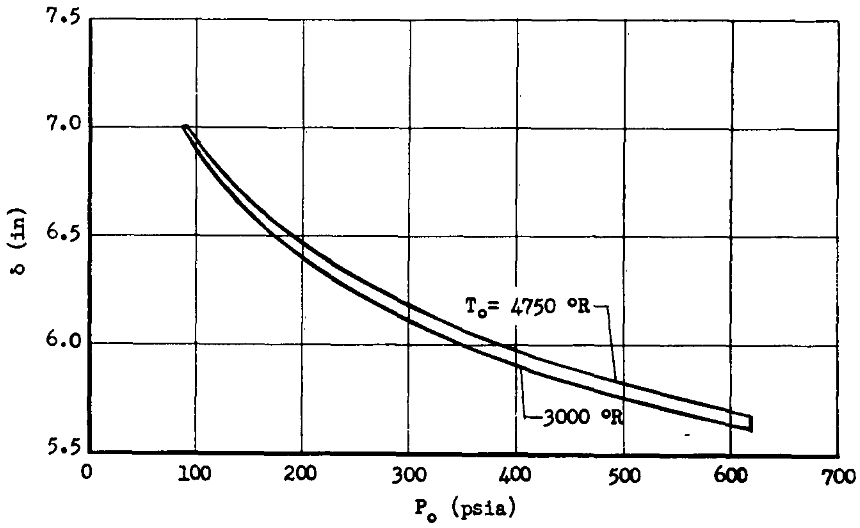

Figure 16 Cont'd

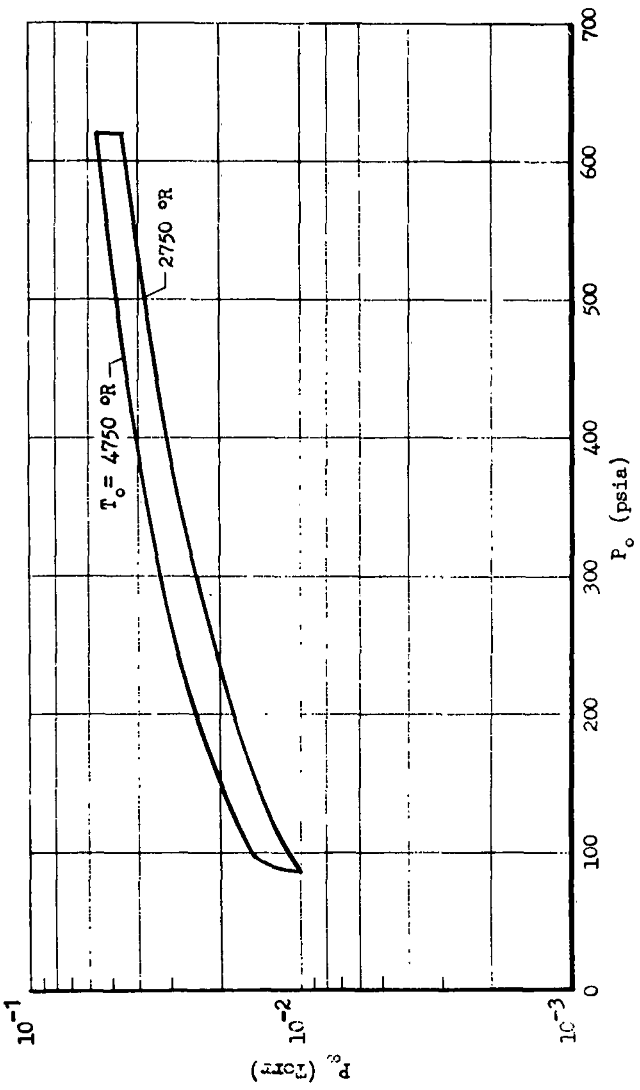

Figure 16 Cont'd

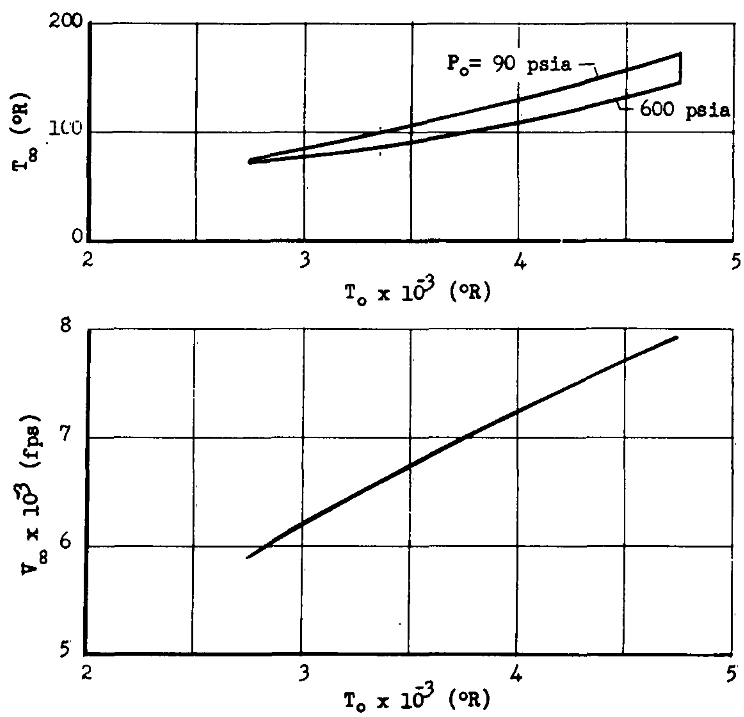

Figure 16 Cont'd

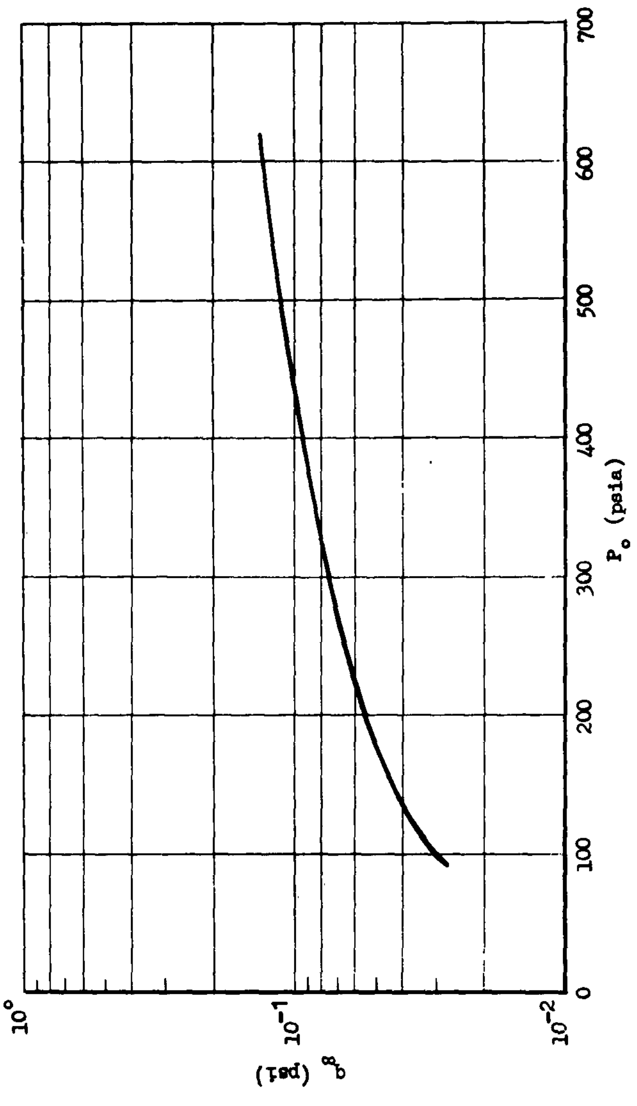

Figure 16 Cont'd

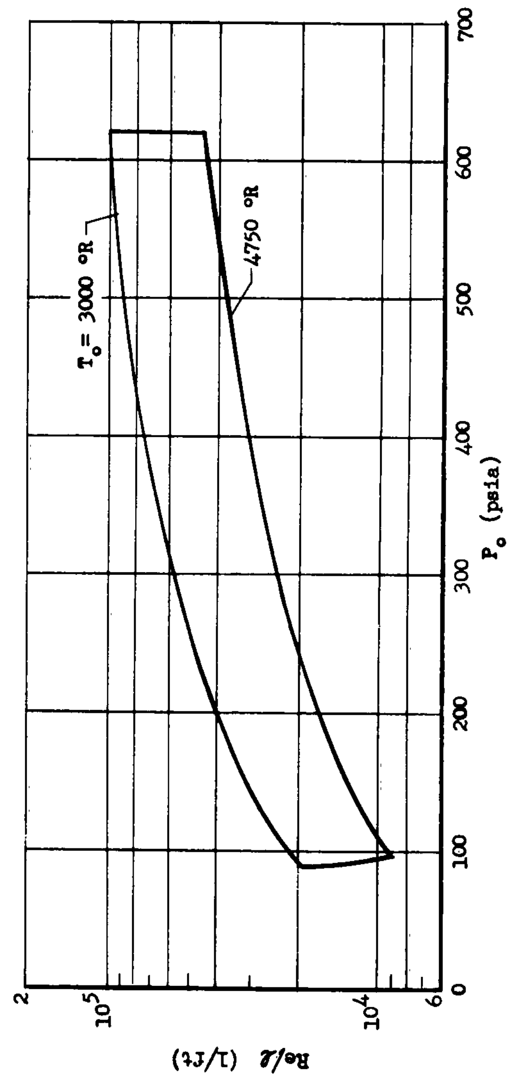

Figure 16 Cont'd

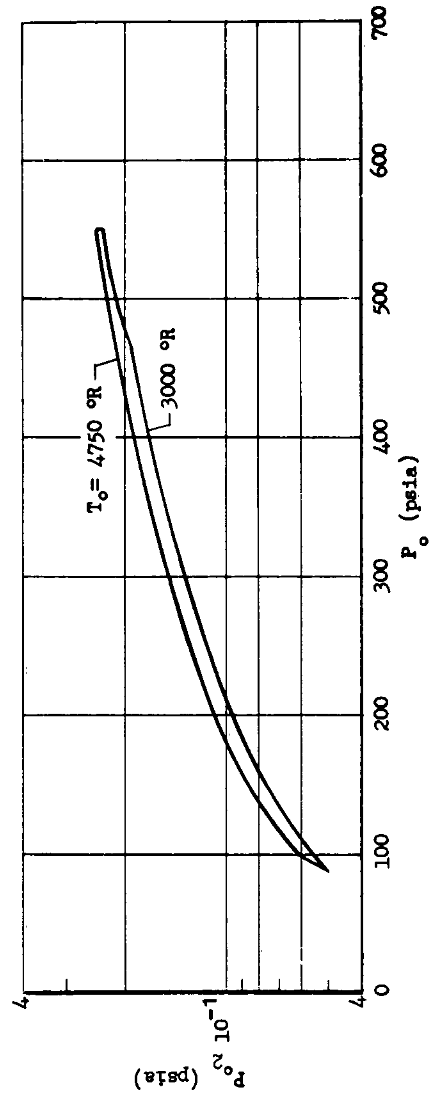

Figure 16 Cont'd

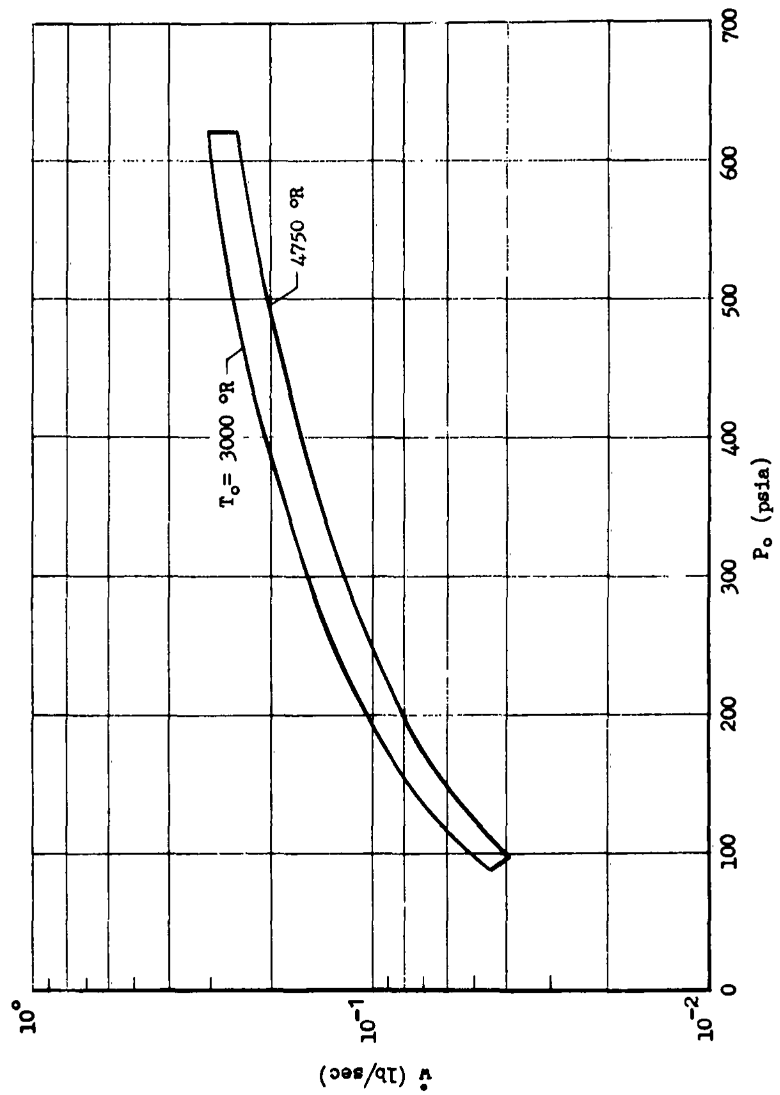

Figure 16 Cont'd

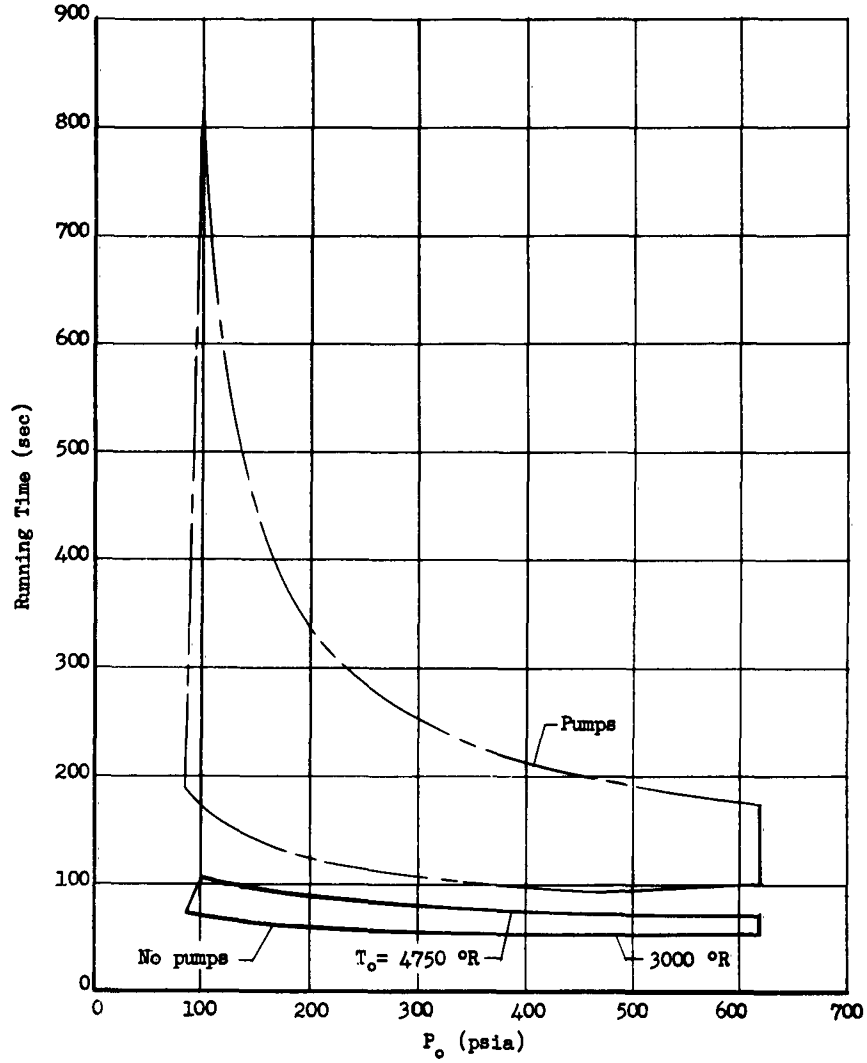

Figure 16 Cont'd

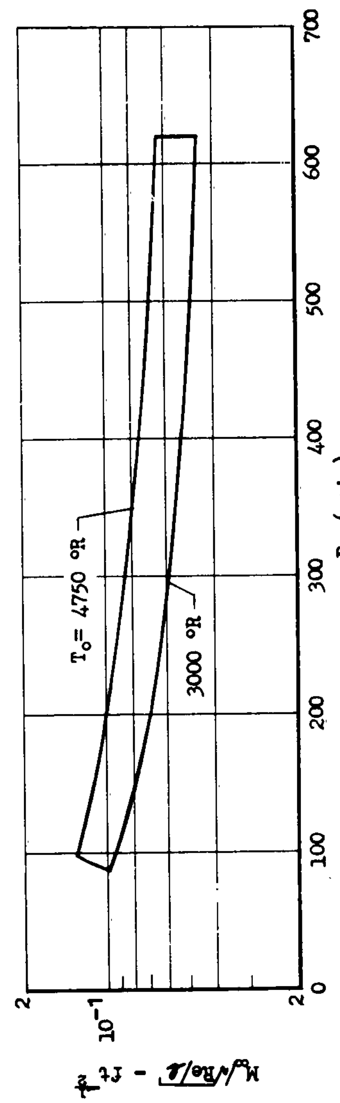

Figure 16 Cont'd

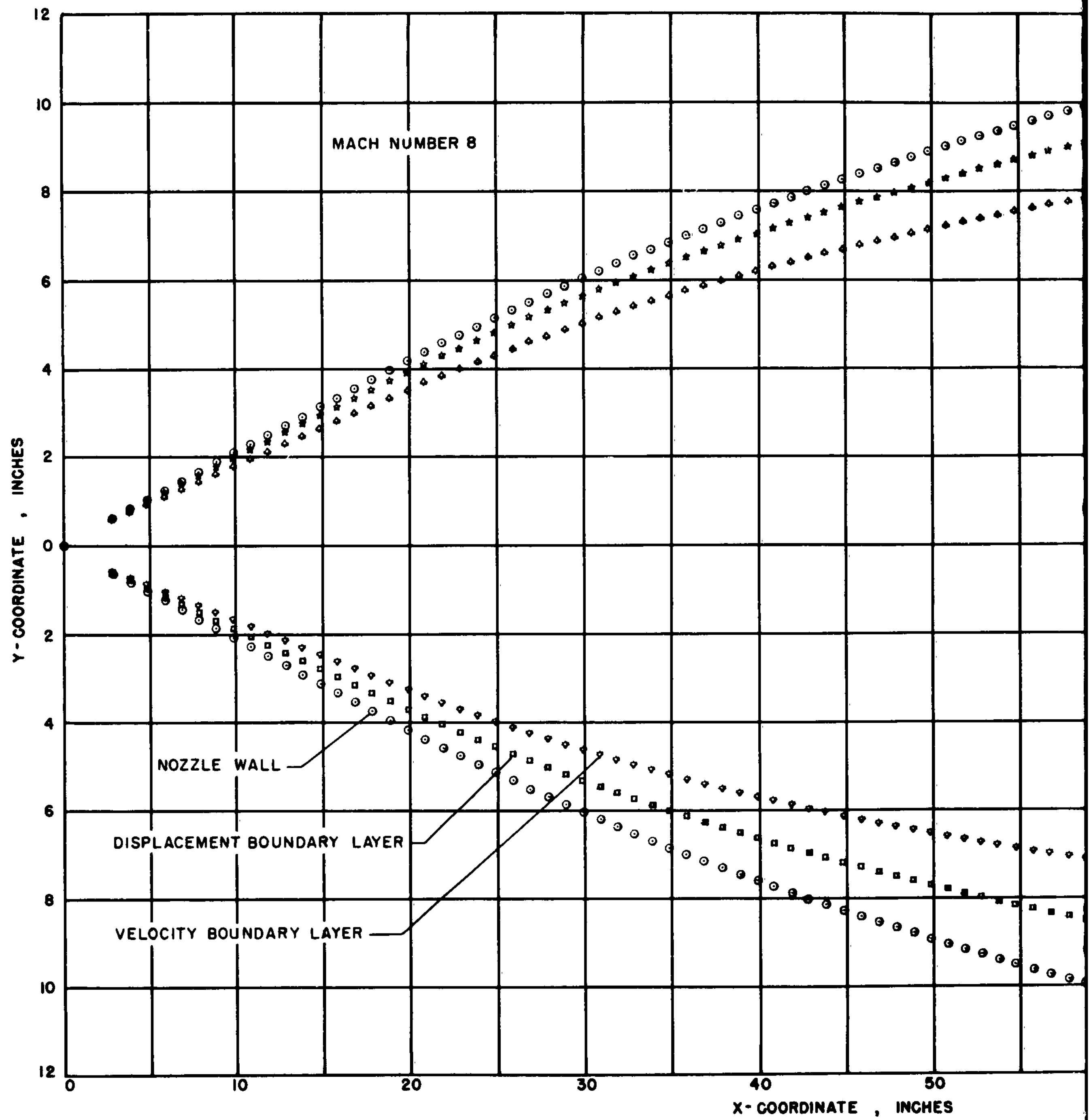

Figure 17. Nozzle Boundary Layer Growth

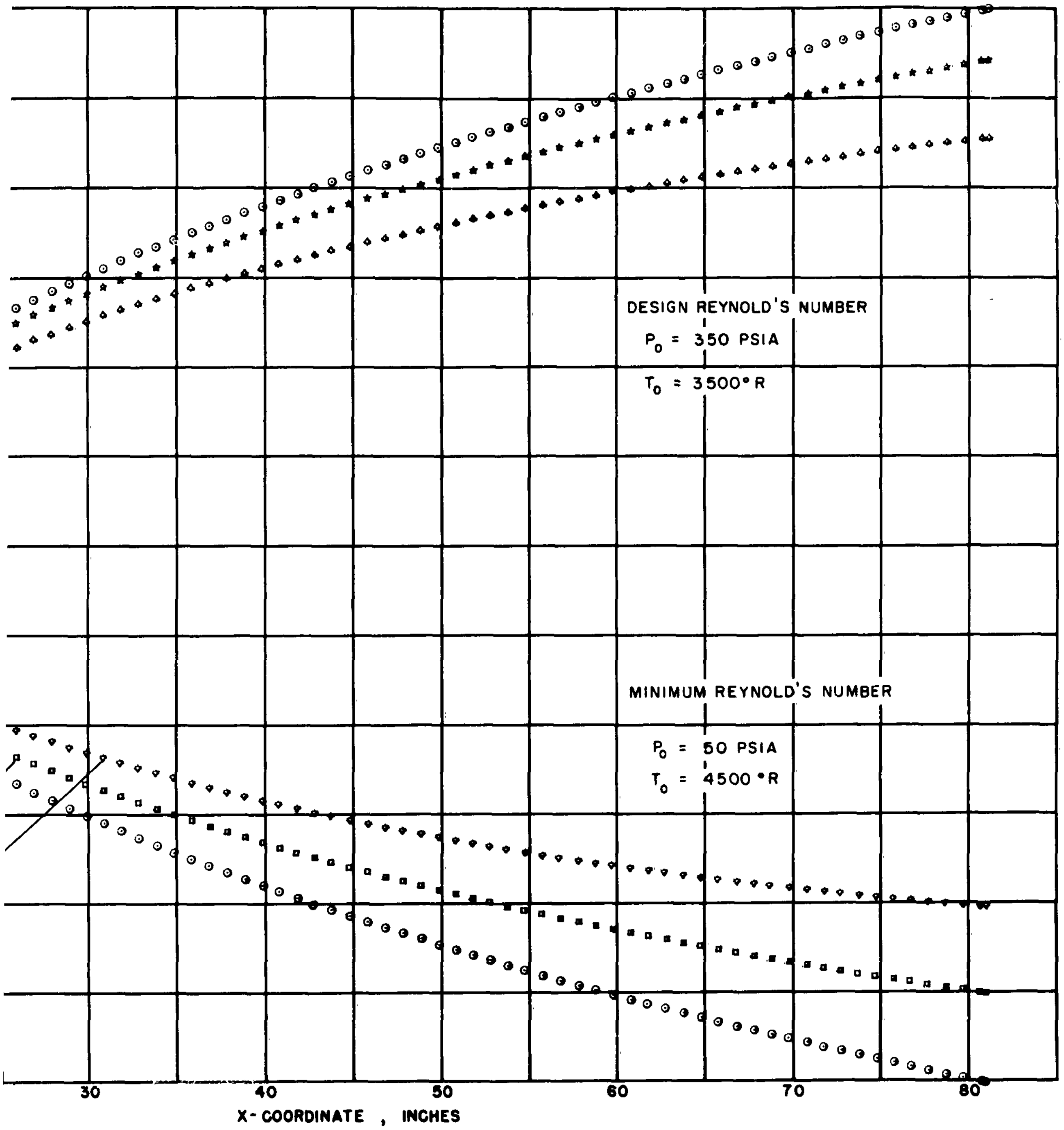

Figure 17. Nozzle Boundary Layer Growth

2

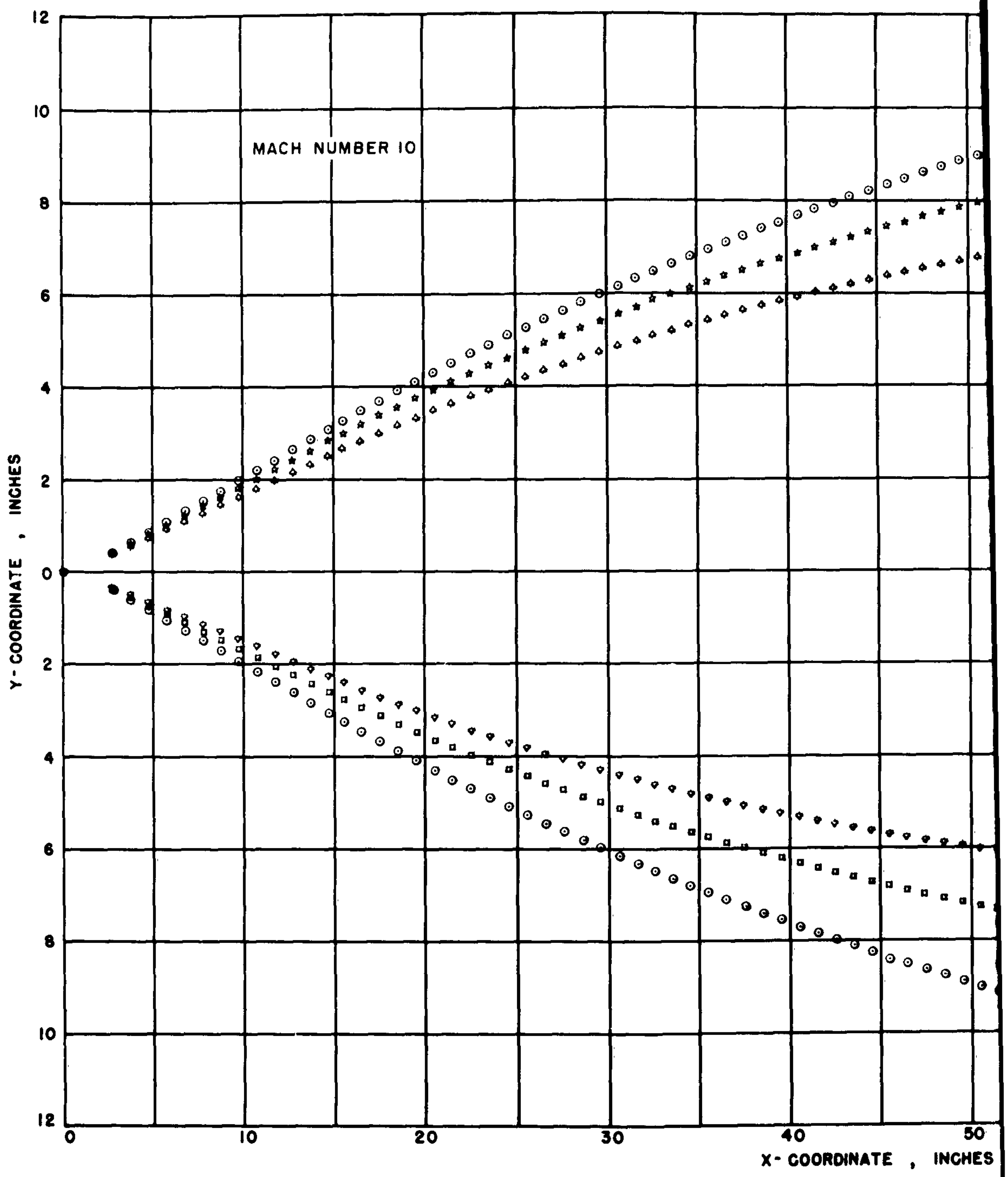

Figure 17 Cont'd

1

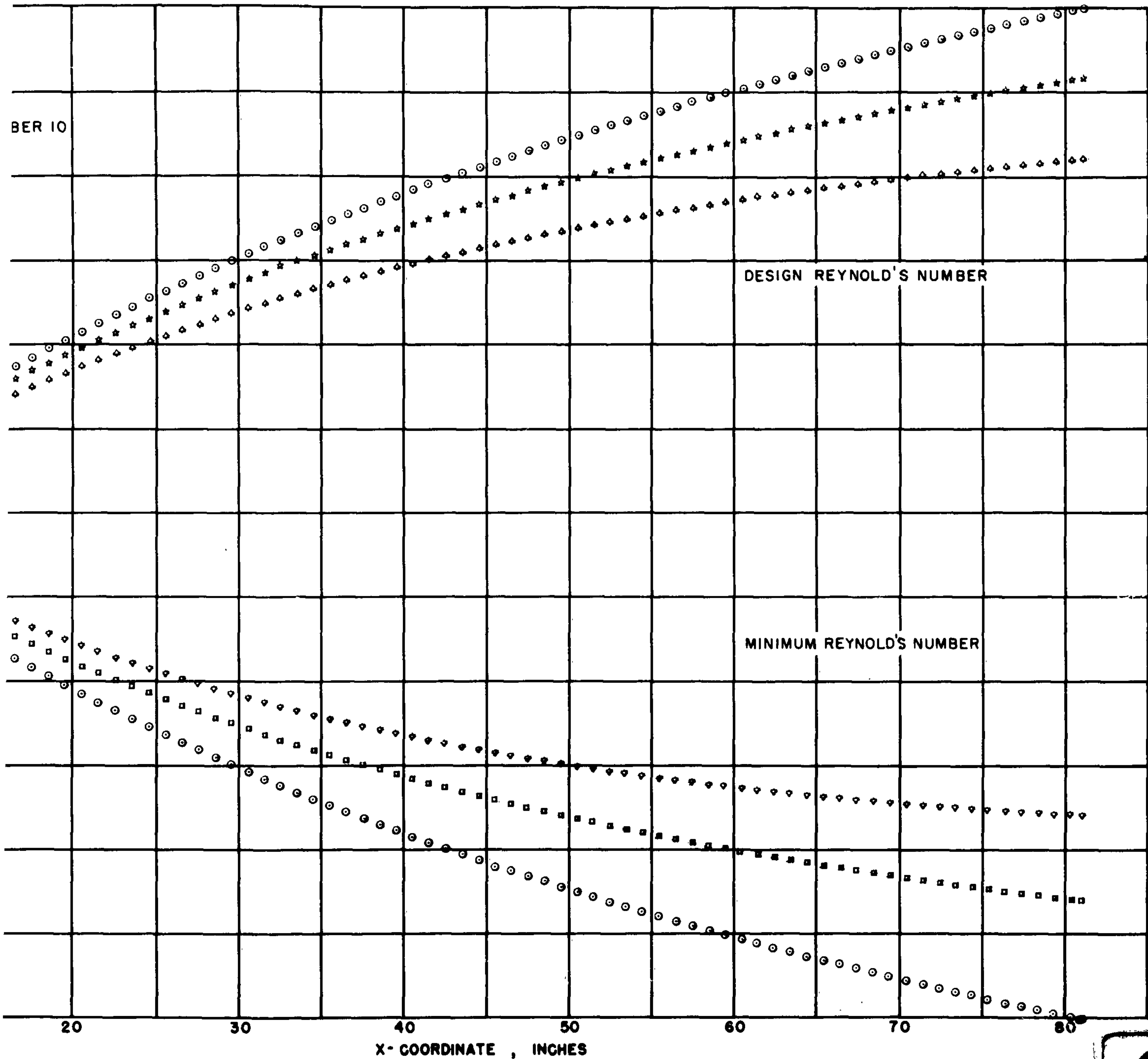

Figure 17 Cont'd

2

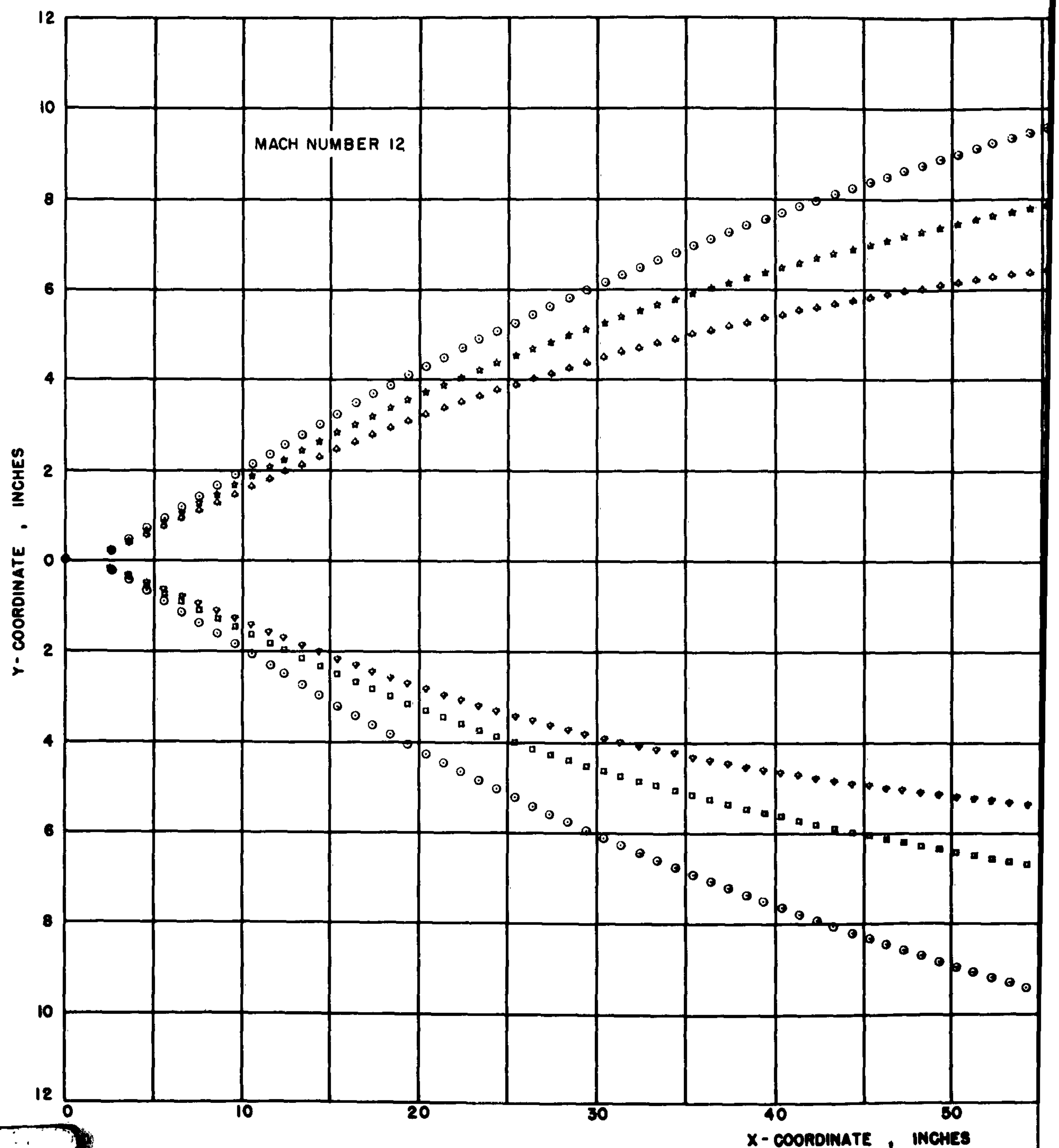

Figure 17 Cont'd

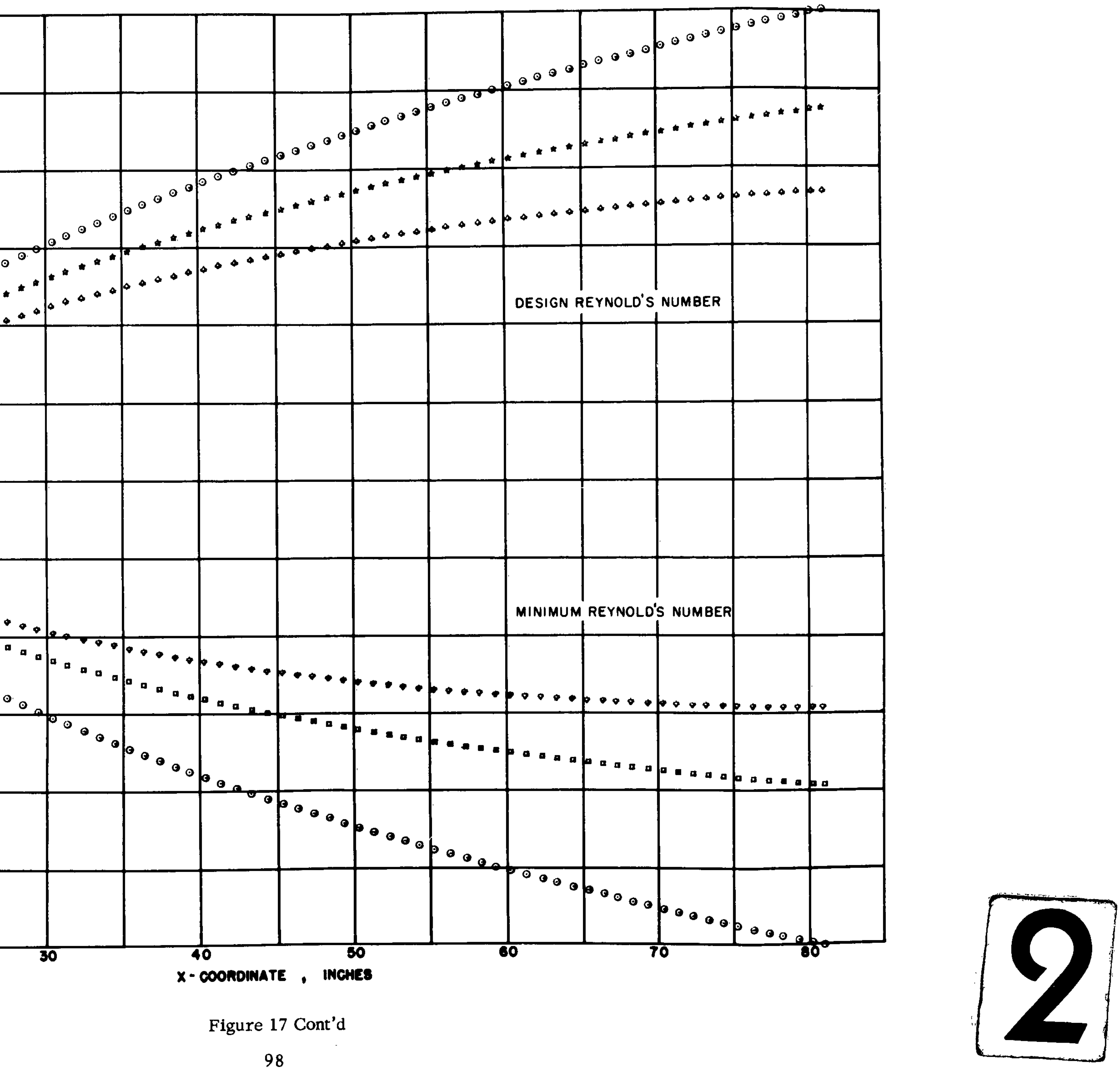

Figure 17 Cont'd

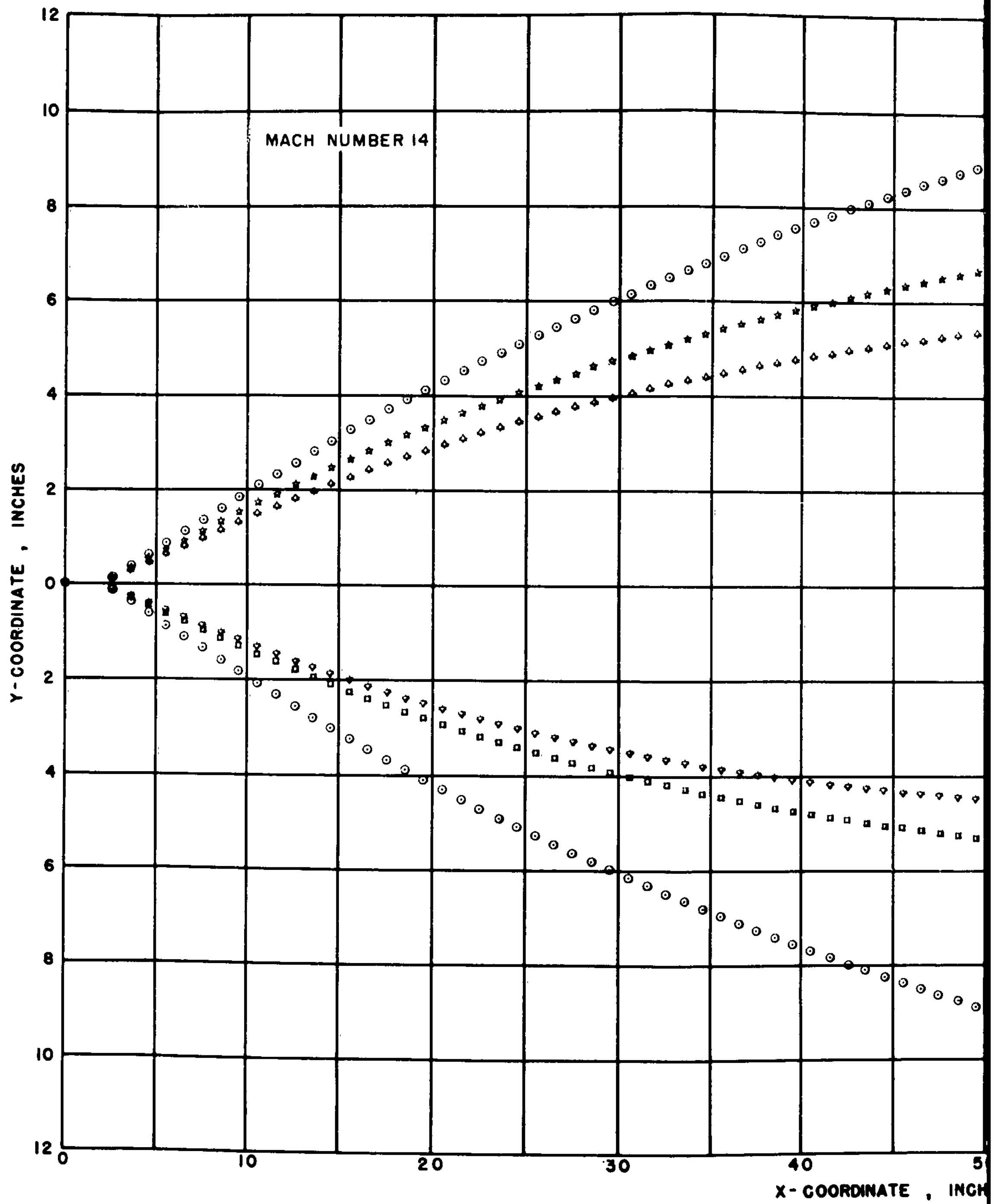

Figure 17 Cont'd

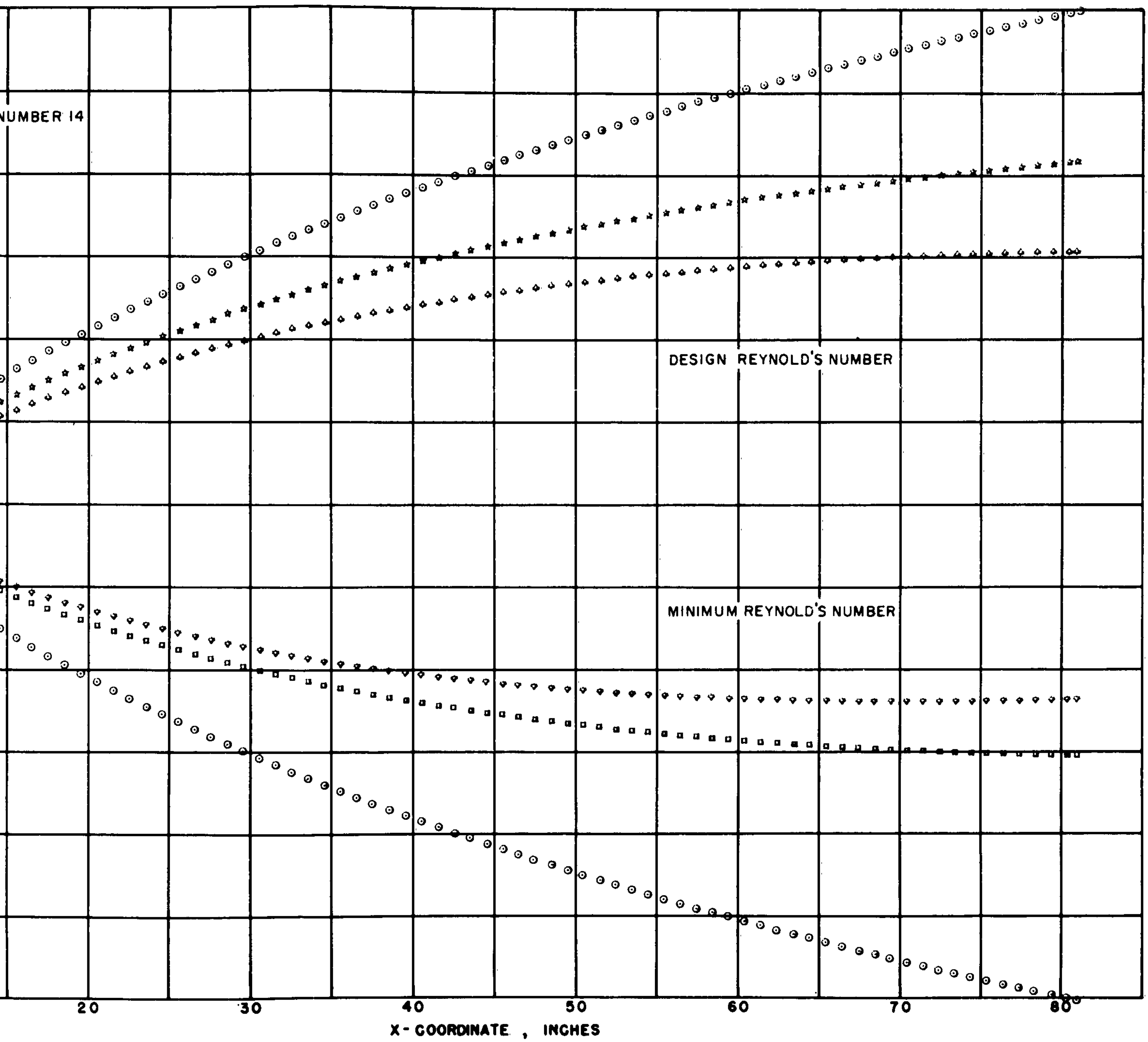

Figure 17 Cont'd

2

Aeronautical Systems Division, Directorate of Engineering Test, Deputy for Test and Support, Wright-Patterson AFB, Ohio.
Rpt No. ASD-TDR-63-456, THE HIGH TEMPERATURE HYPERSONIC GASDYNAMICS FACILITY ESTIMATED MACH NUMBER 6 THROUGH 14 PERFORMANCE. Final report, Jun 63, [illegible] p. incl illus., tables, 16 references.

Unclassified Report

The High Temperature Gasdynamics Facility was developed as a result of the Aeronautical Systems Division's effort to extend the state-cf-the-art in hypersonic aerodynamic simulation. The High Temperature Facility is a hypersonic wind tunnel

(over)

1. Wind Tunnel
2. Hypersonic
3. High Temperature
4. Performance

I. AFSC Project 1426 Task 142601
II. Paul Czysz
III. Aval fr OTS
IV. In ASTIA collection

supplied with high pressure air, heated from a zirconia dioxide pebble heater. The maximum stagnation pressure and temperature is 40 atmospheres and 4700°F, respectively. This facility is one of four of its kind in this hemisphere and the only Air Force facility of its type. This report discusses the modification of the facility to a two-foot diameter test section with a Mach number range of 6 through 14 and its expected performance. This facility is scheduled to be operational in the Fall of 1963.

Aeronautical Systems Division, Directorate of Engineering Test, Deputy for Test and Support, Wright-Patterson AFB, Ohio.
Rpt No. ASD-TDR-63-456, THE HIGH TEMPERATURE HYPERSONIC GASDYNAMICS FACILITY ESTIMATED MACH NUMBER 6 THROUGH 14 PERFORMANCE. Final report, Jun 63, [illegible] p. incl illus., tables, 16 references.

Unclassified Report

The High Temperature Gasdynamics Facility was developed as a result of the Aeronautical Systems Division's effort to extend the state-cf-the-art in hypersonic aerodynamic simulation. The High Temperature Facility is a hypersonic wind tunnel

(over)

1. Wind Tunnel
2. Hypersonic
3. High Temperature
4. Performance

I. AFSC Project 1426 Task 142601
II. Paul Czysz
III. Aval fr OTS
IV. In ASTIA collection

supplied with high pressure air, heated from a zirconia dioxide pebble heater. The maximum stagnation pressure and temperature is 40 atmospheres and 4700°F, respectively. This facility is one of four of its kind in this hemisphere and the only Air Force facility of its type. This report discusses the modification of the facility to a two-foot diameter test section with a Mach number range of 6 through 14 and its expected performance. This facility is scheduled to be operational in the Fall of 1963.